OPTIMAL WATER PUMP SCHEDULING IN AN OPEN RESERVOIR WATER-TREATMENT SYSTEM, INCORPORATING EVAPORATION AND SEEPAGE EFFECT

By

NGANCHA BONJA PATRICK

Thesis submitted in fulfilment of the requirements for the Degree:

Doctor of Engineering in Electrical Engineering

In the Department of Electrical, Electronic and Computer Engineering

Faculty of Engineering, Built Environment and Information Technology

Central University of Technology, Free State

Promoter: Prof. K. Kusakana

Co-Promoter: Prof. E.D. Markus

August 2022

DECLARATION

I, NGANCHA BONJA PATRICK, student number _____, do hereby declare that this research project, which has been submitted to the Central University of Technology Free State, for the degree: Doctor of Engineering in Electrical Engineering, is my own independent work and complies with the Code of Academic Integrity, as well as other relevant policies, procedures, rules and regulations of the Central University of Technology, Free State.

This project has not been submitted before by any person in fulfilment (or partial fulfilment) of the requirements for the attainment of any qualification.

N.B. Patrick Date: 03 August 2022

DEDICATION

Firstly, I thank the Almighty God for the strength he bestowed on me throughout my studies. “For the Lord is my strength and my shield, my heart trusts in him, and he helps me. My heart leaps for joy and with my song I praise him”.

Secondly, I would like to take this opportunity to thank my beloved wife, Ndi Gooh Vera Ngancha, for her inspirational guidelines throughout these studies, the family support at a time when it’s needed the most; indeed, this is our success.

I am indebted to the Bonja’s family for their enduring love and for believing in me for so long. I could have never done this without their faith, support and constant encouragement, particularly to my Mother, Mama Chancho Catherine Bonja and the rest of the extended family, for their trusted love, care and patient support in my studies.

Furthermore, I dedicate this research and tribute to my late father, Philip Bonja, for encouraging me to pursue a meaningful career path… may your spirit continue to live with us forever. To my former classmates at the “Community Technical and Commercial College (COTECC Bafut)”, thank you for the strength and the time we spend together, figuring out ideas to better our studies.

Last, but not least, I would like to sincerely thank the prayer community, for their spiritual support is greatly appreciated.

ACKNOWLEDGMENTS

I would like to express my sincere appreciation to my supervisors, Prof. Kanzumba Kusakana and Prof. Elisha Didam Markus who were supportive of this study. Their continual guidance, support and knowledge were indeed invaluable. They provided me with motivation and ongoing encouragement throughout the study, for through them a Dr. is found within me.

I furthermore want to thank my CUT electrical research group mads, especially Dr. Percy Hohne, for their constant inspiration and moral support in furthering my studies.

Thank you to the Central university of Technology (CUT), Free State, for granting me the opportunity and financial assistance to undertake my studies; the Manufacturing, Engineering and Related Services Sector Education and Training Authority (merSETA), for their financial support.

ABSTRACT

Bulk water extraction and purification, in most countries, occurs in distant areas, where running rivers or lakes are available. To achieve the goal of obtaining potable water, water from dams or lakes is pumped into a treatment reservoir, to undergo purifying operations. Electrical energy is required for the supply of these electric pumps, to pump water from one level to another, during the process.

Looking at the energy management point of view, the main problem is the rising cost of electrical energy used to pump water from the dam to the reservoirs. This could be owing to inadequate management of the pumping system, as well as the fact that water reservoir pumping systems are subject to exogenous variables, including evaporation, precipitation, seepage and leakage.

A review of water-pump energy management steps in a bulk-water purification system, was conducted, to understand the problem and find the best possible solution in enhancing the energy usage in a water pumping system. This survey provides a complete overview of current control strategies in water pumping energy management activities. The review is led by the performance, operation, equipment and technology (POET) concept, which includes a review of current water pumping technologies, as well as advancements, ideas, evaluations and improvements.

This POET framework discussed the long term viability of a broad energy management program, as an application of the commercial bulk water development scenario. The case study established that the POET based energy management system may save energy in a coordinated and effective manner. It may be able to successfully obtain the energy saving prospects of water pumping processes, as well as laying the groundwork for a future project in water treatment systems.

This research proposes different energy management models, to meet the pumping water demand while minimizing the amount of energy required during the operation. The first model was based on the mathematical model for water pumping controller systems and is

known as the research's baseline model. The system takes into consideration the impacts of evaporation, rainfall and seepage to make the model more realistic and it uses the flood switching principle, regulating the pumping operation of a water facility. To assess the initial model's performance, simulations were run in two scenarios: first, evaluating the flood switching control system without taking into account the effects of rainfall, evaporation, and seepage, and second, with all of these constraints taken into account.

The second model was based on the principle of timer-setting control. When the effects of evaporation, rainfall, and seepage losses were all considered, the performance of the suggested electrical timer switching control system was evaluated. The simulation of the second model was carried out using two scenarios: first, a time control system was applied to a fixed water pump, and second, a timer-setting control system was incorporated with the VFD power control pump.

The optimal switching control system was used in the third model. Evaporation, rainfall, and seepage losses were all elements taken into account in order to make the model more realistic. The simulation of the third model was divided into two categories: first, an optimal control system was applied to a fixed water pump, and second, the optimal control system combined with the VFD power control pump.

The main objective of this research was to optimise the pumping operation of a water pumping system, with the aim of obtaining a lower energy consumption cost. MATLAB-SCIP optimization software was used to implement the developed models. Hence, the model's energy-saving capabilities were validated through simulation. In comparison to the baseline case, in which the developed model is simulated with the impacts of evaporation, rainfall and seepage; and then again without these disturbances, the results of the first model show an energy savings of 683ZAR per day, when the effect of evaporation, seepage and rainfall are all taken into consideration in a flood switching control system.

The simulated results of the second model are compared to the baseline flood switching control system, to estimate the economic benefit of the developed model. As compared to the baseline case, where the flood switching control system is used to accommodate the load

demand, the simulated results for the selected day of operation have shown that, using the proposed timer-setting control model with fixed speed motor pump, a 316 ZAR reduction in the operating cost is achieved, compared to the baseline flood switching control system. Looking further, when a VFD control motor pump is added to the timer-setting control system, the simulated result shows that a 1022 ZAR decrease in operating cost per day may be saved, when compared to the baseline flood switching control system.

In a separate simulation of the third model, the results are compared to the baseline flood switching control system, to estimate the economic benefit of the developed model. When the optimal control system is employed to meet the load requirement, the simulated results for the chosen day of operation demonstrate that, when compared to the baseline flood switching control system, the proposed optimal control model with fixed speed motor pump, saves 1204 ZAR in operating costs. When a VFD control motor pump is introduced to the optimal control system, the simulated result shows that, when compared to the baseline flood switching control system, a 1725 ZAR reduction in operating cost per day may be achieved.

These findings further revealed that the grid's energy demands are significantly reduced when the proposed optimal control models are combined with a VFD control motor pump in a water pumping system. As a result, the initial cost of acquiring energy is reduced. Further services, such as maintenance, could benefit from the savings. In the end, this may assist in lowering the initial cost of water sold to consumers.

TABLE OF CONTENTS

LIST OF FIGURES

LIST OF TABLES

LIST OF ABBREVIATIONS AND SYMBOLS

AC	Alternating Current
ACO	Ant Colony Optimization
BCR	Benefits-to-Cost Ratio
C_{EC}	Cumulative Electricity Costs
$C_{initial}$	Initial Cost
C_0	Summer off-peak rate
C_{OM}	Operation and Maintenance Costs
C_p	Summer peak rate
C_{rep}	Replacement Cost
C_s	Summer standard rate
DC	Direct Current
DWS	Department of Water and Sanitation
Δt	Sampling Time
EMS	Energy Management System
HMI	Human-Machine Interface
kW	Kilowatt
kVA	Kilovolt-Ampere
kWh	Kilowatt Hour
LCC	Life Cycle Cost

LCD	Liquid Crystal Display
MATLAB	Matrix Laboratory
MD	Maximum Demand
MPC	Model Predicting Control
OI	Innovations Conference
OPTI	Optimization
PBP	Payback Period
Pm	Post meridiem
POET	Performance, Operation, Equipment and Technology Efficiency
Ppump	Power of pump
PV	Photovoltaic
RESWPS	Renewable Energy Source Water Pumping System
RoR	Rate of Return
RPM	Revolution Per Minute
SABS	South Africa Bureau of Standards
SCADA	Supervisory Control and Data Acquisition
SCIP	Solving Constraint Integer Programs
SPP	Simple Payback Period
ToU	Time-of-Use
US	United State
US$	United States Dollar

VFD	Variable Frequency Drive
VSD	Variable Speed Drive
VSP	Variable Speed Pump
WTW	Water Treatment reservoirs/Works
ZAR	South African Rand

CHAPTER 1: INTRODUCTION

1.1. BACKGROUND

Globally, water is known as one of the most important commodities to life [1]. However, more than 348 million people face severe water scarcity, since they live in regions where existing water resources require a high cost of water purchase [2]. Since the 1990s, global water demand has more than tripled, relying primarily on the availability of surface water resources, including rivers, groundwater and lakes [3]. Water consumption for household, agricultural and industrial purposes, has skyrocketed [4]. Municipalities are tasked with purifying and distributing drinkable water in most countries, including South Africa [5, 6].

The Covid-19 pandemic is one major challenge that has heated the world, South Africa included, adding to all the water challenges such as drought, that have a detrimental impact on South Africa, in terms of water crises, although climate change has yet to be fully realized. Water, hygiene and sanitation are critical for the prevention and treatment of Covid-19 infections, according to the Institute of Development Studies' 2020 report [7,8]. Increased home water demand, on the other hand, will simply exacerbate the water problem in cities that already have water scarcity. In the South African area, water allocation to agriculture and irrigation constitutes 52% of the total annual consumption. The second largest water consumption, accounting for 19% of the total annual consumption, is the environment. 11% of the water is used for industrial and commercial purposes. 10% is classified as domestic use, and 8% is for forestry water [9].

In most developing countries, South Africa included, potable water harvesting and purification depend on the availability of surface water resources, such as rivers, ground water and lakes [10]. A structure built across a stream, a river, or an estuary to retain water, is known as a dam. Figure 1.1 shows a location of a water dam situated in the Bloemfontein area, where untreated water is pumped before the purification process begins.

Figure 1.1: Rustfontein Dam

According to the 2019/2020 annual report of the Bloemfontein utility firm that delivers potable water to the city, direct operating costs account for 53.2% of overall costs, with 41.5% attributed to energy consumption. Pumps are the most energy-intensive component of a water treatment facility. Because of the high pumping costs associated with water pumping systems, as well as the fact that pumping occurs regardless of the time of use (ToU) tariff structure, which varies depending on the time of day, the current pumping system has a considerable energy cost. [11, 12].

Water loss of 7.29% in the year 2019/2020, was reported [12]. However, additional consideration is given to the volume of water that is lost. This is water loss that may be attributed to the effect of seepage and evaporation [13].

The South African Government, through the Department of Water and Sanitation (DWS), takes water development seriously, as its mandate is to provide reliable, sufficient and clean water, to promote socio-economic progress. This is combed out in accordance with the criteria of water-related laws and legislation, which are vital in realizing the population's rights to better social well-being, adequate food and water, economic growth and poverty eradication [14, 15].

The study's focal point is the Bloemfontein Mangaung Metropolitan water treatment system. The case study consists of the metro water system's geographical area. Water is moved from the Orange and Caledon river systems to meet current water requirements. The main transfer water supply schemes are:

- The Caledon Bloemfontein transfer, which supplies Bloemfontein, Dewetsdorp and small users with water from Welbedacht Dam,
- The Maselspoort scheme,
- The Caledon Modder (also known as the Novo transfer scheme), via the Rustfontein treatment works, supplies Bloemfontein, Botshabelo and Thaba Nchu.

There are mainly three systems that served the Mangaung metropolitan area, namely, the Rustfontein Dam, Mockes/Maselspoort Dam and Groothoek Dam. Water is pumped from these dams to their respective water treatment reservoirs/works (WTW) [16, 17].

Several academics have been working on solutions to reduce water loss in the water system. Their strategy is divided into two groups; the supply side, which includes the water catchment and pumping facility; and the demand side, which includes the numerous consumers.

This study takes a look at present control approaches for water-supply pumping systems. The optimization model, energy tariff fluctuations, electrical pump control methods and the effect of evaporation and precipitation in an open reservoir, are all included.

The aforementioned challenges, prompted the conduct of this study in the field of water pumping systems, which includes an optimal control water pumping system, that attests to changes in the water load demand, while taking into account constraints, such as evaporation, seepage and rainfall effects in an open reservoir water pumping system.

1.2. PROBLEM STATEMENT

Electrical energy required for water pumping to reservoirs and distribution to customers, is growing increasingly expensive and it continues to be one of the largest cost drivers in water delivery to consumers, followed by equipment repairs and maintenance [18]. This could be due to ineffective water pumping tactics, given that a continuous pumping system results in a high rate of energy consumption, which translates to a high water cost to the user.

Most of the literature on water pumping in an open reservoir system ignores critical exogenous variables, such as evaporation, rainfall influence on the open reservoir and leakages, treating them as constants [19, 20, 21 and 22]. However, Friegrich et al. [23] and Craig et al. [24] analyse the impact of these factors on reservoir water volume in their research. Therefore, the above problem has resulted in the pumping of more water in the reservoir, to cater for evaporation and seepage, in the given system.

Additionally, the pumping method adopted in most stations is based on a constant water level, that should be maintained and operated until the reservoir level reaches a 90% level (rated as full capacity). When the water level lowers to 10%, pumping resumes. Pumping costs are rising, due to leaks and evaporation losses in the system, as well as the fact that, with flood management, water demand fluctuations are not traceable in the process. As a result, the above water pumping method is seen as unreliable and costly.

1.3. AIM AND OBJECTIVES

The aim of this research is to develop optimal energy control models for managing water pumping systems, in order to minimize the total energy consumption costs, taking into account the time of use (ToU) tariff, in the context of South African electricity supply, as well as the effects of evaporation, seepage and precipitation. Therefore, to achieve this aim, the objectives were as follows:

- To develop a model and simulate the operation of a water-pump system, based on Scheduled timer-setting control switching, applied to a fixed speed water pump. This control operation is similar to a binary ON/OFF switching. The control is compared to a baseline flood switching control system, in view to understand the cost benefit in pumping, when applying the idea system. The control operator is guided by the historical data, to set up the timing sequence of the operation.
- To develop and simulate an optimal control model, to automatically schedule the pumping operation of a fixed speed water pump and compare the system to a baseline control system, in determining the energy saving capability of the system.
- To develop a model and simulate a timer based control model driving a VFD pumping system and to compare the output to a baseline flood switching control water pumping system, then determine the techno-economic benefit of the proposed method.
- To develop a model and simulate an optimal control system driving a VFD power control water pump, for a reservoir water catchment system, comparing the result to a baseline flood switching control system.
- Conducting a techno-economic analysis of the four models developed, determines their performances, in terms of its energy cost consumption, as compared to the baseline, while operating in the same demand and environmental conditions.

1.4. RESEARCH METHODOLOGY

To achieve the objectives of the study, the methodology is as follows:

- Literature review: A detailed survey of literature related to pumping systems, the effect of evaporation in reservoir water, effect of losses due to seepage, pump operation together with pumping strategies and electricity tariff in pump stations, was reviewed.
- Model description: The first model consists of a timer switch controlling a fixed speed pump based on the reservoir water level, turning ON at minimum and OFF at maximum (Model 1), the second involves an optimal control water pumping system applied to a fixed speed pump (Model 2). The third model is a timer switch controlling a VFD power control water pumping system (Model 3). While the fourth involves an optimal control model, driven a VFD power control water pumping system (Model 4). All four models had considered the constraints, such as the evaporation effect, rainfall effect and seepage losses.
- Data collection (input variables) and case study: Real input variable data collected from SCADA systems at a water plant in the Bloemfontein area, Free State was used, which includes:
  - Water load demand.
  - Net radiation data, latent heat of vaporization and density of water.
  - Saturation vapour pressure, ambient air vapour pressure and vapour transfer coefficient.
  - Rainfall data.
  - A pump rated power, water pump processes, sizing and other equipment, etc.
  - ToU tariff electricity pricing.
  - Permeability of material, height of reservoir water, number of potential drops and number of flow channels.

- Models' development: The various steps in developing the optimal energy management models for the proposed water pumping systems are shown in Figure 1.2: The mathematical models were developed and applied using MATLAB software.

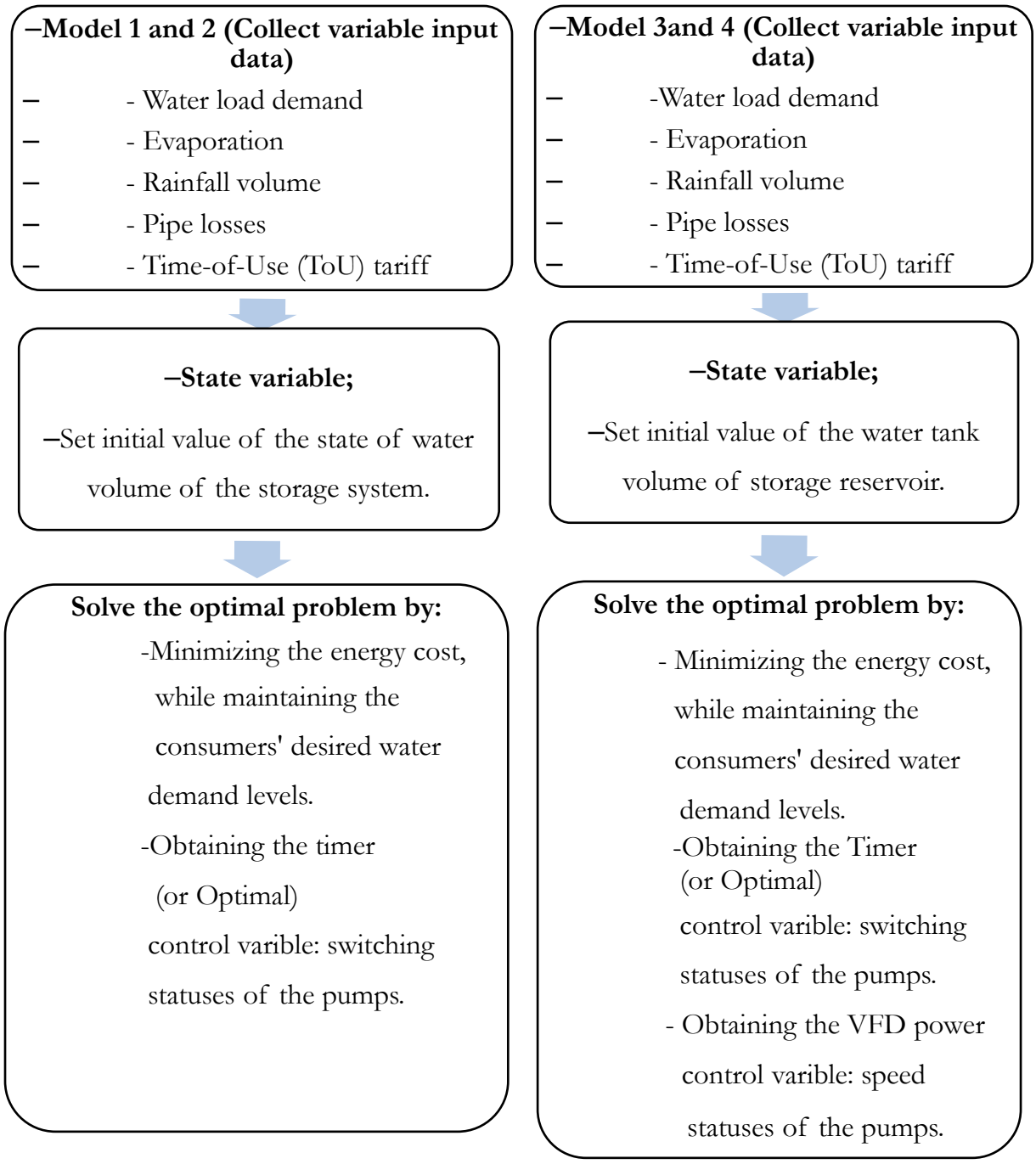

Figure 1.2: Block diagram of methodology and research design

Based on the changing nature of water-pump power flow control of the various models and taking into consideration several restrictions, such as evaporation, rainfall, seepage and pipe losses. The developed model uses mixed-integer non-linear programming, to solve the objective function and constraints. Because the optimization problem incorporates nonlinear constraints, the SCIP Optimization solver in the MATLAB OPTI Toolbox is utilized [25].

- Simulation results and discussion:
  - Simulations are carried out for the water system supplying the storage reservoir to assess the efficacy of the proposed energy management models, in terms of flood switching control. Timer-setting control of a fixed-speed motor-pump, optimal control of a fixed-speed motor-pump, flood switching control of a VFD control motor-pump, timer-setting control of a VFD control motor-pump and optimal control of a VFD control motor-pump.
  - For the flood switching control in a water pump system, simulations are conducted to evaluate the baseline level of energy management in the model, which is applied to the reservoir water pumping for a 24 hour full-load cycle. Two main aspects are simulated and discussed. This is the flood switching cycle that operates the power ON/OFF of the pump and the simulation of the reservoir water volume levels.
  - For the timer-setting control water pump system supplying the reservoir, simulations are conducted to evaluate the effectiveness of the proposed energy management model, applied to a constant speed (or VFD control) water pumping system for a 24 hour full-load cycle. Two main scenarios are simulated and discussed. These are the timer switching cycle that operates the power ON/OFF of a fixed speed pump and, the second, a VFD power control water pump. The simulation of the reservoir water volume level and the simulation of a 24 hour economic analysis of the system.
  - For the optimal control water pump system supplying the reservoir, simulations are conducted to evaluate the effectiveness of the developed energy management model applied to the water pumping system of a 24 hour full load cycle. Two

main scenarios are simulated and discussed. These are the optimal scheduling switching cycle that operates the power ON/OFF of a fixed speed pump and optimal control scheduling switching cycle with a VFD power control water pump. A 24 hour simulation of the reservoir water volume level and the simulation of a 24 hour economic analysis of the system.

- For the techno-economic analyses, the findings of the four developed models are compared to the baseline (flood), in terms of daily operation, as well as lifecycle costs.

1.5. CONTRIBUTIONS TO KNOWLEDGE

The primary contributions of this research, when compared to the various researches currently available on the energy management of water pumping systems, are as follows:

- The impact of exogenous variables, such as precipitation, evaporation, seepage and storage are included, to actualize the models.
- Most studies have used a control method, such as the flood switching control, to manage the operation of a water pump in a water pumping system. In this study, further operating strategies, such as models 1, 2, 3 and 4 (timer-setting control switching, applied to a fixed speed water pump, an optimal control switching model, applied to a fixed speed water pump, timer-based control model driving a VFD pumping system and an optimal control switching model, driving a VFD pumping system) have been developed and their respective techno economic performances have been assessed through simulation.
- Social impact:

  The research provides an opportunity for municipal water pumping cost minimization. This may, in return, provide more affordable water to the community, while maintaining a reliable water supply to meet the demand.

1.6. HYPOTHESIS

- More accurate results will be obtained by including the various effects, such as evaporation, seepage and rainfall volume, in optimising the pumping operations of a water pumping system.
- The four developed models have achieved a lower daily energy consumption cost, as well as lifecycle cost, as compared to the flood system currently used in the water plant.

1.7. DELIMITATION

The study was conducted with the following limitations:

- This study is limited to modelling and simulation of timer based and optimal control, applied to both the fixed speed pump and VFD power control pumps. Further control options will be solely reviewed, not modelled.

1.8. PUBLICATIONS DURING THE STUDY

Conference papers:

- Ngancha, P.B., Kusakana, K. and Markus, E.D., 2018, October. Optimal Pump Scheduling in an Open Reservoir Water-Treatment Incorporating Evaporation and Seepage Effect. In *2018 Open Innovations Conference (OI)* (pp. 102-106). IEEE.

Journal articles:

- Ngancha, P. B., K. Kusakana, and E. D. Markus. "Energy Management Methodology for Sustainable Water Development and Servicing, Considering the POET Based Concept." In *Journal of Physics: Conference Series*, vol. 1577, no. 1, p. 012043. IOP Publishing, 2020.
- Ngancha, P. B., K. Kusakana, and E. D. Markus. "Energy savings configuration for a water-pumping system. " *International Journal of Smart Grid and Clean Energy* 9 (2022):805-812.
- Ngancha, P. B., K. Kusakana, and E. D. Markus. "Optimal pumping scheduling for municipal water storage systems." *Energy Reports* 8 (2022): 1126-1137.
- Ngancha, P. B., K. Kusakana, and E. D. Markus. "Timer switching control applied to a water pumping system". *Accepted.*
- Ngancha, P. B., K. Kusakana, and E. D. Markus. "Flood switching control applied to a water pumping system". *Submitted.*

1.9. THESIS LAYOUT

This thesis has been divided into six Chapters, with the main research results being presented in Chapters 3 to 5.

Chapter 1 presents an introduction to the thesis, which introduces the background on the research study, the problem statement, aims, objective, methodology, contributions to knowledge, hypothesis, as well as delimitations of the study.

Chapter 2 outlines the major water-pump energy management steps in a bulk-water purification system and provides a complete overview of current control strategies in water pumping energy management activities. The review is led by the POET concept, which

includes a review of current water pumping technologies, as well as advancements, ideas, evaluations and improvements.

Chapter 3 describes the modeling of the flood switching control, which will further be used as a baseline for comparison of all the methods that will be developed in this work. The system takes into account the effects of evaporation, rainfall and seepage; to control the pumping operation of a water facility, it uses the flood switching principle. The SCIP Optimization solver in MATLAB OPTI toolbox software was used to implement the generated model.

Chapter 4 analyzes the simulation results of the developed timer-setting control model. The performance of the suggested electrical timer switching control system when applied to firstly a fixed motor pump and, secondly, when applied to a VFD control motor pump. The results are compared to the baseline flood switching control system to estimate the economic benefit of the created model. Evaporation, rainfall and seepage losses, were all elements that were taken into account.

Chapter 5 discusses the created model's simulation results. Application of the proposed optimal switching control system, to a fixed motor pump performance and, on the other hand, when applied to a VFD control motor pump. The results are compared to the baseline flood switching control system, to estimate the economic benefit of the generated model. The influence of evaporation, rainfall and seepage losses are all factors that were considered.

Chapter 6 presents the techno-economic analysis of the proposed control system. Evaluating the energy savings and lifetime costs of the proposed timer control, VFD-timer control, optimal control and VFD-optimal control water pumping systems, in comparison to the baseline, for the same operating conditions.

Chapter 7 presents the conclusions of the findings and makes recommendations for future research in the field of water pumping control technology.

CHAPTER 2: LITERATURE REVIEW

2.1. INTRODUCTION

In this Chapter, the available literature published, related to the energy efficiency in the water pumping system, is reviewed and discussed. The studies are related to performance, operation, equipment, or technology efficiency of water pumping systems. The review Chapter structure is as follows: In Section 2.2, the overall system operation is described, with the main components of the water pumping processes highlighted; in Section 2.3, a review of the pumping system energy management is presented; and in Section 2.4, the POET literature on water pumping energy management systems (EMS) is summarized. Section 2.5 presents the POET analysis for energy management systems. Section 2.6 outlines a review of control methods used in the water pumping system. The review's principal findings and recommendations, are summarized in Section 2.7. The Chapter is summarized in Section 2.8.

2.2. PROPOSED SYSTEM DESCRIPTION

The general configuration of the proposed water-pumping system is shown in Figure 2.1. The setup has three sections, starting with the grid supply, which is the main power source that the system receives from the municipality. The grid supplies a three-phase electrical energy to the water pump via a controller, which controls the pumping schedule of the pump, according to the tariff structure ToU energy cost.

The main source of water, for water catchment, is a dam. Therefore, electrical pumps are used to pump water from the Dam to the reservoir, during the pumping operation, the pump 1 unit elevates the water from the dam (river), to the main water reservoir, while the pump 2 unit services the storage tank at the top of the hill. The purpose of placing a water

storage tank higher is to allow for the water to be released (dispersed) to the end-user using gravity [26].

Figure 2.1, further shows the various exogenous variable, such as the rainfall, evaporation and seepage that affect the water pumped volume and level in the reservoir, depending on the amount of rain received at a given time interval, the water level will increase and therefore, the need of water pumped from the dam will decrease. Evaporation, on the other hand reduces the amount of water in the reservoir and will lead to more water pumped into the reservoir. Adding to the seepage that occurs, water leaks, as a result of a pipe burst or a broken pipe while transporting water from one level to another. Considering this, a model is being developed that takes into account these many aspects of the water pumping system, in order to optimize the pumping system.

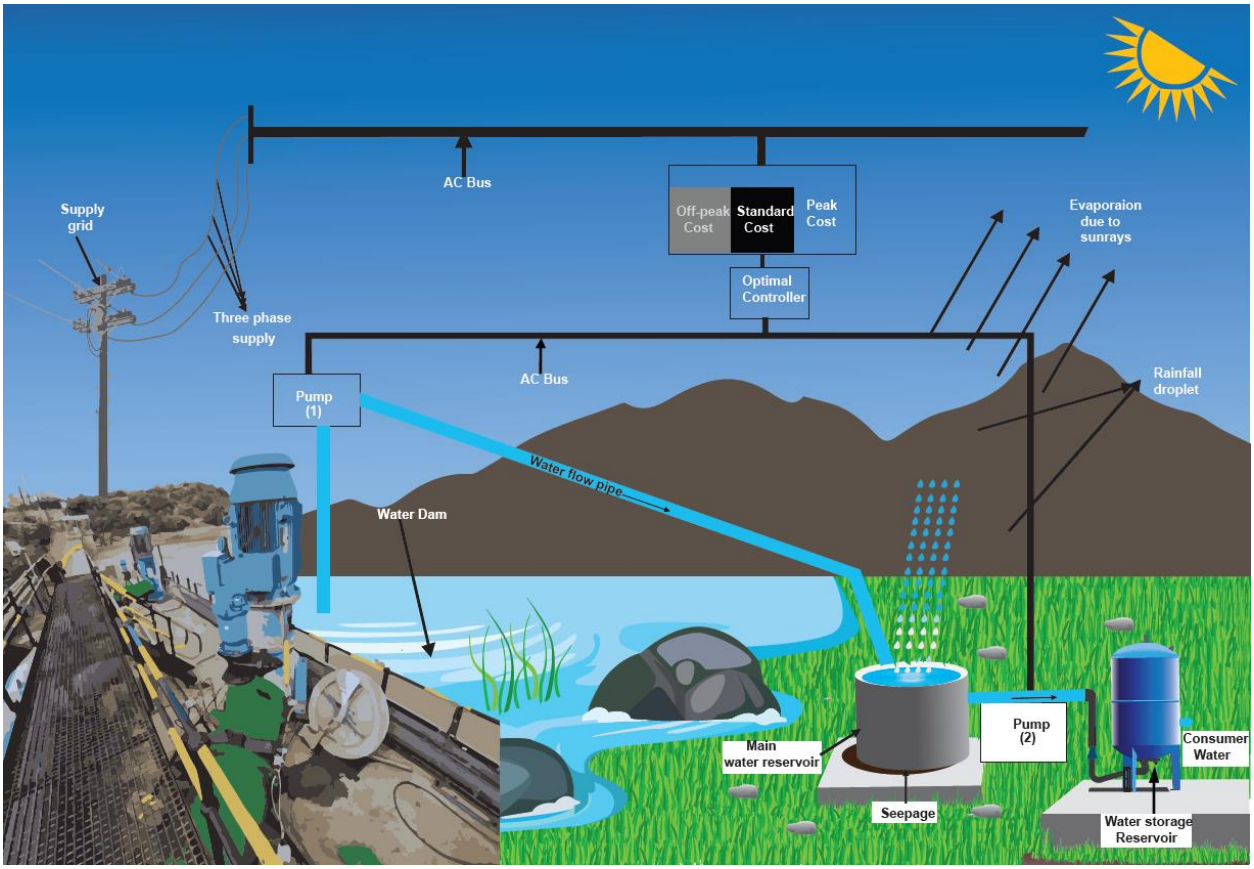

Figure 2.1: Proposed water pumping system schematic

2.3. REVIEW OF THE PUMPING SYSTEM'S ENERGY MANAGEMENT

The advancement of energy management technologies, has prompted several conventional high-power-consumption businesses to reconsider their strategies. The water-treatment plan pumping system is one of them and it consists of numerous pumping phases. The water harvesting and purification procedure, includes pumping this water through a series of steps, such as water screening, straining, corrosion inhibition, pH balance, dental health, coagulation, flocculation, sedimentation, filtration and disinfection, as well as storage [27, 28].

Pump systems are complex operative systems in industrial applications and, as a result, they should be taken into account when making energy-saving decisions. Many options are examined for energy management in pump systems, according to Ormsbee and Lansey, such as employing renewable energy sources to subsidize the conventional energy supply and, on the other hand, using control mechanisms to lower the energy consumption cost [29].

Gopal et al., looked on the advancements in renewable energy source water pumping systems. The comparison of several renewable energy water pumping systems and their limitations is the most appealing aspect of this review. It was concluded, by recognizing the significant reduction in traditional energy sources, as well as the environmental benefits of using renewable energy sources in pump systems [30].

The idea of the hybrid energy system, according to Ramos et al., is to merge a number of energy sources to reduce energy demand from the utility grid, by giving precedence to renewable energy supply and compensating during volatility between sources [31].

Tawanda works on an effective pump-scheduling model for a reservoir water pump system in another submission. Electricity costs are lower at night than during the day under this arrangement. To determine which pump combination is turned on and at what hour, linear programming is used. The result reveals a switching sequence, that is combined, to obtain the optimal output capacity [32].

Reca et al., employ the linear programming approach (LP), to establish an optimal pumping schedule in a water reservoir, taking into account the effects of evaporation and the different price structures of electrical tariffs. The study created a pumping policy for the water distribution system, that takes evaporation losses into account [33].

It is vital to emphasize the difficulties that other academics are working on and their potential solutions, in order to proceed with the energy cost optimization of a water pumping system. Different restrictions that impact the water-reservoir pumping system, such as the effect of rainfall, the evaporation, seepage effect and head losses in the water pipes, are given a larger analysis.

The operation of a water pumping system, is a challenge that has been emphasized by numerous studies. An improved operation control scheme, may result in less energy usage.

In an ideal world, an electrical pump is required to transport water from one location to another. Nevertheless, the usage of pipes to transport water from one stage to another, as well as the alleged water losses, due to leaks or evaporation, may all contribute to a high consumption rate [34, 35 and 36].

It is critical to look at the many research, that involved the water harvesting/pumping system, in order to appropriately coordinate the four key pillars that interface with the POET concept, in relation with water pumping. The literature that relates to the POET concept on water pumping and energy management, is presented in the next section.

2.4. POET RELATED LITERATURE IN WATER PUMPING ENERGY MANAGEMENT SYSTEM

POET establishes a comprehensive framework for energy management. Performance efficiency (P), operation efficiency (O), equipment efficiency (E) and technological efficiency (T), are the four components of energy efficiency in POET. Technology efficiency is defined as the ratio of useable work performed in energy conversion. These comprise of processing,

transmission and utilization, with natural laws as a constraint. Operation efficiency is evaluated, by considering the appropriate coordination of various system components. Equipment efficiency is a measure of an isolated piece of energy equipment's energy output, in relation to its technological design specifications. An energy system's performance efficiency is a measure of energy efficiency, that is defined by deterministic external system variables, such as production, cost, energy sources, environmental impact and technical indicators, among others [37, 38].

The literature regarding energy management, using the POET based characteristics in terms of the water harvesting/pumping field, specifically energy efficiency. Wanjiru and Xia looked at energy and water optimization of typical systems, such as rooftop harvesting systems. Their research is based on the capturing of rainfall water for garden irrigation [39, 40]. Zhanbo et al. analyzed and compared the energy storage devices that aid in producing the most efficient output, in terms of their differed coordination [41]. Matsubayashi et al. work on the energy management systems that provide information on energy serving recommended equipment. The theory is archived by calculating and comparing the power consumption estimates based on the various equipment information [42]. Sallem et al. presented an intelligent algorithm, based on the fuzzy rules that make a decision on the interconnection, an instance of photovoltaic installation components. The result shows an improved operating time for more than 5/hours [43].

These works are fundamentally within the category of energy efficiency, however, the adopted approach and vision are not systematically cascaded, to obtain a common goal; thus, they are a challenge to interpret. In view of the above challenge, this section aims at developing the systematic water developmental energy efficiency mechanism for water catchment purposes. However, it recognized the established research framework; specifically, the developed POET (Performance, Operation, Equipment, Technology) energy management framework [38].

2.5. POET BASED ENERGY MANAGEMENT EFFECT

2.5.1. Energy efficiency effect relating to performance

The performance efficiency, in this case, will focus on the environmental effect, the effect of evaporation in water transformation and technical indicators [38].

2.5.1.1 Evaporation effect

The issue of water losses in an open reservoir as a result of evaporation, is a serious concern. This is emphasized by Shalaby et al., who mention 50% water losses in reservoirs, due to evaporation [44]. Supported in another article by Saggai and Bachi, who describe Algerian experience in water reduction owing to the influence of evaporation, adding to the reality that the country is located in a water-scarce environment [45]. Condie and Webster, research the details of the numerous variables that affect evaporation rate and provide evidence of how evaporation changes occur [46]. Benzaghta and Mohamad, studied evaporation in an open reservoir and several methods of reduction. Physical and chemical reduction strategies are discussed in this review. The chemical cover is based on the use of long chain alcohols, to generate a thin layer on the water surface, whereas, the physical approach involves the application of a floating cover as a protecting portion of the water surface. The research findings reviewed that physical approaches may efficiently reduce evaporation without causing environmental harm, whereas chemical treatments have a negative impact on water quality and solely reduce evaporation by a tiny margin [47].

Martinez-Granados et al. assess "the economic impact of evaporation losses from great dams (GDs) and on-farm agricultural water reservoirs (AWRs) in the semi-arid Segura River basin, SE Spain". Evaporation losses were computed using Class-A pan evaporation data and pan coefficients in their approach and their economic impact was examined, using an

economic mathematical programming model, that replicates land and water allocation in the basin's various irrigated zones. Annual evaporation from GDs and AWRs, accounts for 8.7% of the water, currently available for irrigation in the Segura basin, according to their findings. The economic impact of such losses is projected to be a 6.3% decline in the value of agricultural produce and a 5.4% fall in farm net margins [48].

Mousavi et al. worked on improving a pumped hydro storage system, by taking into account the influence of evaporation. Their model aims to reduce the large inaccuracy, in by calculating the stored energy, taking into account the essential factors. To begin, all losses caused by the pump, pipes and fittings, are calculated. Thereafter, the volume of water in the upper reservoir is then calculated using a water balance approach, that takes into account inflow, outflow, precipitation and evaporation. To conclude, the turbine power is computed as a function of reservoir water levels, taking into account turbine, pipe and fitting hydraulic losses. A physical system's experimental results are used, to validate the provided model. The model's accuracy is compared to that of further well-known models. The findings show that the suggested approach reduces the estimated stored energy inaccuracy, from 13.17% to 0.74% [49].

Given that evaporation is a complex issue that affects the reservoir's water volume, understanding the numerous factors that influence the occurrence of evaporation, may aid in establishing the real evaporation volume. The various factors that influence the rate at which evaporation occurs, are shown in Table 2.1 below.

Table 2.1. Factors affecting the rate of evaporation [50, 51, 52 and 53].

Factors	Influence on evaporation
Force of attraction	A greater force of attraction will result in a less rate of evaporation
Temperature	An increase in temperature causes the kinetic energy of molecules to increase, allowing more surface molecules to overcome the force of attraction and leave as gas. (The kinetic energy of the molecules is proportional to the temperature.)
Surface area	When there is less surface area, fewer molecules leave as gas and when there is more surface area, more evaporation occurs.
Wind	More molecules escape from the surface area as the wind speed increases, resulting in a faster rate of evaporation.
Humidity	The amount of water vapor in the air is known as humidity. As the humidity in the atmosphere rises, so does the amount of water vapor in the atmosphere. As a result, the rate of evaporation is reduced.
Nature of liquid	This has to do with fluid viscosity and density. Density refers to the space between the particles of a fluid, whereas, viscosity relates to its thickness or thinness. Temperature, which affects the rate of evaporation, has an impact on both attributes.

The above factors depend on geothermal conditions, which, in most cases, are influenced naturally. However, the surface area may be controlled in the case of water processing systems. The overall observation, in terms of performance efficiency, reviewed that evaporation losses in water reservoir create a deficit in water volume and it is as a result of a number of factors, listed in Table 2.1. However, solely the surface area could be considered

as a variable that could be controlled, whereas the others are dependent on the natural hemisphere. The study recommends that future construction of a water reservoir, or storage tank, should be constructed in a semi-conical shape. This should further reduce the rate of wind speed to the water surface.

2.5.1.2 Reservoir and transmission pipe leakages effect

According to the review by Puust et al., water leakage studies are divided into three subcategories: leakage detection methods which primarily aim in detecting leakage hotspots, leakage control models aim at effectively controlling current and future leakage levels and leakage assessment methods, which aim to quantify the amount of water loss [54]. In a further study, conducted by Hunaidi et al., water pipe losses are classified in the area of transmission and distribution pipes leakages [55]. This study, focuses on estimating the amount of water lost, as a result of a pipe rupture or further water transmission channel losses, as well as the impact on reservoir water volume.

The water sector reported that merely 76% of treated water reaches the consumer, a level considered unacceptable by the regulator [56]. Underground pipes are used to transport urban water on a regular basis. El-Zahab and Zayed, on their review of leak detection in water distribution networks, indicates that water transmission pipelines lose 20% to 30% of the water that flows through them on a regular basis and in older systems, particularly those that have been subjected to poor maintenance, the figures may rise to over 50%. Using "visualization tools VOSviewer and CiteNetExplorer", they were able to determine that there are two types of leak detection systems: static leak detection systems and dynamic leak detection systems. Finally, in order to provide a general overview of the leak detection sector, this article includes a summary of popular leak detection systems [57].

Another study by Bond et al., used a non-destructive condition assessment technology, to develop a method for determining the exact location and magnitude of leaks in large diameter (12 inch (300mm) and above) water transmission pipelines. The system is inserted

into a live pipeline, through any 2 inch (50mm) tap. The tethered sensor head, carried by the flow of water, may further traverse up to 6,000 feet (1,850 meters) down the pipe per survey, notifying the pipeline operators of each leak, as it is discovered. Using this technology, an average water loss of 57,000 gallons per day, per mile surveyed (134,000 liters per day per kilometer surveyed), was avoided [58].

Given that, this study focuses on leakages that occur around the water treatment area, as shown in Figure 2.1, and that leaks that occur within these facilities are easier to identify, according to the review, and may be repaired in a short period. This work takes the position that the leaks are significantly small tiny or non-existent.

2.5.1.3 Reservoir seepage effect

Seepage is the passage of water from the upstream side of the reservoir/dam, to the downstream side, via a foundation or base embankment. Seepage occurs when water slowly filters down through an earth fill dam's foundation and the dam itself [59]. Omofunmi et al. research on the types, conditions and causes on seepage in the earth dam. They began by describing the many forms of earth dams, including “homogeneous embankment, zonal embankment, and diaphragm embankment”. The author mentions the following possibilities, when discussing the different seepage situations:

- Water level drops rapidly, or falls below what is anticipated with general use (sudden drawdown condition),
- The moist areas and aquatic plants (such as cattails), beneath the dam.

The potential causes of seepage, are identified as: rodent holes, rooted tree roots, effects from piping, internal erosion, internal pressure/suctioning/saturation, uplift, heave and blowout [60].

Oblinger et al. worked on “A pragmatic method for estimating seepage losses for small reservoirs with application in rural India”, using a technique called "monte carlo analysis", to

measure the degree of uncertainty in the total volume of water that was contributed to the subsurface. The Monte Carlo simulation, revealed that the available data could limit subsurface reservoir losses, however, that additional observations are required to regulate reservoir inflows. The research estimate of seepage from the reservoir, is 3.5 times more than the expected recharge volume, when solely considering reservoir volume changes. This finding indicates that, when reservoir inflows are not explicitly included in models, water influx, as a consequence of the precipitation effect, may be greatly underestimated [61].

In another research by Yu et al., an investigation of the seepage, deformation and stability of clay and sand slopes, with varying permeability anisotropy properties that are influenced by reservoir water level changes, is presented. The "SIGMA/W and SLOPE/W" modules in Geostudio, are used to carry out the numerical simulation of Caipo slope, under the drawdown of the reservoir water level and the anisotropy ratio, as well as the anisotropy direction. Results show that the soil's ability to absorb water, is reduced by the anisotropy ratio and anisotropy direction, which raises the infiltration line's hysteretic height and maximum horizontal displacement, and lowers the minimum safety factor[62].

The many reviews have aided in understanding how seepage affects water reservoirs and have further highlighted the various factors that may contribute to seepage. The reviews show that these aspects of water loss are significant, considering the amount of water lost. To ensure the dependability of the water supply to consumers, care should be taken, when modeling the pumping water ratio to the reservoir.

2.5.2. Energy efficiency effect relating to the operation

Operation impact, in this case, relates to the time at which pumping should take place, which is informed by various factors, such as the electricity tariff structure of the locality, as well as the water demand alteration (load flow diagram).

In South Africa, just as in many other countries, electricity cost varies with the type of tariff structure it has adopted. Table 2.2 details the pricing tariffs utilized by several countries around the world, based on various category structures [63].

Table 2.2. Types of electricity tariff [63, 64].

Tariff Category	**Descriptions**
Simple rate tariff	A fixed rate is applied for each unit of the energy consumed
Flat rate tariff	Unchanging charge that allows the user to consume up to a maximum amount.
Two-part tariff	Electrical energy is charged on the basis of maximum demand (MD) of the consumer and the units consumed
Block rate tariff	When a given block of energy is charged at a specified rate and the succeeding blocks of energy are charged at progressively reduced rates
Maximum demand tariff	Maximum Demand Tariff consists of two parts, i.e. demand charge and energy charge. The demand charge is based on the maximum demand in kVA, while the energy charge depends on the energy consumption in Unit (kWh) of that period
Power factor tariff	The tariff in which power factor of the consumer's load is taken into consideration
Three-part tariff	When the total charges to be made from the consumer is split into three parts, fixed charge, semifixed charge and running charge

In South Africa, electricity cost varies with the time of use of the day, alongside the period of the year. Electricity time-of-use (ToU) tariffs, the pricing tariffs used by South African electrical utility (Eskom), has been adopted in this study, according to the various pricing structures [64]. The Gentlex ToU tariff scheme is used for customers who consume energy supplied by Eskom. The tariffs are divided based on two seasons, alongside the periods of the day. It is observed that using electricity during the peak period may cost more, as opposed to the off-peak periods, whereas the high-demand season may charge more than the low-demand season. In the case of water supply, load flow describes (or informs) the evolution of the changes in water demand in a specific period (or time). It is critical to evaluate the system capability to adequately supply the load, while staying within the appropriate energy consumption range.

According to the ToU tariff structure adopted by Eskom and based on the operating efficiency, it is recommended that pumps should be operated during the off-peak periods, since the cost of electrical energy is relatively more affordable.

2.5.3. Energy efficiency effect relating to equipment

In this category, measuring the energy out of the different individual output equipment and their unique technological design, is an emphasis on the utility pump. The overall operating principle of a water pump system may be seen towards the application of "Boyle's law", that elaborates on the relationship by using the following quantities: pressure, volume and temperature [65]. Electric pumps are known for their ability to effect a change of movement in fluid, solid and gas. Pump systems technology has grown over time, from the manual actuator, to various forms of energy controllers [66, 67]. Table 2.3 shows the various categories of pump groups, their principle of operation, mechanisms of pumping, possible multiple stages, advantages and disadvantages.

Table 2.3. Pump grouping, operating mechanism, advantages and disadvantages.

Pump group	**Operation types**	**Pumping mechanisms**	**Multiple Stages**	**Advantages**	**Disadvantages**
Positive displacement pumps	Reciprocating	Piston [68]	Yes	- Performance at low speeds. - May achieve greater pressures at low flow-rates. -No internal leakage Smaller hydraulic shock pressure spikes. - Long service interval. - High accuracy.	- Pulsed output. - Higher sheer on pumping stroke. - Cannot dry run. - Not efficient with particulates.
		Plunger [69]	Yes	- High reliability. - Easily controlled by stroke adjustment or variable speed. - May develop high pressure in a single stage.	- Slow speed operation. - Lower flow rates. - Costly in large size.
		Diaphragm [70]	Yes	- Self priming. -Variable speed and pressure. - Handle slurries and solids. - High viscosity handling. - High suction life capacities.	- Non- constant flow. - Vibration. - Inlet pressure limitations. -Acceleration head.
	Rotary	External Gear [71]	Yes	- High speed. - High pressure. - Quiet operation. - Variety of building material operations Complete rotary motion. -Easily control speed. - Easily control	- Bushings wear in liquid areas. - Fixed end clearances.

				direction.	
		Internal Gear [72]	Yes	-Smooth/pulseles flow. -Slightly more horsepower for size.	- Higher cost. - Limited size range. - Low to moderate pressure ratings. - Few sources of manufacture.
		Lobe [73]	Yes	- Ability to handle medium sized solid particles in the pumping fluid -No metal-to-metal contact -Long term dry run (with lubrication to seals) -Non-pulsating discharge	- Low pressure. - External gears. -Reduced lift with thin liquids
		Vane [74]	Yes	-Low viscosity fluids at high pressures. - Dry run for short periods. -Develops acceptable vacuum.	- Complexity. - Unsuitability for high pressure. - Does not run high viscosity fluids.
		Peristaltic [75]	Yes	- Good flow ranges. - Liquid contained in tubing suction lift. - Dry running. - Good chemical compatibility.	- Tubing is a consumable. - Flow rate and pressure limited by the tubing.
		Screw /Progressive cavity [76]	Yes	- Metering accuracy. - Higher viscosity liquids. - Volumetric efficiency	- Larger number of moving parts. - High maintenance.

				(lower power and more flow). - Low shear.	- Larger footprint.
Dynamic/ Centrifugal pumps	Impeller construction	Radial flow [77]	Yes	- No leakages in fluid. - Last longer. - Less maintenance. - Pump and motor are apart from each other hence no heat transfer is possible. - Less friction.	- Energy loss because of coupling. - Chances of coupling slips due to intense loads. - Low flow may lead to overheating of the pump.
		Axial flow [78]	Yes	- Wide range of pressure, flow & capacities - Fewer moving parts - No excess pressure build-up - Produce high flow rates necessary for industrial applications	- Not well-suited for high-pressure applications - Do not handle high-viscosity fluids well - No suction lift capabilities
		Mixed flow (part radial, part axial) [79]	Yes	- Initial and maintenance cost are comparatively low -Their size is compact and may be installed in limited space -Their mechanism is simple. Less skilled labour is required for its operation and repairs. -May be operated with high speed electric motors, or gas engines and steam turbines -Discharge is steady and non-pulsating	-Requires priming. -For higher head, efficiency is low. -The discharge pipe should be provided with a check valve, to avoid the backflow when the pump suddenly stops due to power failure. -Discharge varies with the

				-May be used for pumping water containing silt, sand etc. -Durable and safe against pressure.	head of water. -Their ordinary suction lift is limited (about 6m or so).

A Positive displacement pump causes fluid movement, by trapping a fixed amount of the fluid and providing a certain force, in the form of kinetic energy that trapped volume into a discharge pipe (or discharge system). On the other hand, dynamic pumps produce additional kinetic energy to the same flow at a given speed (RPM), regardless of the discharge pressure [80, 81 and 82]. An efficient understanding of pump selection should be provided when selecting a pump and for the particular application.

Another form of equipment that is prevalent with water pumping, is an electric motor. The motor efficiency has an impact on the energy efficiency of pumping. The applicability of common electric motor types, to an industrial pumping system, is examined by Ahonen et al., their research compare the motor efficiency characteristics and analysis on how motor efficiency and sizing, impact the energy consumption of the resulting pumping system, with a typical load profile. The purpose of their research, is to offer recommendations on motor sizing, so that the majority of energy-efficient alternative, to the specified pumping system, will be chosen [83].

Burt et al. perform an investigation into how well motors perform, when subjected to different loads and speeds (caused by a variable frequency drives (VFD) controller). Additionally, to provide designers with sufficient information, to calculate the total amount of power used by the pumping system, when it is controlled by a VFD. VFD control motors, were tested and the readings measured across the supply line and VFD. When compared to a correctly built, full-load system, the result shows that the efficiency of an electric motor pumping system with a VFD may be, on average 8% less efficient. However, as VFDs may effectively modify speeds to match those conditions and, thereby, save energy overall, the 8% could be made up, in terms of energy costs [84].

Trianni aet al. presented an overview of electric efficiency measures (EEMs), for electric motor systems (EMS), based on scientific and industrial literature, by stressing their qualities and

advantages for productivity. EEMs are presented on their review, in accordance with four key categories: hardware, motor system drives, plant management of motors and power quality. According to their conclusions, the classification is useful in assisting research into the creation of a new framework, to reflect the primary variables influencing the adoption of EEMs for EMS. Additionally, it may aid in locating and quantifying the productivity advantages for such EEMs. Finally, it may produce a useful instrument, that offers many viewpoints to industrial managers, technology suppliers and industrial policy makers, as decisions are made [85].

By guiding the understanding in this area of motor efficiency, a standardised system has been put in place by the National Electrical Manufacturers Association (NEMA) and International Electro-technical Commission (IEC), by classifying the various motors and arranging them, according to their various characteristics[86, 87]. When comparing their classification of motor efficiency, it may be seen that the higher power rated electric motors have less variability in efficiency. Since the motors used in water treatment pumping facilities have large power ratings, it may be concluded that the efficiency effect in choosing an electrical motor, is not a major issue. When employing their classification table, the most effective equipment is supported by equipment efficiency.

2.5.4. Energy efficiency effect relating to technology

Modern technology in energy resources edifies on how important and affordable renewable energy could be in our daily life [88, 89]. However, the many challenges involving the renewable sources warrant a different approach towards its application. Hence, the introduction of the hybrid system in pump stations for the pumping of water is of viable significance. Gopal et al. present an intensive "review on renewable energy source water pumping systems (RESWPSs)". In this review, the energy sources were categorized into five major groups. The author in his article acknowledges the importance of combining these sources, obtaining a more affordable and stable energy supply to the pump. Therefore, it is concluded that the renewable energy sources play an important role in reducing the energy drawn from the conventional energy source [90]. Xia and Zhang provided a new perspective

on achieving technical efficiency, in the sense of technological innovation, which frequently challenges older technologies, by pushing scientific boundaries. Their method is demonstrated by regulating a heavy haul train and it is found to be promising in dealing with all aspects of energy efficiency [91].

In the case of a water pumping system, the concept of incorporating new technology and choosing the best option for integrating diverse technologies into a pumping application, will result in the greatest possible energy savings and perfect energy management performance.

2.6. CONTROL METHOD USING POET

A variety of management techniques have been used in the recent past, to manage the level of water contained within the tank. To increase pump efficiency, Zhang et al. established an ideal pump sizing model, based on energy efficiency classifications, by regulating the pump's functioning, using a closed-loop model predictive control technique. Their models demonstrate that the pumping system energy efficiency study may be classified, according to system performance, operation, equipment and technology (POET). By balancing the contributions of load shifting and energy efficiency during operation, this control technique shows the reduction in energy cost [92].

Moreira and Ramos studied the "Fátima" water supply system in Portugal. To find the most effective operation point, various pump characteristic curves were examined and modeled. The major objective, was to identify which pumps and what daily scheduling permitted the greatest economical solution; in comparison to a manual override technique, a genetic algorithm optimization included in the modeling program, was taken into consideration. At the end of the analysis, a 43.7% reduction in the initial daily energy costs, was possible. This was accomplished by adding higher quality pumps and configuring them to operate in an intelligent manner [93].

Tang et al. applied an integrated method to the general optimal control problem of pumping stations, to create an optimal control problem, that takes into account pump switches and an optimal control problem that further, takes into account a cumulative operating time. The newly formulated challenges are resolved, using the particle swarm optimization technique, using a case study of an intake pump station. Their findings demonstrate that, load shifting and energy efficiency, may both be accomplished using the optimal control strategies, The optimal control strategies, may save approximately 30% of your energy costs. The majority of the savings are produced, by changing the pumps' time-of-use (TOU), tariff-based operation status [94].

After understanding about the background of the POET concept, applied to the area of energy management in a water pumping system. This section will mainly deal with how to apply the operational tool "O" in POET, to manage the energy usage in a water pumping system. However, the operation will depend on the specific technology, that may require different equipment, which, in the end, will produce a set performance [95]. This study proposes four control techniques used in reducing energy consumption in a water pumping system, which include:

- Flood switching control; indicates the water level at the top and bottom of the reservoir,
- Timer switching control; operates using the pump's programming switching schedule,
- Optimal control; works in real-time switching scheduling of the pump,
- Timer switching control incorporated to a VFD power controlled pump.

2.6.1 Flood switching control

Flood switches control the top and bottom level of water in the reservoir. There are three types of float switches: internal counterweight, which floats on the liquid, external counterweight, where the counterweight is positioned at a preset height and without

counterweight, where the switch is installed without a counterweight in the tank or basin using, for example, try-raps [96, 97]. Bakheet uses a microprocessor to regulate the fluid level in a tank. The system communicates information to the microcontroller through flood switches, which, in turn, send a signal to the driver to start or stop the pump. The results demonstrate the efficacy of a flood switch in turning ON and OFF the pump when the water level rises above (or falls below) a predetermined level [98].

Debenedictis et al. present an overview of controlling the operational energy-efficiency improvement in water pumping [99]. In this research, the authors review the flood switching control method applied to a water pumping system. Ahmad and Atikol presented a modified water level control scheme, based on float switching, in which they developed a model that allows the pumping of underground water, based on the upper flood switch when the water level drops by 5% to refill the rooftop tank during the off-peak period and, by 30%, during the peak period. When compared to model predictive control (MPC), their approach saved nearly the same amount of energy. However, utilizing the flood switch method, would have avoided the high processing capacity and a sophisticated analog feedback level sensor [100].

2.6.2 Timer-setting control

Timers have long been in existence and are classified into analogue and digital timers. Their main function is to provide timing control to a number of electrical system operations. In this research, we shall base our selection on a digital timer, which usually comes in compact sizes and incorporates a three-digit LCD display, has a programmable timing range and supports high load control systems and is a weekly programmable timer. It contains 20 ON/OFF timer settings and is a relay-type of timer; it provides automatic and manual mode. [101, 102].

Timer switches are divided into two types: OFF-delay and ON-delay, based on the operator's switching settings, delays the operation for a predetermined amount of time. Pavushetti et al., work on a solar powered water pump for irrigation purposes. In this setup,

the electrical pump is turned ON and OFF by an electronic timer. The results show that a reliable PV energy may be generated for irrigation purposes, by using battery storage in a solar system and scheduling the pump period, with the use of a time switch [103].

Getu and Attia, research on controlling an agricultural pump based on soil moisture sensing and timer. The timer program is set for the period of pumping during the pump ON time, and sensors are used to determine the moisture content of the soil before turning the pump ON/OFF. The result shows great enhancement of crops, saves energy and provides appropriate water management. [104].

2.6.3 Optimal control

Optimal control is the process of minimising the energy consumption of a dynamic system by determining the control and state trajectory over a setting period [105]. To schedule the water pumping in a water distribution system, an open-loop optimal control system is formulated, with the understanding that priority is given to the periods when grid energy is considered at its lowest cost (off-peak) or second lowest cost (standard) and the peak tariff energy cost is not used. Unless, under the very tired conditions, when the load demand is so high in such a way that the off-peak and standard energy costs are insufficient to meet the load demand. This decision shall be informed by the real-time data collected from the various measuring (instrument) sensors, located at the outlet of a water reservoir. The aim is to minimize the electrical energy drawn from the grid during the peak period and to maximize energy when the energy cost is relatively more affordable, to meet the demand of the pump-stations loads.

An understanding is drawn from Bagirov et al. research, who uses a technique known as the "Hooke and Jeeves direct search approach". The method iterates between the optimization model and the hydraulic simulation model "EPANet", until the ideal solution is identified. In order to identify the ideal cost minimization in a pumping system, the system uses uncertainties, such as polyhedral and ellipsoidal [106]. Another application by López-

Ibáez, employed "Ant colony optimization (ACO)", to manage pump energy consumption, by arranging pump running periods, based on electricity costs. The outcome demonstrates improved savings, when compared to others who used a simple evolutionary algorithm, based on the binary representation [107].

A variable speed pump (VSP), runs at multiple speeds; they adopt the principle of variable frequency drive (VFD) to control the electrical motor that drives the pump. VFD works by adjusting the frequency of the motor by adjusting the revolution per minute (RPM). Shankar et al. concentrate their review on VFD control strategies for improving pumping system efficiency. In addition to the control approaches, this article covers component selection and system dimensioning. It reveals that a VFD provides better chances for energy savings than component selection and dimensioning of the pumping system [108].

2.7. KEY FINDINGS AND SUGGESTIONS

2.7.1 POET analysis

After reviewing the main available publications on the POET energy management framework in the area of a water pumping system, it is reviewed that the POET energy management framework is an effective tool for evaluating and improvement in water pumping system.

This Chapter analyses and highlights the key areas of emphasis, in terms of water and energy efficiency, regarding sustainable water development and servicing. It stretches the preferred approach, in terms of energy reliability and managing efficiency, drawing from the POET concept:

- The overall observation in terms of performance efficiency reviewed that, evaporation is a result of a number of factors, listed in Table 2.1. However, solely the

surface area could be considered as a variable that could be controlled, whereas, the others are dependent on the natural hemisphere. The study recommends that future construction of a water reservoir or treatment plant should be constructed in a semi-conical shape. This should further reduce the rate of wind speed to the water surface.

- According to the tariff structure and based on the operating efficiency, it is recommended that pumps should be operated during the off-peak periods, since the cost of electrical energy is relatively more affordable. In addition, during the peak periods, the pumps may be switched off for cooling and maintenance.
- Equipment efficiency endorses the optimal equipment selected for a given task. In the case of a commercial bulk water pumping and focusing on the various pumps listed in Table 2.3, care should be given to the following factors, when selecting a pump: pumping mechanism, the possible number of stages, advantages of the pump as well as the energy consumption.

- In the case of a water pumping system, technological efficiency will embrace newly developed technology that is on the market and the combination of these technologies and the configuration of the different energy sources will aid in obtaining the most efficient energy savings.

2.7.2 Control system analyses

The review of the different control techniques to manage the pump operations, in terms of energy saving, is an integral part in this Chapter. According to the different reviews based on energy management, the following were observed:

- A flood switching control system applied in water pumping system has the ability to control the turning ON/OFF of the pump when the water level reaches the bottom and top levels of the reservoir. Its operation is similar to that of a binary switch. As a result, it has the limitation of not being able to determine the period during which

electrical energy is slightly more affordable, owing to the Eskom utility supply's ToU tariff structure. Consequently, the pumps are continuously running at any given time, consuming more energy.

- A timer switching control system is a pre-programmable control system, the programming is dependent on historical data collection, it works efficiently in turning OFF the pump when electrical energy costs are at their highest and turning ON the pump when energy costs are slightly lower. Furthermore, it takes into account exogenous conditions, such as rainfall, evaporation, seepage and pipe losses. However, its limitation is based on the operator information in the programing of the timer, which depends on the historical data. This form of control system is accurate, if the load demand remains constant.

- An optimal control system was chosen to address the difficulty of real-time load demand variations and the requirement that the pumps be turned ON/OFF solely when the cost of energy is deemed more affordable under the ToU tariff structure. In addition, it takes control of the external variables, such as the effect of rainfall, evaporation, seepage and pipe losses.

2.8. SUMMARY

Water harvesting and pumping are considered in an intensive survey mechanism, the following were the observations:

- A number of studies have looked at how to manage the energy consumption of pumping systems using a power supply type mechanism, where they looked at how to use renewable energy to supplement traditional energy sources.
- Available studies use principles like linear programming to manage pumping activities, based on the pump's scheduling intervals. However, in determining the pumping time, this research is limited to the ToU tariff period. Other variables, such

as evaporation, are taken into account in another application, however, they are treated as a constant factor impacting the reservoir's water level.

- The POET energy management framework has proposed matching cost-cutting measures. Based on the four pillars of the POET idea, the classification of the energy management concept is realized. The performance, operation, equipment and technological aspects of water pumping and storage plant activities, all affect energy consumption efficiency. The study indicated that the POET-based energy management technique has an effective coordinated energy-saving potential, allowing it to obtain the energy-saving opportunities of water pumping processes and laying the groundwork for a future water pumping project.
- Control systems have been utilized to manage the operation of water pumps in many of the studies mentioned in this Chapter. Several studies have used the flood switching control principle to control the water pump in a water pumping system, while taking changing load demand into consideration. The fact that various disturbances, such as rainfall filling the reservoir, evaporation, seepage and pipe loss, all affect the water level in the reservoir in a real-time dynamic environment, has been overlooked in their approach. As a result, the cost of energy use is quite significant.

Judging from the reviews, this study proposes to use an optimal control method, to control the pump in a water pumping system in a real-time changing load demand, while taking into account the changes in the reservoir water volume, that occur on a continuous time basis, due to evaporation, seepage and precipitation.

CHAPTER 3: FLOOD SWITCHING CONTROL APPLIED TO A WATER PUMPING SYSTEM

3.1. INTRODUCTION

In this Chapter, a model is developed to control the water pumping, based on the flood switching control system. This control system is constraining the pump to operate solely between two present water levels in a tank, using the same principle as a temperature thermostat.

As a contribution, exogenous variables, such as the evaporation as well as precipitation, that may influence the water level in the reservoir, are incorporated in the model.

This Chapter further establishes the proposed system baseline, in order to assess the water pumping system economic performance, under various control methods. The baseline is made up of the complete existing water pumping system, both with and without constraints. The baseline is simulated with the same model and input parameters.

A water utility company based in Bloemfontein, South Africa, is used as a case study. The load profile, reservoir size and pump size are all inputs to the model that was developed.

To assess the economic performance of the developed model, simulations for a 24 hour pumping cycle, using a flood switch control water pumping system, were used.

Simulations using MATLAB, are conducted, to assess the performance of the proposed model, which will then be used as a baseline for techno-economic comparisons with the other control methods, that will be developed in the subsequent Chapters.

3.2. FLOOD SWITCHING CONTROL SYSTEM MODEL

Figure 3.1 shows the flood switching control configuration. The water level in a reservoir (or tank) is determined by flood sensors, which are positioned at the top and bottom of the reservoir, to detect the upper and lower limits of water level. As the level rises or falls, the control switch (S_w) turns the pump on/off.

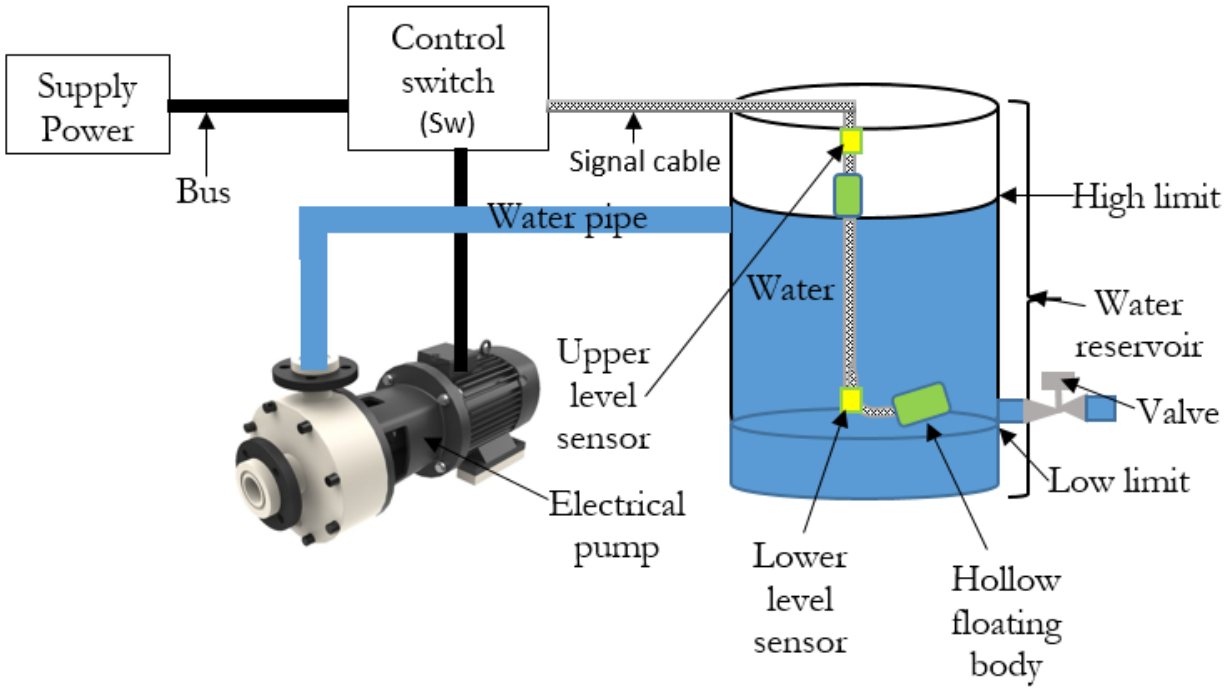

Figure 3.1: Proposed float switching control water pumped system schematic

3.3. MATHEMATICAL MODEL DEVELOPMENT

In this section, the flood control switching model was developed, taking into account, the demand, storage, as well as the exogenous variables influencing the operation.

3.3.1. Evaporation model

The evaporation may be modelled as the amount of water lost, changed into vapour, due to the effect of the sun, as well as the temperature at the surface.

The following are the methods by which evaporation occurs:

-Evaporation due to the energy balance principle (E_r) is proportional to the net radiation (R_n) and inversely proportional to the product of the latent heat of vaporization (l_v) and the density of water (ρ_w) [109, 110].

$$E_r = \frac{R_n}{l_v \rho_w} \tag{3.1}$$

Where: (R_n) is the radiation emitted and (R_i) the radiation absorbed

-Based on aerodynamic E_a(mm/ (day*m^2), which is how the wind moves the moisture away from the surface [111].

$$E_a = B(e_{as} - e_a) \tag{3.2}$$

Where: (e_{as}) is the saturation vapor pressure, (e_a) the ambient air vapor pressure and the vapor transfer coefficient (B).

3.3.2. Losses in pipes

Water losses in the pipe are a contributing factor to a lower reservoir water level and they have a negative impact on water volume stability in reservoir water level calculations, as this

water flow is not accounted for and does not serve the customers. As a result, these effects should be considered when pumping balances are made.

Pipes are the primary carrier of water and are subject to two types of losses: major losses (h_f) caused by friction and minor losses (h_b), caused by elbows and pipe bends, losses at the entry and exit of pipes and losses caused by valves and further fittings [112, 113]. As a result, the pipe loss (E_p) may be expressed as:

$$E_p \approx h_f + h_b \tag{3.3}$$

Where: (h_f) is the head loss due to friction and (h_b) losses due to pipe bend.

3.3.2. Rainfall model

Rainfall filling up an open reservoir, without the need for an electrical pump, reduces the operation time of the pumping system [114]. However, due to its natural occurrence, great care must be taken when regulating reservoir water volume, in order to ensure reservoir stability.

By multiplying the actual height of rainfall in the reservoir during that period (R_a) in meters by the cross-sectional area of the top section of the reservoir, the estimated volume of rainfall water (V_{R_a}) filling-up a reservoir may be derived.

$$V_{R_a} = R_a * A \tag{3.4}$$

Where: (A) is the cross-sectional area of the reservoir (m^2).

3.3.3. Seepage

Seepage is the slow escape of water from a reservoir through porous concrete material or small holes [115]. Because the seepage impact affects the amount of water in the reservoir, it should be considered when balancing the water in the reservoir.

The seepage quantity (q) per unit width may be expressed as follows:

$$q = Kh\frac{N_f}{N_d} \tag{3.5}$$

Where: (K) is the permeability (meters/sec.) of the material of the reservoir concrete; (h) the height (meters) of the water in the reservoir; (f) is the number of potential drops; and (d) the number of the flow channels.

The total volume of water lost due to seepage ($m^3/sec.$) is calculated as:

$$V_s = qL \tag{3.6}$$

Where: (L) is the length (meters) of the returning wall of the reservoir.

3.3.4. Pumped water volume

The electrical power (P_e) of a water pump used to pump water into a water reservoir is calculated by multiplying the mass (m) of water, the height (h) of elevation and the force of gravity (g), as a function of the time (t) that the electrical pump is turned on. As a result, the volume of pump water is determined by:

$$V_{P1} = \frac{P_e * t}{gh\rho} \quad (3.7)$$

Where: (ρ) is the density (kg/L) of water pumped into the reservoir

3.3.5.1 Load balance without the effect of evaporation, precipitation, seepage and leakages.

Considering a case where the constraints, such as evaporation effect, precipitation effect, seepage losses and pipe leakages, are ignored in the model. Therefore, the load balance calculation becomes:

$$\dot{V}s = \dot{V_{in}} + \dot{V_{P1}} - \dot{V_{load}} \quad (3.8)$$

Where: ($\dot{V_{in}}$) is the sum of the initial volume in the reservoir, ($\dot{V_{P1}}$) the water pumping-rate and the load demand ($\dot{V_{load}}$), is equal to the change in volume at the reservoir ($\dot{V}s$).

As the pump runs at a constant speed, the flood switching control may be modeled as a binary switch, which controls the pump ON/OFF switch. As a result, as illustrated in Equation 3.8, the load balance may be written as:

$$\dot{V}s = \dot{V_{in}} + (\dot{V_{P1}}) * S_w - \dot{V_{load}} \quad (3.9)$$

Where: $\dot{V_{in}}$ is the state variable; S_w is the control variable and $\dot{V_{load}}$ is considered as the disturbance.

Equation (3.9), is broken down into its separate components, as indicated in Equation (3.10), to generate the state space equation that represents the system. The state space equation is adjusted, so that the subject of the formula is the water volume in the reservoir, which is shown as the state variable [116].

Let (A) stand for the state variable, (B) the decision variable coefficient and (γ) as the disturbances. As a result, in Equation (3.9), the state variable (A), the decision variable coefficient (B) and the disturbances (γ), are all equal [117]:

$$\begin{cases} A = \dot{V_{in}} \\ B = \dot{V_{P1}} \\ \gamma = \dot{V_{load}} \end{cases} \tag{3.10}$$

Therefore, replacing question (3.9) into Equation (3.10), to obtain the simulated outcome in a case, where the limitations are ignored.

3.3.5.2 Load balance with the effect of evaporation, precipitation, seepage and leakages

The incoming water flow volume, exiting water volume, the load demand volume and losses may all be used, to estimate the reservoir water volume at a given time. The load balance, in Equation (3.6), changes, as follows, when the limitations (e.g. evaporation effect, precipitation effect, seepage losses and pipe leakages), are considered in the model.

The sum of the initial volume in the reservoir ($\dot{V_{in}}$), water pumping-rate ($\dot{V_{P1}}$), amount of rainfall rate ($\dot{V_R}$), evaporation rate ($\dot{V_E}$), rate of pipe losses ($\dot{V_{pe}}$), seepage losses ($\dot{V_s}$) and the load demand ($\dot{V_{load}}$), is equal to the change in volume at the reservoir ($\dot{V}s$) in the subsequent sampling interval.

$$\dot{V}s = \dot{V}_{in} + \dot{V}_{P1} + \dot{V}_R - \dot{V}_E - \dot{V}_{pe} - \dot{V}_s - \dot{V}_{load} \quad (3.11)$$

Because the pump runs at a constant speed, the flood switching control may be modeled as a binary switch that controls the pump's ON/OFF. As a result, as illustrated in equation 3.12, the load balance may be written as:

$$\dot{V}s = \dot{V}_{in} + (\dot{V}_{P1}) * S_w + \dot{V}_R - \dot{V}_E - \dot{V}_{pe} - \dot{V}_s - \dot{V}_{load} \quad (3.12)$$

Where: $\dot{V}_{in}$ is the state variable; S_w is the control variable; $\dot{V}_R, \dot{V}_E, \dot{V}_{pe}, \dot{V}_s$ and $\dot{V}_{load}$ may be considered as the disturbance.

Equation (3.12), is broken down into its separate components, as indicated in Equation (3.13), to generate the state space equation that represents the system. The state space equation is adjusted, so that the subject of the formula is the water volume in the reservoir, which is shown as the state variable [116].

Let (A) stand for the state variable, (B) the decision variable coefficient and (γ) for the disturbances. As a result, in Equation (3.12), the state variable (A), the decision variable coefficient (B) and the disturbances (γ) are all equal:

$$\begin{cases} A = \dot{V}_{in} \\ B = \dot{V}_{P1} \\ \gamma = \dot{V}_R - \dot{V}_E - \dot{V}_{pe} - \dot{V}_s - \dot{V}_{load} \end{cases} \quad (3.13)$$

Therefore, replacing Equation (3.13), into Equation (3.12), becomes:

$$\dot{V}s = A + BS_{w(t)} + \gamma_{(t)} \quad (3.14)$$

At an initial state, the state variable $\dot{V}_{in}$ represents the reservoir's actual water volume content. Accordingly, it may be written as $\mathrm{AV}_{(t)}$. Equation (3.15), is obtained by replacing the actual water volume in Equation (3.14) with:

$$\dot{V}s = \mathrm{AV}_{(t)} + \mathrm{BS}_{w(t)} + \gamma_{(t)} \tag{3.15}$$

3.3.6. Discretized reservoir water volume

Knowing that the water volume is of continuous-time function, therefore, transforming the continuous variables (or function) in Equation (3.15), into a discrete form and applying the discretization base on finite difference approximation of derivatives, according to the forward difference method [118, 119].

Equation (3.16) is used to transform the initial continuous problem, which has an infinite number of degrees of freedom into a discrete problem, where the degree of freedom is inevitably limited.

$$\begin{cases} Y(t) \to -Y(k) \\ r(t) \to r(k) \\ \frac{dy(t)}{dt} \to \frac{Y(k+1)-Y(k)}{t_s} \end{cases} \tag{3.16}$$

Where: t_s is the sampling time.

Starting by substituting Equation (3.16) into Equation (3.15), we get the Equation (3.17).

$$\frac{V(k+1)-V(k)}{t_s} = -\mathrm{AV}_{(k)} + \mathrm{BS}_{w(k)} + \gamma_{(k)} \tag{3.17}$$

Multiplying Equation (3.17) through by t_s and making the state variable $(V_{(k+1)})$ the subject of Equation (3.17).

$$V_{(k+1)} = V_{(k)} - t_s A V_{(k)} + t_s B S_{w(k)} + t_s \gamma_{(k)} \quad (3.18)$$

Factorizing the water volume $(V_{(k)})$ in equation (3.18)

$$V_{(k+1)} = V_{(k)}(1 - A t_s) + t_s B S_{w(k)} + t_s \gamma_{(k)} \quad (3.19)$$

After deriving the discrete-time function Equation (3.19) and knowing that V_k is the water volume, or the fluctuation in the reservoir water level. The state variable $V_{(k+1)}$ may now be expressed in terms of its starting value V_0 and the control variable S_w. At each interval, the state variable $V_{(k+1)}$, is computed numerically as:

For $k = 0$, then substituting in (3.19).

$$V_{(1)} = V_{(0)}(1 - A t_s) + t_s B S_{w(0)} + t_s \gamma_{(0)} \quad (3.20)$$

Similarly, for k=1, then $V_{(2)}$ is given as:

$$V_{(2)} = V_{(1)}(1 - A t_s) + t_s B S_{w(1)} + t_s \gamma_{(1)} \quad (3.21)$$

Substituting $V_{(1)}$ into Equation (3.21)

$$V_{(2)}=(V_{(0)}(1-At_s)\ +t_sBS_{w_{(0)}}+t_s\gamma_{(0)})(1-At_s)\ +t_sBS_{w_{(1)}}+t_s\gamma_{(1)} \quad (3.22)$$

Further grouping and simplification of the Equation (3.22)

$$V_{(2)} = V_{(0)}(1-At_s)(1-At_s)+\ t_sBS_{w_{(0)}}(1-At_s)+t_sBS_{w_{(1)}}+\ t_s\gamma_{(0)}(1-At_s)+ t_s\gamma_{(1)} \quad (3.23)$$

Likewise, for k=2, then $V_{(3)}$ is given as:

$$V_{(3)}=V_{(2)}(1-At_s)\ +t_sBS_{w_{(2)}}+t_s\gamma_{(2)} \quad (3.24)$$

Substituting $V_{(2)}$ into Equation (3.24)

$$V_{(3)} = (\ V_{(0)}(1-At_s)(1-At_s)+\ t_sBS_{w_{(0)}}(1-At_s)+t_sBS_{w_{(1)}}+\ t_s\gamma_{(0)}(1-At_s)+ t_s\gamma_{(1)})(1-At_s)\ +t_sBS_{w_{(2)}}+t_s\gamma_{(2)} \quad (3.25)$$

Expanding equation (3.25)

$$V_{(3)} = V_{(0)}(1-At_s)(1-At_s)+\ t_sBS_{w_{(0)}}(1-At_s)+t_sBS_{w_{(1)}}+t_s\gamma_{(0)}(1-At_s)+ t_s\gamma_{(1)}+At_sV_{(0)}(1-At_s)(1-At_s)+At_s\ t_sBS_{w_{(0)}}(1-At_s)+At_st_sBS_{w_{(1)}}+ At_st_s\gamma_{(0)}(1-At_s)+At_st_s\gamma_{(1)}+t_sBS_{w_{(2)}}+t_s\gamma_{(2)} \quad (3.26)$$

Further simplifying equation gives (3.26)

$$V_{(3)} = V_{(0)}(1 - At_s)(1 - At_s)(1 - At_s) + Bt_sS_{w(0)})(1 - At_s)(1 - At_s) + Bt_sS_{w(1)}(1 - At_s) + Bt_sS_{w(2)} + t_s\gamma_{(0)}(1 - At_s)(1 - At_s) + t_s\gamma_{(1)}(1 - At_s) + t_s\gamma_{(2)} \quad (3.27)$$

The state variable $V_{(k+1)}$ in a discrete time function may be expressed as:

$$V_{(k+1)} = V_0(1 - t_s)^{(k+1)} + Bt_s\sum_{k=0}^{n-1}\left(S_{w_k}(1 - t_s)^{(n-k-1)}\right) + t_s\sum_{k=0}^{n-1}(\gamma_k(1 - At_s)^{(n-k-1)}) \quad (3.28)$$

Where: $V_{(0)}$ and $V_{(n)}$ denote the initial and k^{th} water volumes in the reservoir respectively; S_w denotes the k^{th} switching status with the binary operation for ON/OFF switching of the pump; while, t_s is the sampling time.

3.3.7. Constraints

The cost function is subjected to constraint factors, such as the influence of rainfall on the reservoir, evaporation and seepage:

$$V_{min} \leq V_{(k)} \leq V_{max} \quad (3.39)$$

Where: (V_{min}) is the minimum permissible volume level that the water in the storage reservoir may reach and (V_{max}) denote the maximum threshold level that the volume may not exceed, for any given interval and (V) represent the actual volume of water in the reservoir.

Switching of the pump ON/OFF, is represented as a binary operation as follows [120]:

$$S_w \in \{0,1\} \quad (3.30)$$

3.3.9. Solver selection

The developed model may be addressed as a simple ON/OFF problem that is implement on MATLAB software program.

3.4. CASE STUDY DESCRIPTION

3.4.1 Water pumping system side description

The plant water pumping arrangement consists of three electrical pumps that pump water from the Dam to the main reservoir; the pumps are positioned alongside each other and next to the Dam catchment area, suspended vertically, as illustrated in Figure 3.2. A three-phase alternating current (AC) source from the utility grid, is used to power the pumps. The water from the dam is pumped to the main reservoir, which has a cross sectional area of $1{,}26\text{km}^2$, constructed out of concrete, with an open top surface. Electrical pumps, on the other hand, are used to pump the water to the reservoir for storage after it has been entirely treated; these pumps operate on the same principle as the first set of pumps.

The water treatment plant, discussed in this study, was built more than three decades ago and the original design of the adopted case study pump station, was to serve a population far smaller than its current carrying capacity. In the sense that, the pumps in Figure 3.2, were to be operated at different intervals, possibly at different times, thereby controlling the rate of energy consumption. However, the population that relies on this

water treatment plan, has grown to the point that the corporation may solely turn ON two pumps, at any given time, to meet the water volume required for the given load demand [121]. As a result, two of the three pumps, described in Section 3.4.4, were used in this study's modeling, to meet the load requirement, in its current form. Figure 3.3 shows the selected water reservoir in the Bloemfontein area in South Africa.

Figure 3.2: Electrical water pumps

Figure 3.3: Water reservoir

3.4.2 Rainfall, Evaporation and Seepage profile

The evaporation effect caused by the open top form of the water reservoir was another effect examined in this study, after receiving the radiation data for the provided area from SAURAN data services and the computed values supplied in Table A in the appendices, the evaporation data displayed in Figure 3.4, was derived, using the formula shown in Section 3.3.1 [122]. The evaporation water-volume data are displayed for a 24 hour period, as shown in Figure 3.4. It shows evaporation that occurs between the hours of 12h00 a.m. and 19h00 p.m., indicating the period when the sun rises during that day.

The seepage losses are calculated, using Equations 3.5 and 3.6, as explained in Section 3.3.3. Figure 3.4 and Table of the Appendices, show the results obtained.

Figure 3.4, reflects the rainfall level of the selected load demand day, to calculate it. This data, was obtained from a weather station, located approximately 3.2 km from the water treatment plant, in Bloemfontein, South Africa and are tabulated in Table A, in the appendices.

The data used to determine the viability of these models, is versatile, as the model is designed to control the pumping rate, while taking into account that various atmospheric conditions may occur, adding to the consequences of climate change, discussed in Chapter 2 [6, 7]. Not to mention the fact that, as stated in Equation 3.12, Section 3.3.5.2, these constraints are not expected to cause any disruptions to the control model.

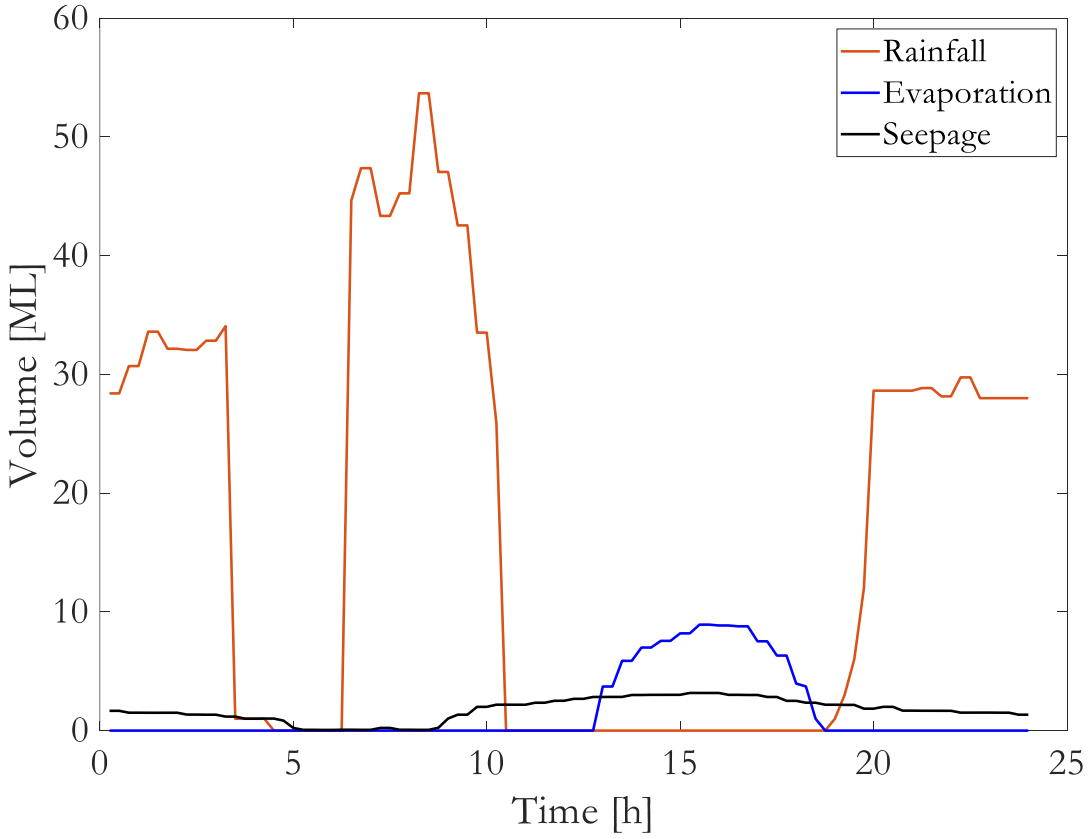

Figure 3.4: 24 hours combined rainfall and evaporation curve

As water reservoirs are built with a big, open top structure, rainfall could be a substantial variable that affects the reservoir water volume. Figure 3.4, reflects the rainfall level of the selected load demand day, shown in Figure 3.5.

The first occurred between 00h00 and 04h00, resulting in a rainfall volume of 34ML; the second occurred between 06h00 and 10h30, resulting in a rainfall volume of 54ML; and, finally, the rain of about 28ML occurred between 20h00 and 24h00.

Seepage is the slow escape of a liquid through porous material or small holes in water reservoir and it is crucial behind water losses. Considering that the storage reservoir in this study represents the load demand, it is therefore understood that the quantity of water loss, because of seepage, depends on the volume of water stored in the reservoir at any giving time. Equations 3.5 and 3.6 are used to determine the seepage losses, as described in Section 3.3.3. The results are displayed in Table A of the Appendices and Figure 3.4.

Figure 3.4, shows the behaviour of water loss owing to seepage over a 24 hour period. A maximum of 3.172ML is lost in the hour of 15h00, which further happens to be the time when the load demand is at its peak, as shown in Figure 3.5.

3.4.3 Load demand profile

Figure 3.5, is drawn from the data shown in the appendices Table A. It illustrates the water utility company's load demand, as detected by a sensor at the outlet of a treatment reservoir in Bloemfontein, South Africa. As shown in Figure 2.1, the water pipe outlet from the main water reservoir, flows to the water storage reservoir, which is considered a load in this system and distributed to small and large scale consumers.

The demand side load profile, is drawn from the accumulated data, recorded from the main water reservoir, collected from the water utility company, situated approximately 60km from the Bloemfontein area and considering that, the storage reservoir in Figure 3.5, creates the load of the system. The distribution pipe leaks, are not included in the scope of this

project for this reason. The name of the water company used as the case study, in this study is kept anonymous, until it has been permitted.

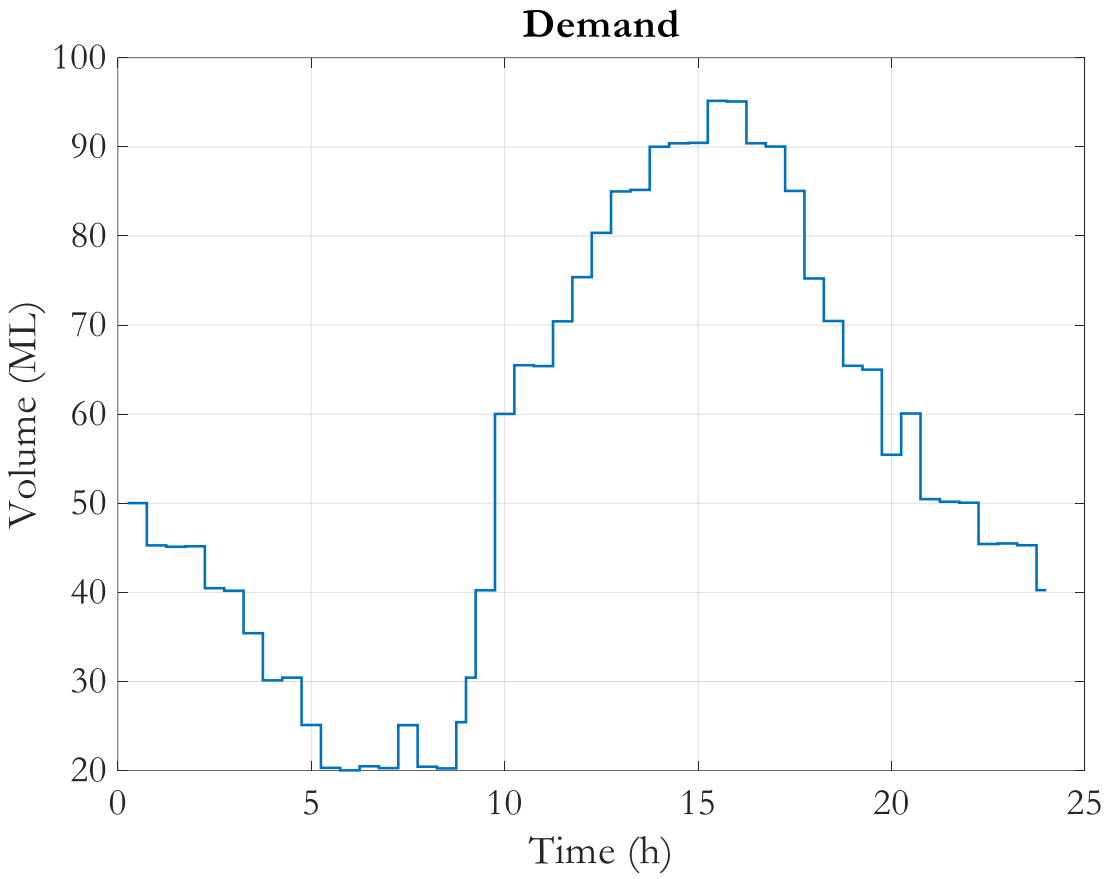

Figure 3.5: 24 hour municipal water demand load-profile

Since the water demand is a continuous process, the pumping of water to the reservoir reciprocates the outflow to the storage tank. Interpreting Figure 3.5, shows a 24 hour water consumption (load demand) for a given day; the water from this reservoir serves Botshabelo, a small village near Bloemfontein, with a population of 447.603 people, who engage in a variety of economic activities [121].

Start of the day referring to Figure 3.5. The day begins at midnight, with a reservoir reserve capacity of 50ML, indicating that this is the time when most economic activities are quiet, as most people are sleeping and most workplaces are closed, implying a low load

demand between 12h00 and 05h00. The demand for water begins to rise early in the morning, between 05h00 and 09h00, when people begin preparing for work. After this time, from 09h00 to 16h00, it is considered the peak water demand period, as shown in Figure 3.5. During this time, it is assumed that the majority of economic activities are taking place and water consumption is at a greater level. Demand begins to decline again near the end of the day, from 16h00 to 24h00, when work places have a chance to resist and go to bed, though there is still a slight demand.

3.4.4 Equipment sizing profile

The system uses three electrical pumps in sizes of 200kW, 200kW and 110kW of a rated frequency of 50Hz, with the 200kW pump having a rated speed of 990rpm. These pumps are used, as shown in Figure 3.4, with the understanding that one of the three pumps is standing by as a backup, in the case of a breakdown, maintenance, or significantly high load demand. Therefore, it has been adopted in this model, an average total capacity pump rating of 310kW, which is the combination of the two pumps. With the system's chosen water reservoir having a cross-sectional area of 1, 26km^2 and a pumping volume capacity of 90ML.

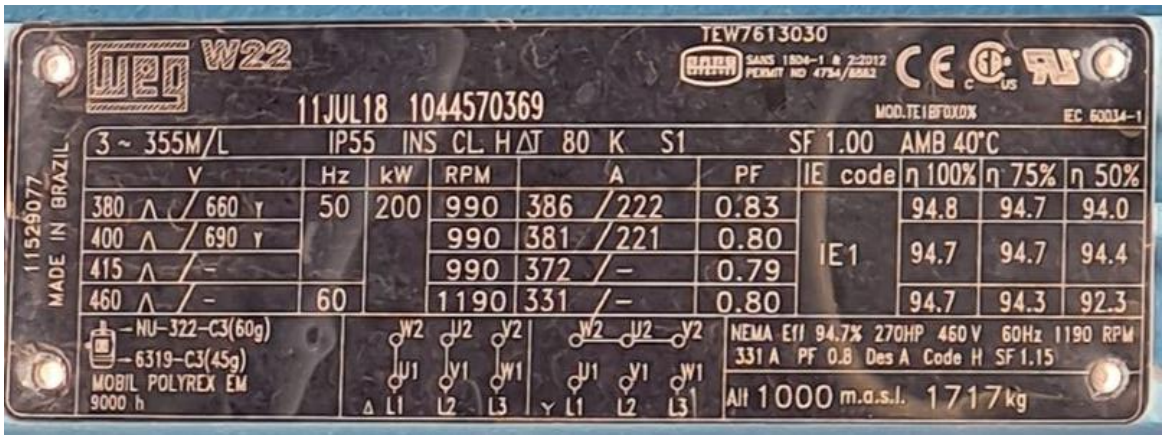

Figure 3.6: Electrical water pump specifications [123].

The specification characteristics of the electrical pump used in these tests are shown in Figure 3.6.

The data obtained during the month of June 2020, was chosen for this simulation for a variety of reasons, including the fact that it is representative of many other days throughout the year. The fact that the cost of electrical energy is significantly greater in the winter than in the summer and that this is the time of year when the demand for water is highest, due to the dryness of the weather, which might result in a humid state that increases the rate of evaporation and seepage. Rainfall is possible at this period, as indicated in Figure 3.4.

3.4.5 ToU profile

The research included Eskom's recent ToU prices for industrial customers [124]. Table 3.1 shows Eskom's ToU tariff pricing between 2020 and 2021. Summer months denoted (September to April) are considered low demand, while winter months are considered high demand (May to August).

Equation (3.32), shows the ToU tariff charges during high demand seasons. This ToU tariff ($\mathbf{C_{e(j)}}$) may be further expressed, according to the South African daily pricing time structure, as shown in Equation (3.32).

$$C_{e(j)} = \begin{cases} C_0; t \in T_k, T_k = [0,6)[22,24); \\ C_p; t \in T_k, T_k = [6,9)[17,19); \\ C_s; t \in T_k, T_k = [9,17)[19,22); \end{cases} \quad (3.32)$$

Where:

C_0 is the cost of energy during the off-peak pricing period (ZAR/kWh);

C_p is the cost of energy during the peak pricing period (ZAR/kWh);

C_s is the cost of energy during the standard pricing period (ZAR/kWh).

The simulation parameters are listed in Table 3.1. To improve the accuracy of the presented water volume variations in the storage reservoir, the sampling time was set to 15 minutes. Furthermore, the data were solely provided at 15 minute intervals.

Table 3.1: Simulation parameters

Parameter	**Value**
Sampling time (Δt)	15 min
C_0 (summer off-peak rate)	0.81 ZAR/kWh
C_p (summer peak rate)	1.38 ZAR/kWh
C_s (summer standard rate)	0.94 ZAR/kWh
C_0 (winter off-peak rate)	1.32 ZAR/kWh
C_k (winter peak rate)	2.83 ZAR/kWh
C_s (winter standard rate)	1.44 ZAR/kWh
Maximum demand rate	135.58 ZAR/kVA
V_{min}	10ML
V_{max}	90ML
P_{pump}	310kW
D (pipe diameter)	9cm
As	1.26km^2
Reservoir capacity	90ML

3.5. SIMULATION RESULTS AND DISCUSSION

3.5.1. Flood switching control and reservoir volume state without the effect of rainfall and evaporation.

The behaviour of the water pump switching system is explained, in accordance to the different tariff-pricing period as highlighted by the sectional view in Figures 3.8 and subsequent switching sequence.

The time when the pump is ON is the duration it takes for the water pumped into the reservoir to reach the pre-defined maximum level of 90%. When the pump is shut off, it remains off until when the volume of water in the reservoir reaches 10ML, lower value considered as a predefined lower level, the OFF-time lags. Point zero "0" on the y-axis in Figure 3.7, indicates when the pump is turned OFF, while point one “1” is when the pump is turned ON.

Figure 3.7, shows the switching sequence for the flood switching control water pump, without taking into account the effects of precipitation and evaporation, whereas, Figure 3.8, shows the volume of water pumped into the reservoir using the pump switching sequence, presented in Figure 3.7.

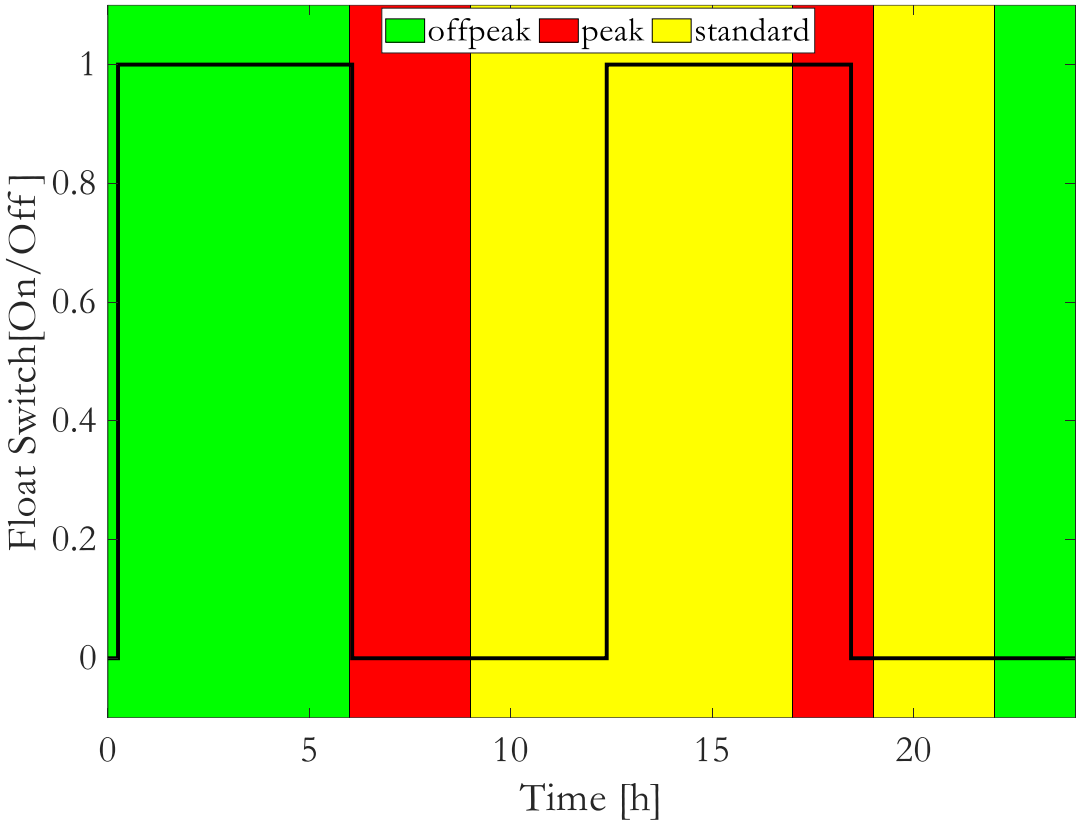

Figure 3.7: Flood switching sequence without rainfall and evaporation effect

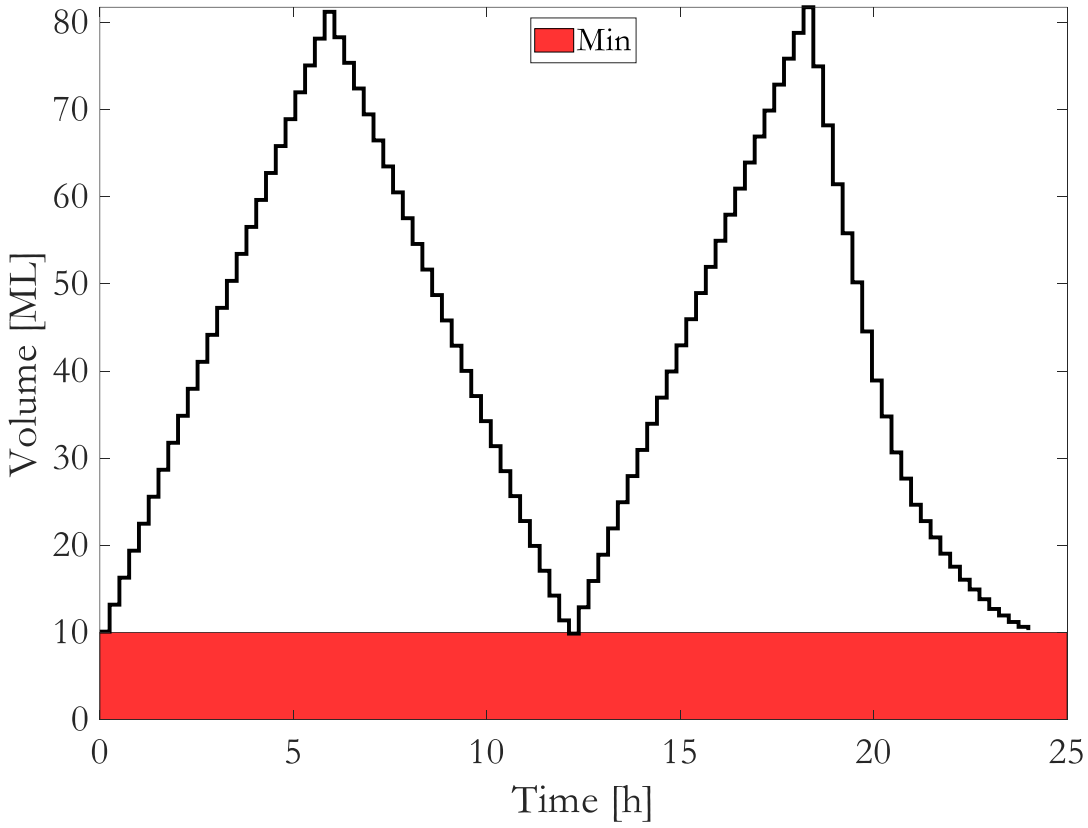

Figure 3.8: Flood switching control state of water stored in the reservoir without rainfall, seepage and evaporation effect

The water volume in the reservoirs, shown in Figures 3.9, explains the differences in the volume flow rate, in order to certify the water load demand requirement. However, the reservoir volume in Figure 3.8, is not affected by rainfall and evaporation. As a result, the total water volume in the reservoir in Figure 3.8, is clearly the water pumped by the switching action in Figure 3.7, revealing the cause for the longer pumping operation in Figure 3.7.

Examining the switching operations of a flood switch, as shown in the Figure 3.8. The principle of the flood switch entails that once the pump is switched ON, it remains ON until the water level in the reservoir reaches maximum before it is switched OFF as shown in Figure 3.8. and will remain in its OFF position until the water level in the reservoir reaches its minimum which is 10ML, as shown in Figure 3.8.

In each price segment, as shown in Figure 3.7, there is a sectional description of what happens to the reservoir pumped volume, referring to Figure 3.8. The load demand referring to Figure 3.5.

3.5.1.1 During the first off-peak (green) pricing period, from 00h00 to 06h00.

The pricing is at its lowest (off-peak) period, as indicated by the delimited periods in green in Figure 3.7. The load demand in Figure 3.5, is on a declining trend at this time, commencing at 50ML. With reference to Figure 3.5, the flood switching in Figure 3.7, displays the ON position of the sampling time, which equals 6 hours of ON-time and the pump turns ON, while pumping water to the reservoir at a level of 80ML.

3.5.1.2 During the first peak (red) pricing period, from 06h00 to 09h00.

This is a time when energy costs are at their highest (peak). Figure 3.5, shows a low load demand. Looking at Figure 3.7, the pumps are switched off, which means the flood switch control is turned off and the energy supply to the pumps is turned off. The electric pumps are turned off at this time and the reservoir volume in Figure 3.8, continues to decrease gradually, due to the low load demand.

3.5.1.3 During the first standard price period (yellow) from 09h00 to 17h00.

The standard costing period is thought to be a kind of middle ground between peak and off-peak pricing. The load demand in Figure 3.5, increases as daily activities begins. The Flood switch control in Figure 3.7, turns the pump ON to start pumping water into the reservoir. During this period, the reservoir volume starts rising as shown in Figure 3.8,

adding to the high load demand, shown in Figure 3.5, implying a large quantity of the pumped water is consumed by the load as the day progresses.

3.5.1.4 Switching during the second peak (red) pricing period from 17h00 to 19h00.

Towards this hour of the day, the load demand starts reducing, however, in a very small rate, which keeps the flood switch control in Figure 3.7, in its ON state. However, because the load demand is high at this time, as shown in Figure 3.5, the rate of water consumption is higher than the rate of pumping at this stage, as shown in Figure 3.9. This increase in cost could further be attributed to the fact that energy tariffs are greater during peak pricing times than during normal and off-peak pricing periods. As a result, using a flood switch to save energy in a water pumping system is not the best option.

3.5.1.5 Switching during the second standard (yellow) pricing period, which runs from 19h00 to 22h00.

During this period, the load demand is seen as decreasing, as shown on Figure 3.5. The flood control switch remains in the OFF state for the entire duration, while the pump is switched OFF, as shown in Figure 3.7. At the same time, the water volume in the reservoir is marginally decreasing, owing to the decreasing load demand, as shown in Figures 3.8 and 3.6, respectively.

3.5.2.6 Switching during the 22h00 to 24h00 hour second off-peak (green) pricing period

The last part of the day is the off-peak costing period, during which the load demand continues on its downward slope, decreasing, as seen in Figure 3.5, the pump is turned OFF,

referring to Figure 3.7. Figure 3.8, shows a downward trajectory of the reservoir volume, indicating that we are approaching the end of the day and that the final state of the pump should be attended to, to appropriately analyse the various situations.

3.5.2. Flood switching control and reservoir volume state with the effect of rainfall and evaporation.

This section takes a closer look at how rainfall, evaporation and seepage affect the reservoir's water volume. Because variables, such as rainfall, seepage and evaporation, have both positive and negative effects on the reservoir water volume, a comparable operation is carried out. The water level increases in the reservoir when rain falls, reducing the pump working duration, while evaporation and seepage cause water loss in the reservoir, requiring more water to be pumped. Figure 3.9, shows the flood switching operation when these effects are taken into consideration.

Figure 3.10, shows the state of water stored in the reservoir at any given time. According to this model, an increase in reservoir water volume is caused by the pump being turned ON, allowing the pump-to-pump water into the reservoir, or rainfall filling the reservoir, whereas a decrease in reservoir water volume is caused by the load demand out flow, evaporation, seepage and pipe losses, as shown in Figure 3.4.

This section will continue to analyse the results when these variables are taken into account.

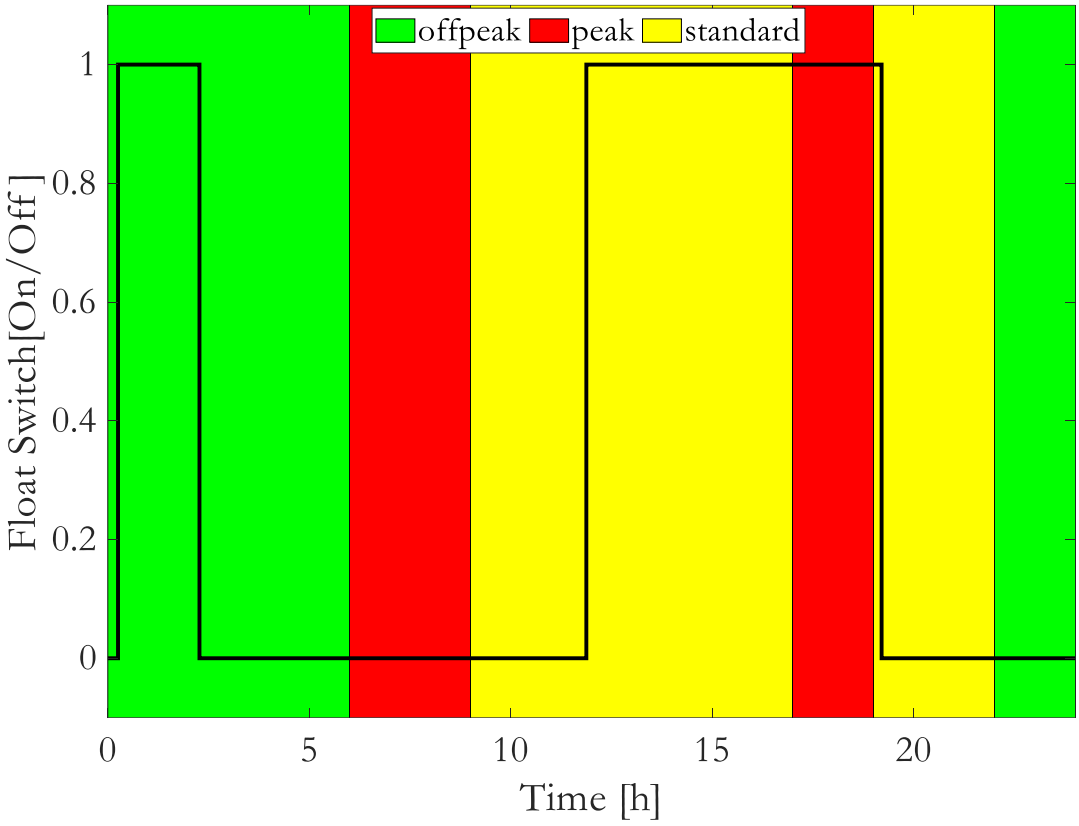

Figure 3.9: Flood switching sequence with rainfall and evaporation effect

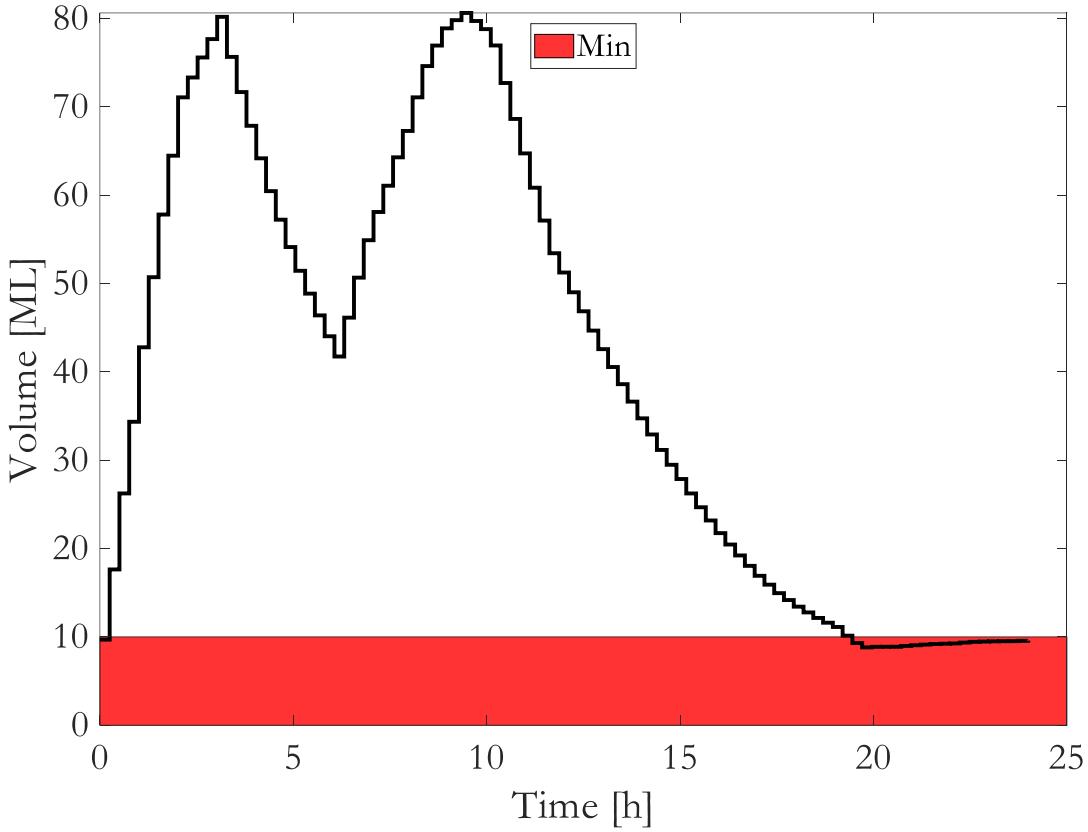

Figure 3.10: Flood switching control state of water stored in the reservoir with rainfall, seepage and evaporation effect

Here, a sectional description of what happens to the reservoir pumping volume when the flood switch controls the pump operation, referring to Figure 3.9 and 3.11, respectively. The load demand, referring to Figure 3.5, evaporation effect referring to Figure 3.4, seepage effect referring to Figure 3.4 and the rainfall effect referring to Figure 3.4, are all variables that affect the water volume in the reservoir [125].

3.5.2.1 During the first off-peak (green) pricing period, from 00h00 to 06h00.

The pricing is at its lowest (off-peak) period, as indicated by the delimited periods in green in Figure 3.9. The load demand in Figure 3.5, is on a declining trend at this time,

commencing at 50ML. With reference to Figure 3.5, the flood switching in Figure 3.9, displays the ON position of the sampling time, which equals 1 hour 51 minutes of ON time and the pump turns ON, while pumping water to the reservoir at a level of 80ML, demonstrating that the rainfall water volume helps in topping up the reservoir, as shown in Figure 3.4. Figure 3.10, shows the water volume in the reservoir, when the rainfall, seepage and evaporations are considered in the simulation, which assisted in reducing the switching ON-time of the pump. Owing mostly to the rainy water volume being added to the pumped water volume in the reservoir. When the reservoir flood switch control is activated, the power supply to the pump is turned off. As a result, illustrated in Figure 3.5, the reservoir's water volume level drops gradually, in response to load demand. Evaporation is recorded as zero during this time.

3.5.2.2 During the first peak (red) pricing period, from 06h00 to 09h00.

This is a time when energy costs are at their highest (peak). Figure 3.5, shows a low load demand. Looking at Figure 3.9, the pumps are switched OFF, which means the flood switch control is turned OFF and the energy supply to the pumps is turned OFF. The reservoir volume in Figure 3.10, continues to increase, the rainfall turns to influence the water volume in the reservoir and, as seen in Figure 3.4, a rainfall water volume of 54ML increases the volume of water in the reservoir. Therefore, at this stage, it turns to raise the water volume and produce a change in the water volume trajectory in the reservoir refers to Figure 3.10.

3.5.2.3 During the first standard price period (yellow) from 09h00 to 17h00, the power flow is switched.

The standard costing period is thought to be a form of middle ground between peak and off-peak pricing. The load demand in Figure 3.5, increases as the day activity is about to

start. The Flood switch control in Figure 3.9, turns the pump ON, to start pumping again. During this period, the reservoir volume continues to decrease, as shown in Figure 3.10, adding to the high load demand, shown in Figure 3.5. An indication that, the reservoir water volume is decreasing as the day progresses. At this time, no rainfall has been reported. However, a small volume of water is evaporated, adding to seepage losses, as shown in Figure 3.4.

During this time, the pump turns on at 11h45, as shown in Figure 3.9. However, because the load demand is so high at this point, it is worth noting that all of these factors, together with evaporation and seepage losses, result in a reduction in reservoir water volume. As a result, it is reasonable to conclude that a combination of high load demand, evaporation and seepage losses consume the volume of water pumped into the reservoir, which explains why the reservoir water volume continues to drop, as shown in Figure 3.10.

3.5.2.4 Switching during the second peak (red) pricing period from 17h00 to 19h00

Towards this hour of the day, the load demand starts reducing. However, in a very small rate, which keeps the flood switch control in Figure 3.9, in its ON state. However, because the load demand is high at this time, as shown in Figure 3.5, the rate of water consumption is higher, as opposed to the rate of pumping at this stage, adding to small evaporation seen at this stage, while the seepage effect is shown in 3.5, resulting to a rise in water volume, as shown in Figure 3.10.

3.5.2.5 Switching during the second standard (yellow) pricing period, which runs from 19h00 to 22h00.

During this period, the load demand is seen as decreasing, as shown on Figure 3.5. The flood control switch remains in the ON state for 15min, before turning OFF while the

pump is running, as shown in Figure 3.9. Simultaneously, the water volume in the reservoir is marginally decreasing, as shown in Figure 3.10. As a result, the pumps are turned OFF and remain so for the remainder of the time. However, the rate of evaporation drops to zero, along with a decrease in seepage loss, as seen in Figure 3.4 and rain begins to fall to fill the reservoir.

3.5.2.6 Switching during the 22h00 to 24h00 hour second off-peak (green) pricing period

The last part of the day is the off-peak costing period, during which the load demand continues its downward slope, decreasing, as seen in Figure 3.5, the pump is turned OFF, referring to Figure 3.9. Figure 3.10, shows a downward trajectory of the reservoir volume, indicating that we are approaching the end of the day and that the final state of the pump should be attended to, to appropriately analyse the various situations. Figure 3.4, shows an approximate 34ML of rainwater filling up the reservoir capable of servicing the load demand in Figure 3.5.

3.6. DAILY ENERGY COST OF THE FLOOD SWITCHING CONTROL SYSTEM

This section discusses and reflects the net-cost in energy consumption, when applying the flood switching control to manage the pump energy consumption of a water pumping system. Figure 3.11, shows the hourly energy consumption rate in a given day. Two scenarios are simulated, the first case shows the cost consumption without the effect of evaporation, seepage and rainfall. The second case is when these variables are taken into consideration.

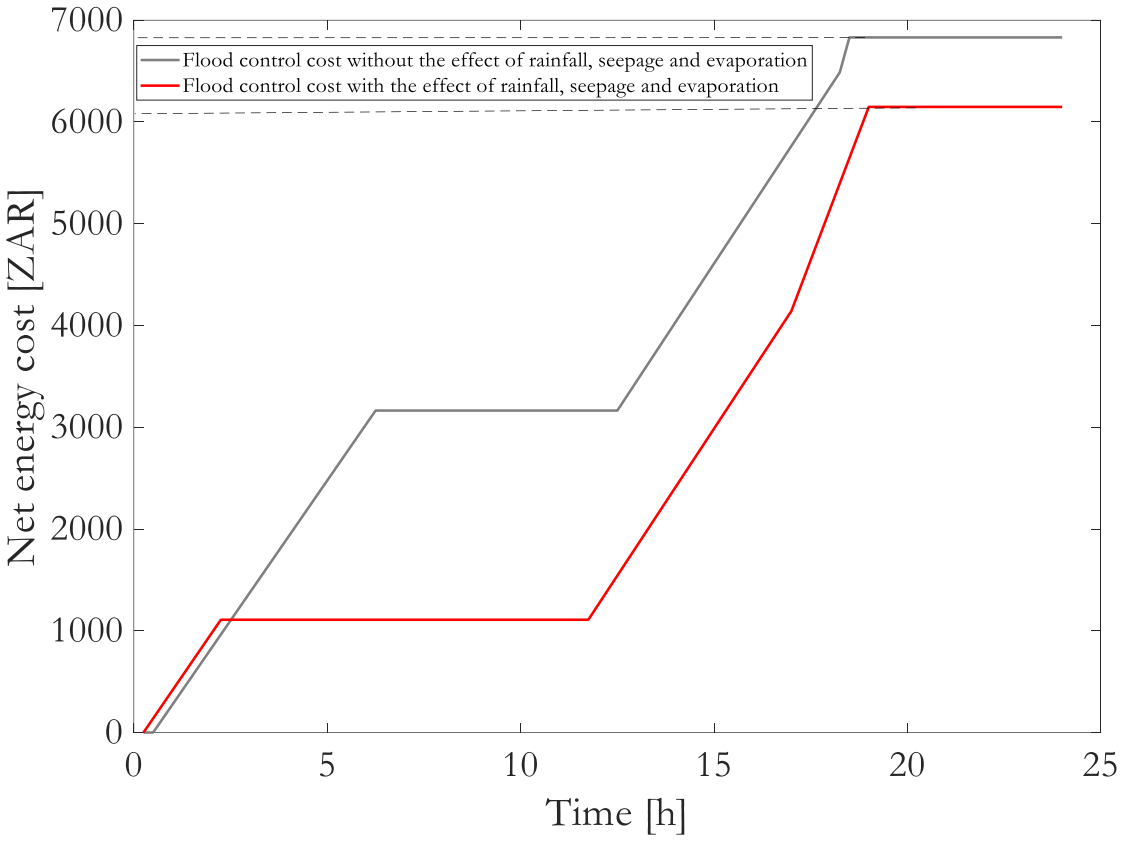

Figure 3.11: Control daily cost

Consider the characteristics of the flood switching controller in Figures 3.7 and 3.10, respectively, as well as what occurs in the reservoir, in Figures 3.8 and 3.11, respectively. It has been found that the cost of energy consumption rises as the water pump volume rises, owing to the pump's ON time operation. During the early hours of the day, when the pumps are turned ON between 00h00 and 05h00, as shown in Figures 3.7 and 3.10, respectively. The pump's energy consumption rises to 3164 ZAR and 1108 ZAR, respectively, indicating that the system that overlooks the effects of rainfall and evaporation takes longer to pump water to the reservoir, resulting in higher energy consumption. The pump is turned OFF for the periods of 05h45 to 12h28; and 02h00 to 11h45, in the respective curves, as illustrated in Figure 3.11. Hence, no energy is consumed by the pump. Figures 3.8 and 3.10 show the pump turned ON again between 12h28 and 18h00, with a cumulative energy usage of 6487

ZAR, in a simulated case, without the effects of rainfall and evaporation and 6148 ZAR in a case with the effects of rainfall and evaporation. As a result, the total amount of energy spent in a 24 hour sample time cycle is 6831 ZAR and 6148 ZAR, respectively, resulting in an energy savings of 683 ZAR between the two situations, as shown in Figure 3.11.

3.7. SUMMARY

This Chapter develops and simulates a control system using the MATLAB software solver, to calculate the water pumping energy cost minimization, when using Flood control switching to regulate the pump switching period. Two scenarios were simulated: one in which variables such as evaporation, rainfall and seepage losses were ignored; the other in which these variables were taken into account.

The study found that by controlling the pump's switching ON/OFF when the water level in the tank reaches its high and low capacity levels, a flood switching control system with an electrical water pump saves energy when the effect of rainfall and evaporation is considered. As a result, the water level in the reservoir will not go below a specific level and it will not overflow.

The simulation results demonstrated that, in a system that considers the effects of precipitation and evaporation, flood control switching may help manage the reservoir's overflow level, while further determining when the electrical pump should be turned ON and OFF. According to the model developed in this Chapter, the precipitation, evaporation, as well as seepage, have a significant effect on the switching of the pump, as well as the resultant operation cost. The importance of experimenting with different control models, to attain a more cost-effective energy consumption cost in a water pumping system, is shown by this quantity of energy consumption.

CHAPTER 4: TIMER SWITCHING CONTROL APPLIED TO A WATER PUMPING SYSTEM

4.1. INTRODUCTION

In this Chapter, a model is developed to control the water pumping, based on an electronic timer-setting control system. This control system compels the pump to operate mainly during off-peak and standard periods, as per the South African energy supply time-of-use (ToU) tariff.

The aim of the model, is to reduce the cost of pumping water from the water catchment to the reservoir, by shifting the time the pump is turned ON/OFF, avoiding the turning ON of the pump as much as possible, during the peak period of the utility energy supply.

Variables such as evaporation, seepage and precipitation, which may affect the water level in the reservoir, are included in the model.

The flood switching control in Chapter 3, is selected as a baseline. The load profile, reservoir size and pump size, are all inputs to the model that was created.

As an improvement to the model, a Variable Speed Pump (VSP) is incorporated into the water pumping system, controlled by a timer switch. VSP employs the variable speed drive (VSD), or variable frequency drive (VFD), principle to adjust the speed of a three-phase motor-pump, by controlling the frequency of the motor-pump, using a power conversion device. In doing so, the power supply to the motor-pump is thus regulated.

The economic performance of the developed model is compared to the baseline, through simulations, for a 24 hour pumping cycle, using an electronic timer-setting controller water pumping system. Various results are simulated using MATLAB, in reviewing the performance of the proposed model; the first is the pump's switching cycle, the second is the water level (volume) in the storage reservoir and the third is the company's 24 hour cost.

4.2. TIMER SWITCHING CONTROL SYSTEM MODEL

Figure 4.1, shows the timer switching control configuration. The water level in the reservoir is dependent on the switching ON/OFF arrangement of the timer switch, which directly controls the pump that pumped water to the reservoir [25].

The timer-setting control unit provides power to the pump. The operator establishes the timing program of this electronic timer, by looking at previous water load demand-data and ensuring that the pumps are turned OFF during the period when electricity prices are at their highest (peak), according to the South African ToU tariff structure.

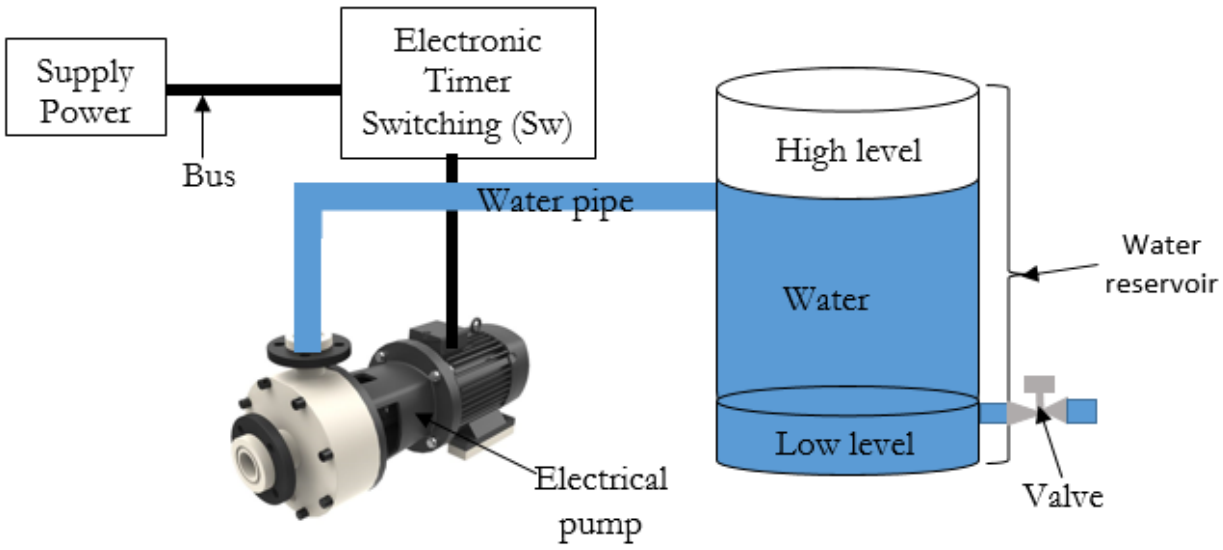

Figure 4.1: Proposed electronic timer switching control water pumped system schematic

4.2.1. Timer switching control system model with VFD incorporated

In order to comprehend how a VFD and a timer-setting controller works in a water pumping system, Figure 4.2, shows the schematic circuit of the VFD-Timer-setting control system, in which the VFD regulates the frequency of the power supply, while the timer regulates the switching period, based on the ToU tariffs and historical load demand data.

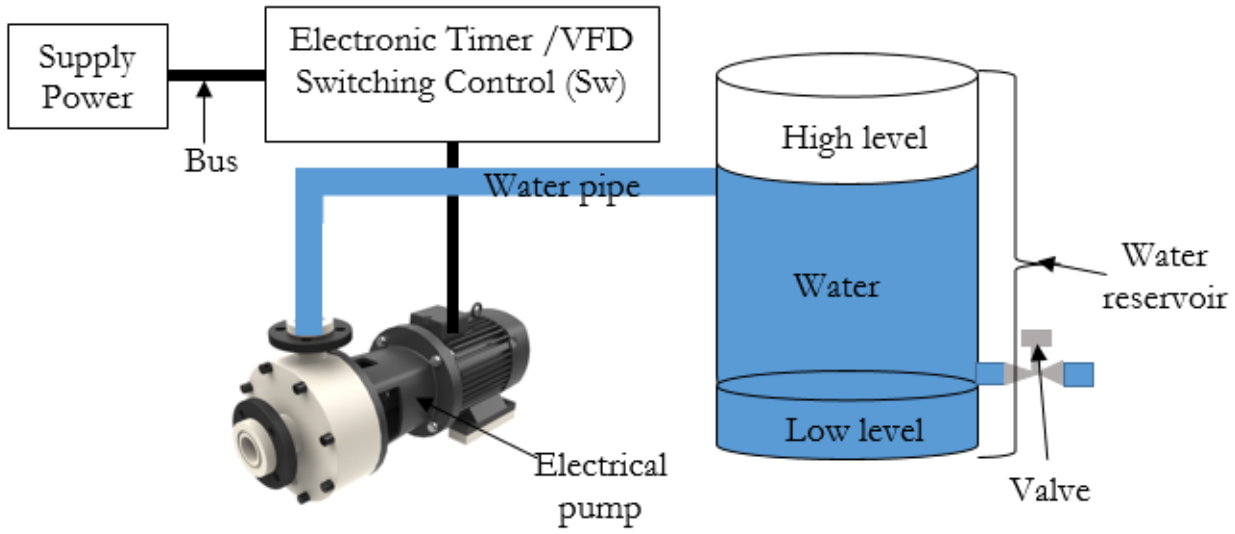

Figure 4.2: VFD-Electronic timer-setting control system

The aim of an equipment management strategy at the pump level, as stated in the POET concept in Chapter 2, is to manage the cost of energy consumption in a given system. In the case of a water pumping system, a variable frequency drive (VFD) alters the speed of the electrical pump during a low demand time, in order to improve energy saving technology in a water pumping system.

Figure 4.3, shows the human machine interface (HMI) of a VFD system, installed within a room, situated few meters alongside the water catchment area, shown in Figure 3.2. The VFD is applied, to control the power consumption of the electric pump. The drive displays the frequency at which the pump is running. Other features include the ability to disengage the VFD control attached to the system and reinstall it.

Figure 4.3: VFD pump control

4.3. MATHEMATICAL MODEL DEVELOPMENT

4.3.1. Timer-setting control model with a fixed motor pump

The timer programmer settings, to control the state of the pump, are turned ON or OFF. The switch (Sw), that controls the power flow to the pump, is represented in Figure 4.1 and serves as the control mechanism of the water pumping system. In this model, the switching principle is like a binary form of control, in which a '1' represents ON and a '0' represents OFF. the pump switching is determined by the Sw_timer, as shown in Figure 4.1, which is the timer predicted programmer settings for the control horizon.

$$S_w = S_{w\_timer} \quad (4.1)$$

Where: (Sw_timer) is the timer's predicted programmer settings for the control horizon.

Switching the pump ON/OFF, is represented as a binary operation, as follows:

$$S_w \in \{0,1\} \quad (4.2)$$

4.3.2. Cost function

The ToU tariff structure is employed, since the cost of energy usage is the major factor to be minimized in this approach. Therefore, in order to address the ToU operating period, the operator switching setting was designed to stop the pump from turning ON, during the peak period. The cost function is further developed, as follows, in order to attain a stable outcome:

$$\text{Min } f = t_s * S_{w\_timer} (C_{e_k} * P_{(pump)_{rated}}) \quad (4.3)$$

Where: f is the cost function; C_{e_k} is the ToU tariff function (R/kWh); $P_{(pump)_{rated}}$ is the electrical pump rated power (kW); S_{w_timer} is the electrical pump operator settings switching state.

4.3.3. Constraints

The cost function is constrained by elements, such as the rainfall effect on the reservoir, evaporation and seepage, and the input parameters remain unchanged, is discussed in Chapter 3. Therefore, this limitation remains the same in this model.

$$\mathrm{V_{min}} \leq V_{(k)} \leq \mathrm{V_{max}} \tag{4.4}$$

Where: ($\mathrm{V_{min}}$), is the minimum permissible volume level that the water in the storage reservoir may reach and ($\mathrm{V_{max}}$) denotes the maximum threshold level that the volume should not exceed, for any given interval and ($V_{(k)}$) represents the actual volume of water in the reservoir.

4.3.4. Timer-setting control with a VFD controlled motor pump

The VFD control, discussed in Chapter 2 and shown in Figure A, at the appendices, is further combined with the timer-setting control model, developed in Section 4.3.1, to generate a combined VFD-Timer-setting control system. Where: the VFD regulates the pump's power during periods of low demand. Therefore, the cost function is given an additional factor, that affects the change in frequency of the motor pump.

4.3.5. Cost function

At this stage, the pump is deemed a control variable, as its power changes as a result of the VFD control concept. Adding to the fact that the control operator set the switching ON time of the timer as seen in Equation 4.1. As a result, the following is the cost function:

$$\text{Min f} = t_s * \ \text{S}_{\text{w\_timer}} \ (\text{C}_{\text{e}_\text{k}} * \text{P}_{(pump)_k}) \tag{4.5}$$

t_s is the sampling time; $\text{C}_{\text{e(k)}}$ is the ToU tariff function (R/KWh), $\text{P}_{\text{(pump)k}}$ is the electrical pump power (kW), at a given interval.

In addition to the constraints shown in Equation (4.8), the VFD control motor pump constraint is as follows:

$$\text{P}_{VFD_{(\text{min})}} \leq \text{P}_{VFD_{(\text{k})}} \leq \ \text{P}_{VFD_{(max)}} \tag{4.6}$$

Where: ($\text{P}_{VFD_{(\text{k})}}$) is the power of the water pump; ($\text{P}_{VFD_{(\text{min})}}$) is the minimum power of the water pump and ($\text{P}_{VFD_{(max)}}$) denotes the maximum threshold level that the pump power should not exceed, for any given operation.

The objective function, as shown in Equation (4.3), is a non-linear function, with a control variable, that should to be solved, in order to obtain the minimum switching cost of operation, in a timer-setting control water pumping system. The developed model is applied to the MATLAB software, which takes into account numerous limitations, such as the evaporation effect, rainfall effect, seepage effect, as well as pipe losses. Given the objective function, as well as constraints, the developed model is non-linear programming. Therefore,

the fmincon solver in MATLAB toolbox is used, to solve the optimization problem, since it contains nonlinear constraints [126].

The mathematical model should to be rearranged to fit the fmincon constraints, in order to solve the nonlinear problem, a function minimizer with linear and nonlinear constraints.

Mathematically, this is written as:

$$min\, fun(x)$$

$$s.t.\, A_x \leq b$$

$$A_{eq}x = B_{eq}$$

$$Lb \leq a \leq Ub$$

$$ceq(x) = 0$$

$$c(x) < 0$$

x_o = initial guess

Where:

$fun(x)$ is the objective function;

$A_x \leq b$ is the linear inequality constraint;

$A_{eq}x = B_{eq}$ is the linear equality constraint;

$Lb \leq a \leq Ub$ is the decision variable bounds;

$c(x) < 0$ is the nonlinear inequality constraint;

$ceq(x) = 0$ is the nonlinear equality constraints;

x is an integer number decision variable;

$j_{(x)}$ is a binary number decision variable;

x_o = initial guess, is the operator switching time settings.

The objective function is consequently replaced with $f(x)$. The decision variable, shown

in Equation (4.1 and 4.2), is a binary value, meaning, solely a 1 or a 0 may be taken as the switching status. The lower and upper boundaries, are therefore shown in Equation (4.4)

The control variable that should be optimized, is therefore constrained, as shown in Equation (4.6).

4.4. SIMULATION RESULTS AND DISCUSSION

As mentioned in Chapter 3, the baseline real-time data recorded from various measuring devices (or sensors), is captured in a spreadsheet, which includes the load demand as captured by the utility company in Bloemfontein, South Africa. The load of the system is determined by maintaining the load demand profile in Figure 3.5.

4.4.1. Timer switching control and reservoir water volume state.

Over the course of a 24 hour period, a timer may be programmed in various operation sequences. It functions similarly to a simple binary ON/OFF switching device. Figure 4.4, shows the electronic timer switching sequence for the water pumping system; the ON and OFF switching time is decided by the operator; in this case, the operator setting (S_{w_timer}) is made in anticipation of historical load demand data and to avoid the energy peak tariff costing period. This is based on the operator experience, as well as to avoid peak tariff period, while supplying the load.

Figure 4.5, shows the present state of the reservoir's water at any particular time. The ON state of the pump, according to this model, allows water to be pumped into the reservoir, filling it. Rain filling the reservoir, on the other hand, causes a rise in reservoir water volume as shown in Figure 3.4, whereas load demand outflow, evaporation, seepage and pipe losses, as shown in Figure 3.4, induces a drop in reservoir water volume.

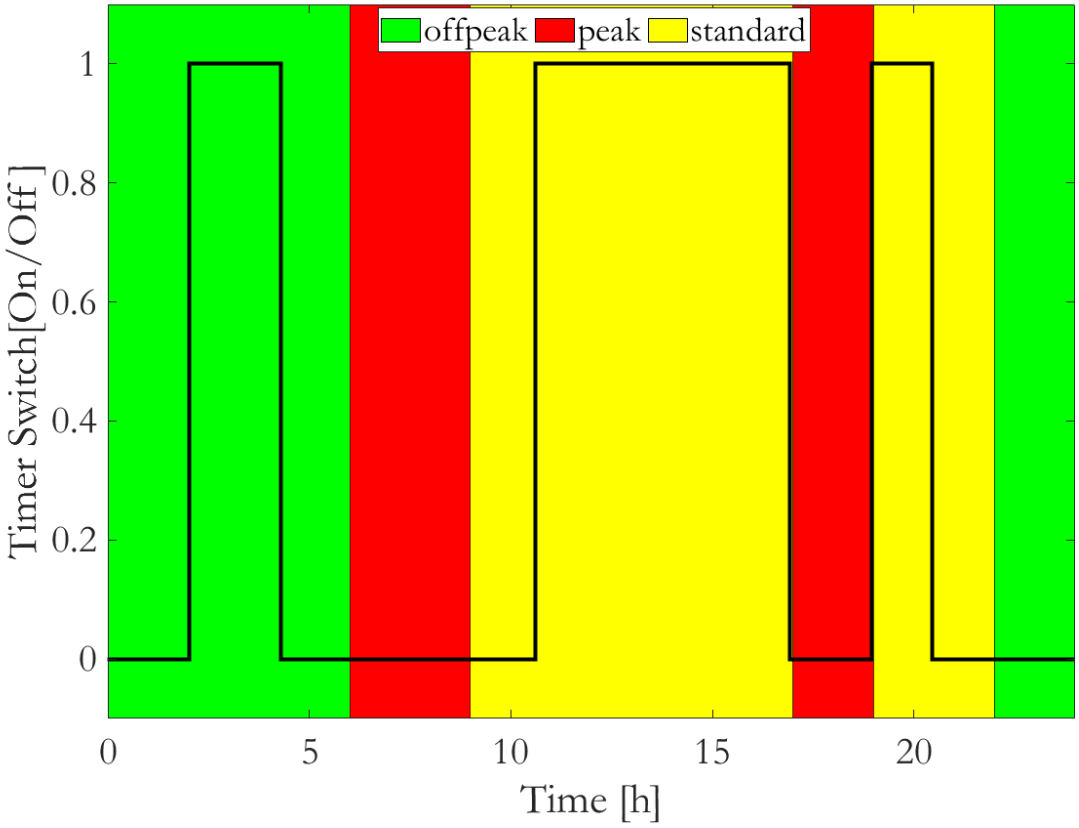

Figure 4.4: 24 hour electronic timer switching sequence

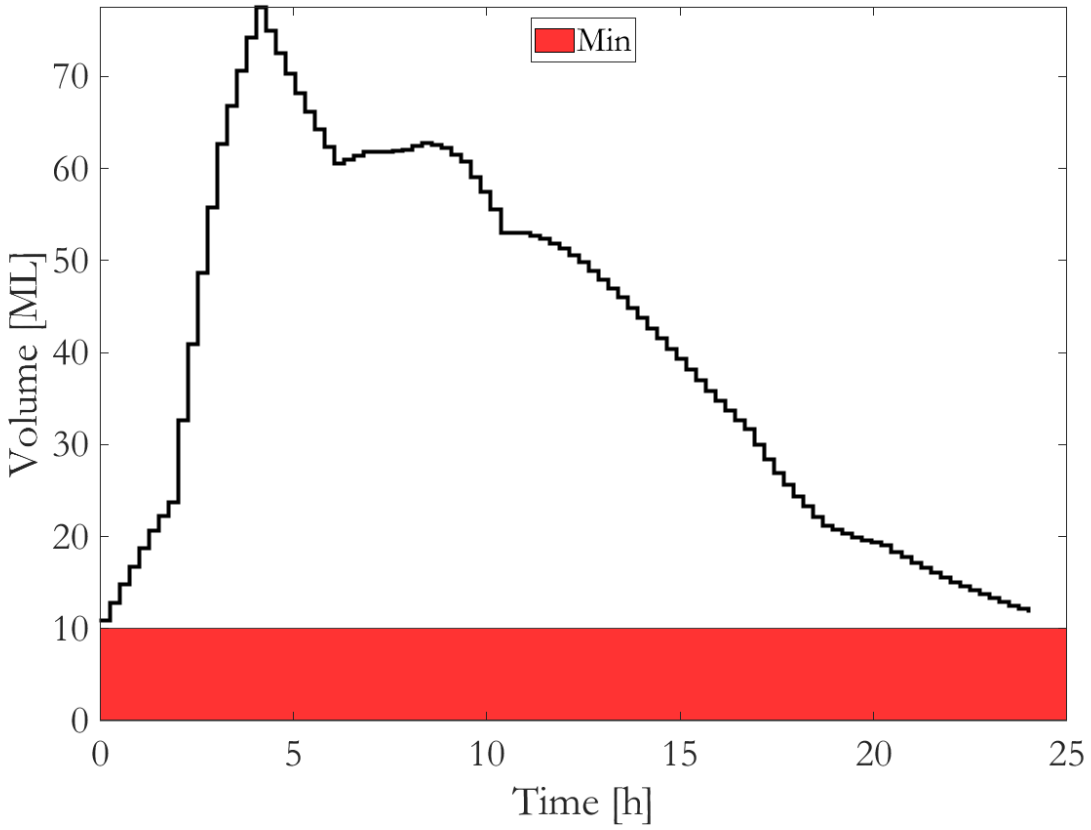

Figure 4.5: 24 hour timer-setting control state of water stored in the reservoir

In a sectional perspective, the water pumping system is explained, in terms of numerous tariff-pricing periods, as shown in Figure 4.4. Figure 4.5, shows the state of the reservoir for a typical switching period, which is the reservoir water volume, corresponding to the operator timer switching, in Figure 4.4.

System operation description, based on the timer set by the operator in each tariff area, as shown in Figure 4.4.

4.4.1.1 During the first off-peak (green) pricing period, from 00h00 to 06h00.

The pricing is at its lowest (off-peak) phase, as illustrated by the green delimited period in

Figure 4.4. The load demand in Figure 3.5, is on a declining trend at this time. The timer switch in Figure 4.4, turns ON after 2 hours of OFF time and remains ON for 2 and a half hours, while pumping water to the reservoir. Figure 4.5, shows a steady increase in water volume at the start of the day, which is mostly due to the rainfall water volume, shown in Figure 3.4, demonstrating that the rainfall water volume helps in topping up the reservoir. Therefore, assisting in reducing the switching ON-time of the pump. Adding to the rainfall water volume, the pump switches ON and pumps water into the reservoir, given the reservoir maximum water volume readings of 77.5 ML during this period. When the timer switch control is switched OFF, the power supply to the pump is turned off. As a result, illustrated in Figure 4.5, the reservoir's water volume level drops gradually in response to load demand. Evaporation is recorded as zero during this time, with a minimal seepage loss recorded.

4.4.1.2 During the first peak (red) pricing period, from 06h00 to 09h00.

This is a period when energy costs are at their highest (peak). Figure 3.5, shows a low load demand. Looking at Figure 4.4, the pumps are switched OFF, meaning that the Timer-setting control switch is turned OFF and the energy supply to the pumps is turned OFF. The reservoir volume in Figure 4.5, maintains a steady increase, which is as the result of the rainfall influencing the water volume in the reservoir. Therefore, at this stage turns to raise the water volume and produce a change in the water volume trajectory in the reservoir, refers to Figure 4.5. Evaporation and seepage remain at zero during this time.

4.4.1.3 During the first standard price period (Yellow) from 09h00 to 17h00.

The standard costing period is assumed to be between the peak and off-peak pricing. The load demand in Figure 3.5, increases as the day activity is about to begin. The timer-setting

control switch in Figure 4.4, turns ON after staying OFF for an hour during this period. It stays ON for the remainder of the time, supplying power to the pump to start pumping again. Adding to the high load demand, shown in Figure 3.5, the reservoir volume continues to decrease as the day progresses, implying that, as the day progresses and because the load demand is so high at this point, evaporation and seepage losses result in a reduction in the reservoir water volume. There has been no rain reported as of yet. However, as shown in Figure 3.4, a small amount of water evaporates, adding to seepage losses.

4.4.1.4 Switching during the second peak (red) pricing period from 17h00 to 19h00

The load demand begins to decrease at this hour of the day, however, at a very slow rate, as shown in Figure 3.5. The timer switch in Figure 4.4, shuts off the power supply to the pumps. The reservoir volume in Figure 4.5, shows a downward slope, implying the load-demand, the evaporation and seepage losses are the significant contribution to the rate of water decline in the reservoir, reference to Figure 3.4. Adding to the fact that the operator timer-setting control setting is set to avoid the switching ON of the pump, during the peak period.

4.4.1.5 Switching during the second standard (Yellow) pricing period, which runs from 19h00 to 22h00

During this period, the load demand is seen as decreasing, as shown on Figure 3.5. The timer-setting control switch turns ON and remains in the ON state for an hour and 50minutes before turning off, while the pump is running, as shown in Figure 4.4. At the same time, the water volume in the reservoir is marginally decreasing, as shown in Figure 4.5. As a result, the pumps are turned OFF and remain so for the remainder of the time.

However, the rate of evaporation drops to zero, along with a decrease in seepage loss, as seen in Figure 3.4 and rain begins to fall, filling the reservoir.

4.4.1.6 Switching during the 22h00 to 24h00 hour, the second off-peak (green) pricing period

The last part of the day is the off-peak costing period, during which the load demand continues to fall, as shown in Figure 3.5 and the pump is turned off, as shown in Figure 4.4. Figure 4.5, shows a declining trend in the reservoir water level, suggesting that the day is ending and that the final state of the pump should be addressed, in order to adequately analyse the various situations. Figure 3.4, shows an estimated 29ML of rainwater filling the reservoir, capable of meeting the load demand, in Figure 3.5, as well as the reserve reservoir water content.

4.4.2. VSD-Timer based switching control and reservoir water volume state.

The switching performance of the water pumping system is explained, in terms of the ToU pricing structure of the South African utility power supply, as shown in Figure 4.6. The VFD-Timer-setting control switching sequence, is shown in Figure 4.6, which shows that the pump is turned ON and OFF, according to a predetermined period, as shown on the time scale (X-scale). Secondly, the vertical scale (y-scale), shows how the VFD controls the motor's rotational speed at various intervals, based on the load demand level of the system. As a result, the pumped water level is as projected, in Figure 4.7.

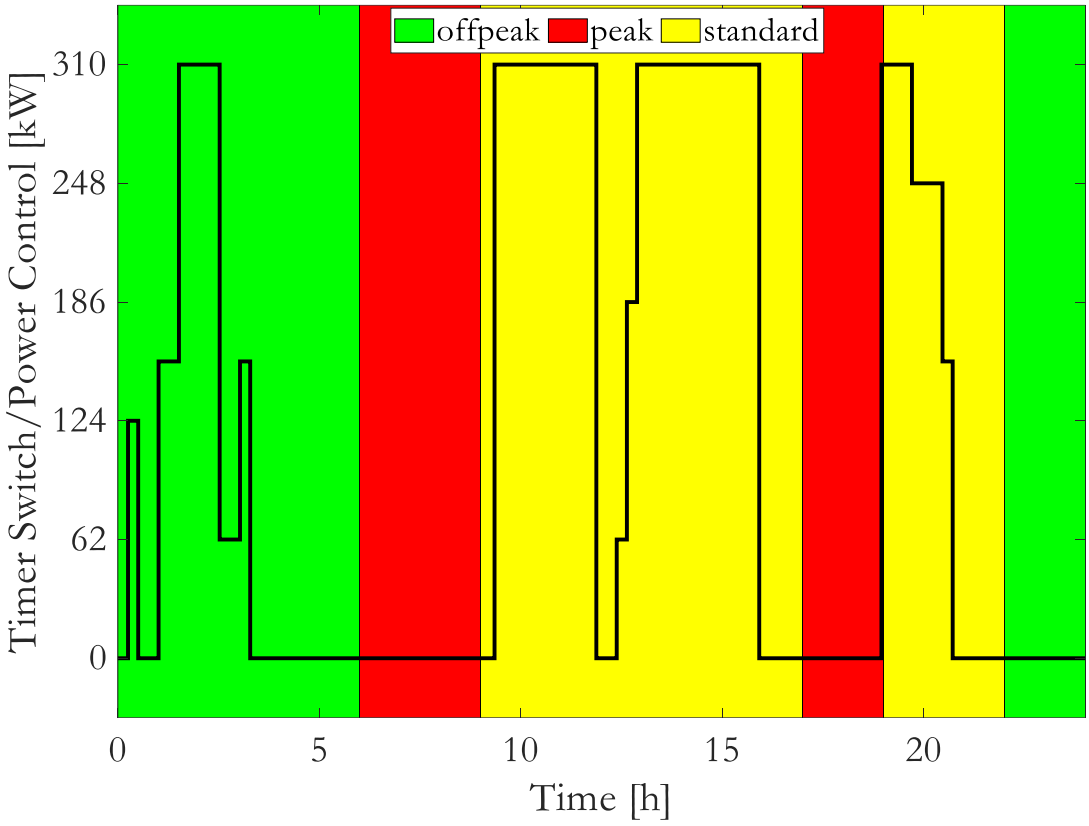

Figure 4.6: Electronic timer with VFD switching sequence

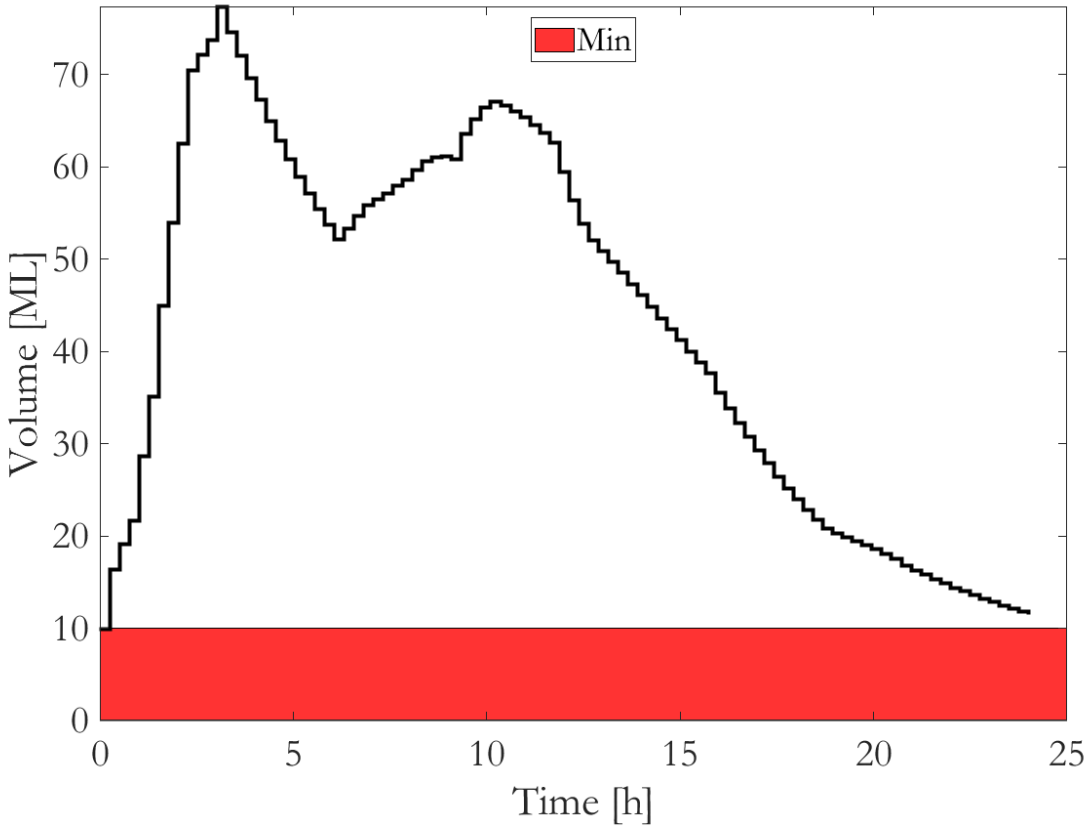

Figure 4.7: Timer-VFD control state of water stored in the reservoir

Explaining the pump switching outcome, as it pertains to the reservoir in each tariff period, as shown in Figure 4.7.

4.4.2.1 During the first off-peak (green) pricing period, from 00h00 to 06h00.

The pricing is at its lowest (off-peak) phase, as illustrated by the green delimited period on Figure 4.6. The load demand in Figure 3.5, is on a declining trend at this time. At the start of the day, the combined VFD-Timer-setting control switch, in Figure 4.6, turns the pump ON, while consuming 124kW from the supply. An indication that the rotational speed varies based on the load demand at the time, affecting the power supply to the pump directly.

Figure 4.7, shows a steady increase in water volume at the start of a day, which is further due to the rainfall water volume, shown in Figure 3.4, demonstrating that the rainfall water volume assists in topping up the reservoir. As a result, it assists the VFD in limiting the speed of the pump. While the pump continues to run as time passes, the power consumption increases to the pump maximum of 310kW. Water is pumped to fill up the reservoir, given the reservoir maximum water volume readings of 77.3 ML, during this period. When the timer switch control is switched OFF, the VFD power control stops operation, since the VFD power flow is interlocked with the timer-setting control switch. The power supply to the pump is turned OFF. Accordingly, as illustrated in Figure 4.6, the reservoir's water volume level drops gradually, in response to load demand. Evaporation is recorded as zero during this time, with a small seepage loss recorded.

4.4.2.2 During the first peak (red) pricing period, from 06h00 to 09h00.

This is a time when energy costs are at their highest (peak). Figure 3.5, shows a low load demand. Looking at Figure 4.6, the pumps are switched OFF, which means that the VFD-Timer-setting control switch is turned OFF and the energy supply to the pumps is zero kilowatt (kW). The reservoir volume in Figure 4.7, maintains a steady increase, which is an indication that rainfall influences the water volume in the reservoir, as shown in Figure 3.4. Therefore, at this stage, turns to raise the water volume and produces a change in the water volume trajectory in the reservoir, as seen in Figure 4.7. Evaporation and seepage remain at zero during this time.

4.4.2.3 During the first standard price period (Yellow) from 09h00 a.m. to 17h00.

The standard costing period is assumed to be between peak and off-peak pricing. The load demand, in Figure 3.5, increases as the day activity begin. After staying OFF for 34

minutes at the start of this period, the timer-setting control switch in Figure 4.6, turns ON, with a VFD power level regulated to 310kW. It stays ON for 2 hours and 55 minutes, without changing the regulated power, then turns OFF for 50 minutes before turning back ON, with the VFD still controlling the pump power, by slowing it down when the pump turns ON, stepping the power incrementally to 62kW, 186kW and 310kW, as shown in Figure 4.6. While the pump pumped water to the reservoir, the high load demand, shown in Figure 3.5, added to the evaporation and seepage losses, shown in Figure 3.4, permits the reservoir volume to decrease as the day progresses, implying that the load demand, evaporation and seepage losses, result in a reduction in reservoir water volume. Rain is reported as zero, as shown in Figure 3.4.

4.4.2.4 Switching during the second peak (red) pricing period from 17h00 to 19h00

The load demand begins to decrease during this period of the day, but at a very slow rate, as shown in Figure 3.5. The timer switch in Figure 4.6, shuts OFF the power supply to the pumps, implying no VFD operation is seen. The reservoir volume in Figure 4.7, shows a downward slope, implying the load-demand, the evaporation and seepage losses, are the significant contribution to the rate of water decline in the reservoir; refer to Figure 3.4. Adding to the fact that, the operator timer setting control, is configured to prevent the pump from switching ON during the peak period, while maintaining a zero kilowatt power.

4.4.2.5 Switching during the second standard (Yellow) pricing period, which runs from 19h00 to 22h00.

During this period, the load demand is seen as decreasing, shown in Figure 3.5. The timer-setting control switch turns ON and the VFD sets the power to 310kW. It's remains in the ON state for an hour and 70 minutes, before turning OFF; the VFD still controls the

pump's power, by slowing its power down to 248kW and 155kW, respectively, while the pump is running, as shown in Figure 4.6. At the same time, the water volume in the reservoir is marginally decreasing, as shown in Figure 4.7. Consequently, the pumps are turned OFF, resulting in zero kilowatts of power and will remain that way for the rest of the time. However, the rate of evaporation drops to zero, along with a decrease in seepage losses, as seen in Figure 3.4 and rain begins to fall, filling the reservoir.

4.4.2.6 Switching during the 22h00 to 24h00 hour, the second off-peak (green) pricing period

The last part of the day is the off-peak costing period, during which the load demand continues to fall, as shown in Figure 3.5 and the pump remains turned OFF, with no power usage, as shown in Figure 4.6. Figure 4.7, shows a declining trend in the reservoir water level, implying that the day and its activities are coming to an end and that the final state of the pump should be addressed, to optimally analyse the various situations. Figure 3.4, shows an estimated 29ML of rainwater filling the reservoir, capable of handling the load demand in Figure 3.5, as well as the reserve reservoir water content.

4.5. DAILY COST AND ENERGY CONSUMPTION

The daily operating cost, is determined by the pump's energy consumption rate; however the cost may vary differently, according to the ToU tariff's effect. In this section, the following control methods is compared in terms of cost and energy consumption when supplying the same load demand [127]. The model considers the influence in the water volume level in the reservoir, in Figures 4.5 and 4.7, when the effect of rainfall, seepage and evaporation is considered in the model.

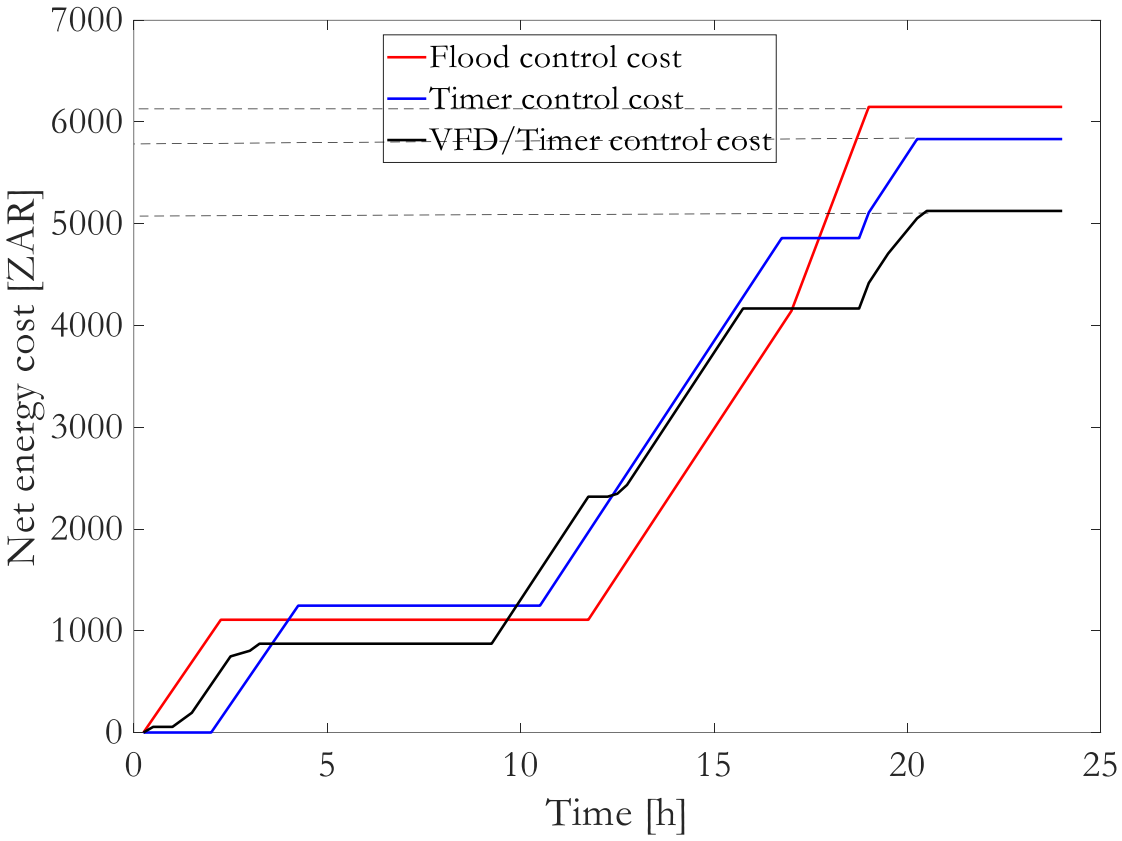

Figure 4.8: Control daily cost

Figure 4.8, shows that the control switching occurs at different intervals in each of the three circumstances, as indicated in Figures 3.10, 4.4 and 4.6, respectively. Starting from the initial value, the flood switching control, timer-setting control and VFD-Timer-setting control models will each record a separate cumulative energy consumption of the pump. Table 4.1, shows the breakdown by time of cost consumption and total energy consumed throughout the course of a 24 hour period. The table equally shows the time at which a change in energy consumption occurs, in each control system.

Table 4.1: Simulation results comparison

Time of operation (hour)	**Cost and energy consumption**					
	Flood switching control		Timer-setting control		VFD-Timer-setting control	
	Cost (ZAR)	Energy consumption (kWh)	Cost (ZAR)	Energy consumption (kWh)	Cost (ZAR)	Energy consumption (kWh)
00:00	0	0	0	0	0	0
02:25	1108	620	138.50	155	609.50	341
03:25	1108	620	692.70	465	872.70	488.30
04:25	1108	620	1247	697.50	872.70	488.30
09:25	1108	620	1247	697.50	872.70	488.30
10:50	1108	620	1247	697.50	1595	875.80
11:55	1108	620	1969	1008	2318	1186
15:55	3420	1783	4281	2248	4167	2178
16:55	3998	2093	4859	2558	4167	2255
17:00	4142	2248	4859	2635	4142	2255
18:55	5897	2713	4859	2635	4167	2255
19:00	6148	2868	5110	2713	4418	2333
20:25	6148	2868	5832	3100	5053	2674
20:50	6148	2868	5832	3100	5126	2713

24:00	6148	2868	5832	3100	5126	2713

The cumulative cost consumption, at every given stage of change in pump power, is recorded in Table 4.1, which is separated into the 24 hour time of day. The cost rating for all the pumps is zero at 00h00, meaning that the pumps are switched OFF and that no power is regulated by the VFD. The VFD-Timer-setting control model consumes a total of 5126 ZAR of energy, at 24h00, compared to 5832 ZAR and 6148 ZAR, for the timer-setting control and flood switching control models, respectively. An indicator that the VFD-Timer-setting control model outperforms the timer-setting control and flood switching control methods, in terms of serving energy, resulting in a lower consumption cost.

Table 4.1 further shows the variations in energy consumption for each control system. Looking at Table 4.1, the energy usage of the flood switching control model, at 17:00 hours, is 2248 kWh, compared to 2635 kWh and 2655 kWh for the timer and VFD-Timer-setting control models, respectively. The flood switching control model, on the other hand, costs 4142 ZAR, while the timer-setting control model costs 4859 ZAR and the VFD-Timer-setting control model costs 4142 ZAR. An indicator that the VFD-Timer-setting control model, by controlling the power of the motor in its operation, assists in cost reduction, while it may consume more energy than the flood switching control model.

4.6. SUMMARY

In this Chapter, the timer-setting control and the VFD are modeled and simulated for a water pumping system. The first model uses the timer-setting control switch to schedule the pumping sequence of the pump, by looking at the historical load and the ToU tariff structure of the utility unit. The second model incorporates the VFD control to the timer-setting control in regulating the power of the pump, according to the load demand level.

Evaporation losses, rainfall effect and seepage losses are all important aspects included in the models.

Comparisons are made in terms of operation and cost, when supplying the same load. The study found that, while the timer-setting control setting is strongly dependent on the operator settings, which are influenced by the historical data collection, the VFD control regulates the pump power, regardless of the operator settings and simply depends on the load demand level.

Results have shown that substantial cost is saved, using VFD-Timer-setting control configuration, as compared to using solely timer-setting control or flood switching control configuration.

CHAPTER 5: OPTIMAL SWITCHING CONTROL APPLIED TO A WATER PUMPING SYSTEM

5.1. INTRODUCTION

In this Chapter, two control models are developed to schedule the pump operation using real-time data in a water pumping system. The first case involves the use of an optimal control method. This control system is constraints the pump to operate solely when the ToU tariff is at off-peak or standard price zone. The model automatically looks at the real-time load demand, before making a switching decision to either turn the pump ON or OFF the pump.

The second case involves a VFD-Optimal control method. A variable frequency drive (VFD), is added to the optimal control water pumping system as an improvement to the model; the VFD adjusts the pump's power, while the optimal controller shifts the pumping period according to the tariff cost and load demand.

As a contribution, exogenous variables, such as the evaporation, seepage, as well as precipitation that may influence the water level in the reservoir, are incorporated into the model.

A water utility company, based in Bloemfontein, South Africa, is used as a case study. The load profile, reservoir size and pump size are all inputs to the model that was developed.

The economic performance of the developed model is compared to the baseline in simulations for a 24 hour pumping cycle. Various results are simulated using MATLAB, in reviewing the performance of the proposed model; the first is the pump's switching cycle, second is the water level (volume) in the storage reservoir and the third is the company's 24 hour cost.

5.2. OPTIMAL SWITCHING CONTROL SYSTEM MODEL

The optimal control model configuration of the water-pumping system, is shown in Figure 5.1. The setup has three sub-models, starting with the grid supply, which is the main power source that the system receives from the municipality and is measured in kilowatt-hours (kWh). The pump stations were made up of several electrical pumps and the optimal controller unit.

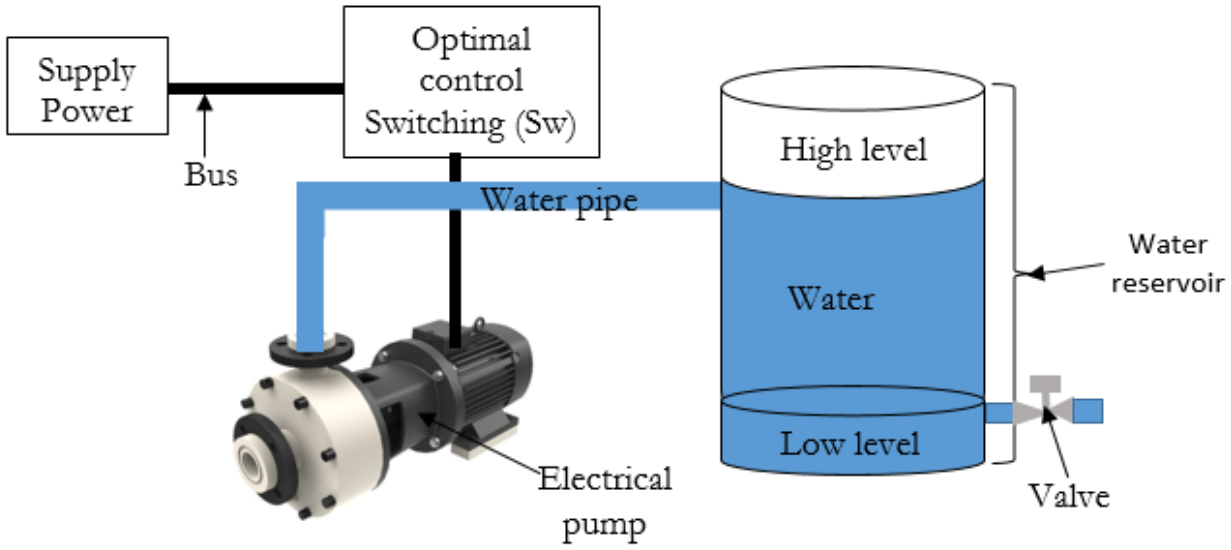

Figure 5.1: Proposed water-pumping control system schematic

5.3. MATHEMATICAL MODEL DEVELOPMENT

5.3.1. Optimal control model

The rated power of the electric pump, the pump flow rate, the reservoir lower and upper water level limits and the price of energy during any particular ToU period are all variables in

a water pumping system. Adding to the nonlinear restrictions, which outer to the fact that, they are based mostly on natural factors, such as evaporation, rainfall and seepage effect.

The control variable (S_w), makes the switching decision based on the ToU tariff cost of electricity that is consumed by the pump, adding to the water load demand at a given time. For the control variable linked to the power flows, Equation 5.1, shows a combined decision variable into one factor, to march the format used by the optimization solver in MATLAB software.

$$S_w = x(1:N) \tag{5.1}$$

Where: (Sw) is a control variable (Switch).

5.3.2. Objective function

The aim of operation cost minimization. is to minimize the energy consumed by the pump during its operation. This is accomplished by controlling the switching ON and OFF of the pump, in accordance with the ToU tariff period. The objective function (f_A), is written as:

$$f_A = t_s \sum_{k=1}^{n} (C_{e_k} * P_{(pump)_{rated}} * S_{w_k}) \tag{5.2}$$

Where:

t_s is the sample period (hours);

C_{e_k} is the ToU tariff function (R/kWh);

$P_{(pump)_{rated}}$ is the electrical pump rated power (kW);

S_{w_k} is the electrical pump switching state function.

x_i is an integer number decision variable.

The pump power rating is incorporated into the objective function, so that the objective function value, after optimization, will result to the total energy cost incurred.

The notion of comparing the water volume load demand, represented as $(V_{(Load)_k})$ to the estimated pumped volume, is known as reservoir water volume stability level minimization. Therefore, to improve on finding the effectiveness of the objective function, additional function is considered, (f_P) is to make the volume difference as low as possible. Therefore, equation (5.3) denotes:

$$f_P = t_s \sum_{k=1}^{n} \left(V_{(pump)_k} - V_{(Load)_k}\right)^2 \quad (5.3)$$

Where: $V_{(pump)_k}$ the estimated water pumped volume.

The fixed final state condition (f_C) is based on the state of reservoir water volume at the end of the control horizon, that should be equal to the water volume at the beginning of the control horizon. This means, the volume of water in the reservoir at the last sampling interval $(V_{(n)_k})$, should be equal to the initial water volume of the reservoir $(V_{(0)_k})$, without forgetting the effect of losses and precipitation.

$$f_C = t_s \sum_{k=1}^{n} \left(V_{(0)_k} - V_{(n)_k}\right)^2 \quad (5.4)$$

Considering the equation (5.2), (5.3) and (5.4), the objective function may be further developed as:

$$\text{Min f} = w_1\left(\text{t}_\text{s}\sum_{\text{k=1}}^{\text{n}}(\text{C}_{e_k} * \text{P}_{(pump)_{rated}} * \text{S}_{w_k})\right) + w_2(\text{t}_\text{s}\sum_{\text{k=1}}^{\text{n}}\left(\text{V}_{(pump)_k} - \text{V}_{(Load)_k}\right)^2 + \text{t}_\text{s}\sum_{\text{k=1}}^{\text{n}}\left(\text{V}_{(0)_k} - \text{V}_{(\text{n})_k}\right)^2) \quad (5.5)$$

Where: w_1 is the weighting factor for energy cost, w_2 is the weighting factor for comfort level, f is the objective function to be minimised, resulting from the power flows from the grid; k is the evaluated kth optimization sampling interval; n is the total number of sampling time in the simulation and Δt_s is the evaluated sampling time in the simulation. As a result, the number of sampling intervals and the optimization sampling intervals, as stated in Equation 5.5, define pump switching in this model.

The objective function is constrained by elements such as rainfall effect, seepage effect and evaporation, as indicated in Chapter 3, no chance is made on the input parameters. Therefore, this limitation remains the same in this model.

Therefore, the optimal control limit variable is specified by:

The minimum permissible volume (V_{min}) level that the water in the storage reservoir may reach, is denoted as:

$$V_{min} \leq V_0(1 - t_s)^{(k+1)} + Bt_s\sum_{k=0}^{n-1}\left(S_{w_k}(1 - t_s)^{(n-k-1)}\right) + t_s\sum_{k=0}^{n-1}(\gamma_k(1 - At_s)^{(n-k-1)}) \quad (5.6)$$

The maximum threshold level that the volume (V_{max}) may not exceed, for any given interval, is denoted as follows:

$$V_0(1-t_s)^{(k+1)} + Bt_s\sum_{k=0}^{n-1}\left(S_{w_k}(1-t_s)^{(n-k-1)}\right) + t_s\sum_{k=0}^{n-1}(\gamma_k(1-At_s)^{(n-k-1)}) \leq V_{max} \quad (5.7)$$

The constraint on the water volume inside the storage reservoir is presented in Equation (5.8):

$$V_{min} \leq V_{(k)} \leq V_{max} \quad (5.8)$$

To address the optimization problem, the mathematical model may be restructured, to match the SCIP constraints.

$$\text{minf}_{(x)} \text{ is such that } \begin{cases} C_{(x)} \leq 0 \\ Ceq_{(x)} = 0 \\ A.x \leq b \\ Aeq.x = beq \\ lb \leq x \leq ub \end{cases} \quad (5.9)$$

Where: $f_{(x)}$ is the objective function; $C_{(x)} \leq 0$ is the nonlinear inequality constraint; $Ceq_{(x)} = 0$ is the nonlinear equality constraints; $A.x \leq b$ is the linear inequality constraint; $Aeq.x = beq$ is the linear equality constraint; $lb \leq x \leq ub$ is the decision variable bounds, in this case the minimum water volume in the reservoir (V_{min}) and the maximum water volume in the reservoir (V_{max}).

5.3.3. Solver selection

With reference to Eq. (5.5), non-linearity of the optimal control problem, may be observed. This means that the developed model, as a whole, may be addressed as a nonlinear

problem. Therefore, the problem, with the proposed objective function, as well as constraints of operation, may be solved using any solver able to contend with a non-linear problem. In this case, the SCIP solver of the MATLAB optimization toolbox, is selected [25].

5.3.4. VFD-Optimal control model

The VFD control discussed in Chapter 2 and 4, is then combined with the optimal control model developed in Section 5.3.2, to generate a combined VFD-Optimal control system. Where: the VFD regulates the pump's power during periods of low demand. Therefore, the objective function, at this stage, is given an additional operator, that affects the change in power of the motor pump.

5.3.5. Objective function

The pump is further considered a control variable at this point, as it changes in power, as a result of the VFD control principle. As a result, the objective function is as follows:

$$\text{Min f} = w_1\left(\mathrm{t_s}\sum_{\mathrm{k=1}}^{\mathrm{n}}(\mathrm{C}_{e_k} * \mathrm{P}_{(pump)_k} * \mathrm{S}_{w_{optimal}})\right) + w_2(\mathrm{t_s}\sum_{\mathrm{k=1}}^{\mathrm{n}}\left(\mathrm{V}_{(pump)_k} - \mathrm{V}_{(Load)_k}\right)^2 + \mathrm{t_s}\sum_{\mathrm{k=1}}^{\mathrm{n}}\left(\mathrm{V}_{(0)_k} - \mathrm{V}_{(\mathrm{n})_k}\right)^2) \quad (5.10)$$

Where: w_1 is the weighting factor for energy cost, w_2 is the weighting factor for comfort level, f is the objective function to be minimised, $\mathrm{t_s}$ is the sample period; C_{e_k} is the ToU tariff function (R/kWh); $\mathrm{P}_{(pump)_k}$ is the electrical pump power (kW), required to meet the load demand; $\mathrm{S}_{w_{optimal}}$ is the electrical pump optimal switching setting.

The constraints and all other parameters mentioned in Chapter 5.3.2, remain the same in solving this VFD-Optimal control system.

The developed model applied to the MATLAB software, to perceive the grid energy savings. Using the optitoolbox in MATLAB, the SCIP Optimization solver is used to solve the optimization problem, since the problem consists of nonlinear constraints.

5.4. SIMULATION RESULTS AND DISCUSSION

As mentioned in Chapter 3, the baseline real-time data recorded from various measuring devices (or sensors), is captured in a spreadsheet, which includes the load demand as captured by the utility company in Bloemfontein, South Africa. The load of the system is determined, by maintaining the load demand profile in Figure 3.5.

5.4.1. Optimal switching sequence control and reservoir volume state.

Optimal switching is a method for determining a dynamical system's automated control horizon over time. This is accomplished by defining an objective function that is guided by particular constraints, in order to obtain a switching parting for the pump operation. The ON and OFF switching times represent the simulated outcome and are dependent on the objective function and other constraints, as shown in Figure 5.2.

Figure 5.3, describes the state of the water in the reservoir at any given time. According to this model, the ON state of the pump permits water to be pumped into the reservoir, thus filling it. Rainfall causes a rise in reservoir water volume, whereas load demand outflow, evaporation, seepage and pipe losses, cause a reduction in reservoir water volume, as shown in Figure 3.4.

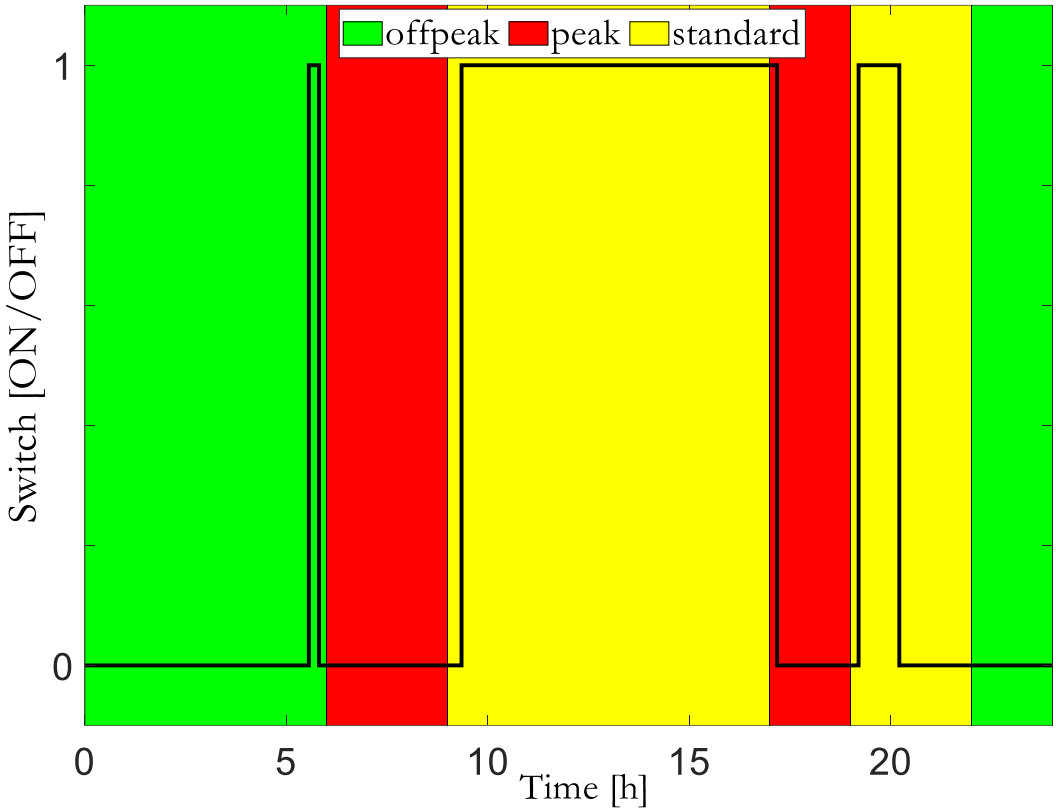

Figure 5.2: 24 hour optimal switching sequence

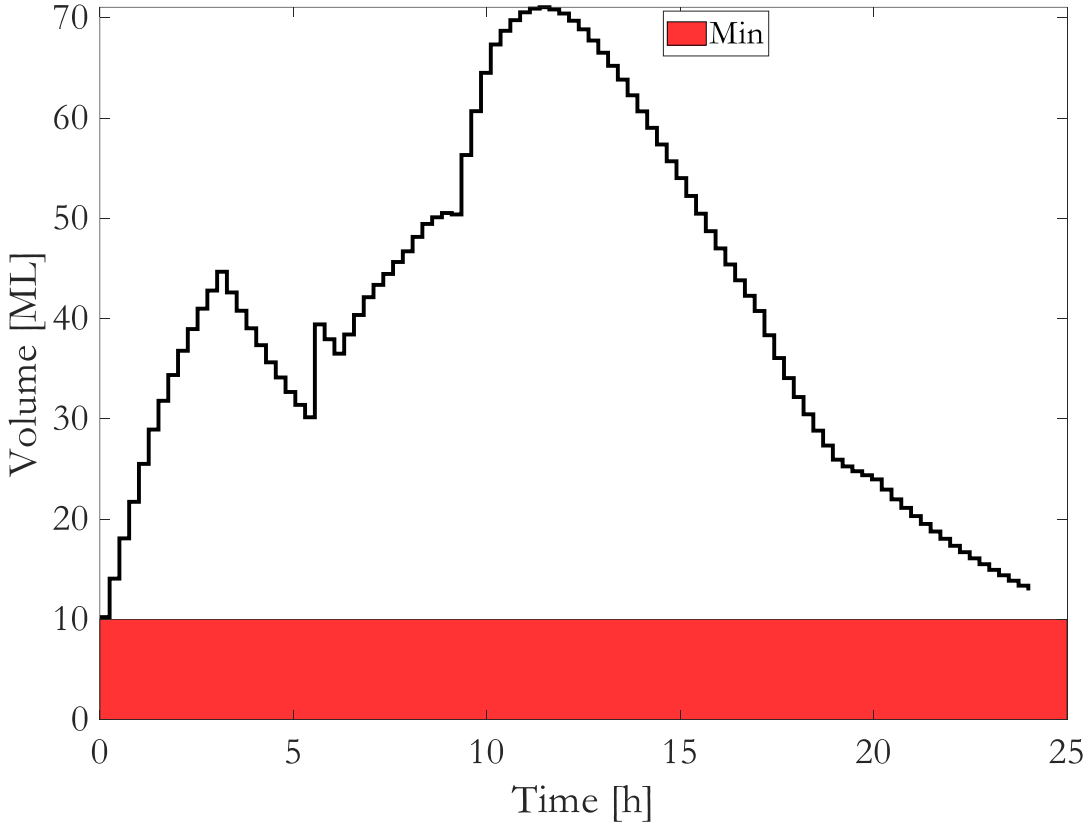

Figure 5.3: 24 hour optimal control state of water stored in the reservoir

The interpretation of the optimal switching control in Figure 5.2, together with the state of water stored in the reservoir in Figure 5.3, has been shared into the different tariff-pricing periods, as per the utility ToU rating.

5.4.1.1 During the first off-peak (green) pricing period, from 00h00 to 06h00.

The pricing is at its lowest (off-peak) phase, as illustrated by the green delimited period on Figure 5.2. The load demand in Figure 3.5, is on a declining trend at this time. After an initial 5 hours and 35 minutes OFF time, the optimal control switch in Figure 5.2, turns ON for 24 minutes, while pumping water to the reservoir. Figure 5.3, shows a steady increase in

water volume at the start of the day, which is mostly due to the rainfall water volume, shown in Figure 3.4, demonstrating that the rainfall water volume, helps in topping up the reservoir, assisting in reducing the switching ON time of the pump. During this period, the reservoir maximum state of water volume reading stands at 44.68 ML. When the optimal control switches OFF the pump, the power supply to the pump is turned off. As a result, as illustrated in Figure 5.3, the reservoir's water volume level drops gradually in response to the load demand. Evaporation is recorded as zero during this time, with a small seepage loss recorded, as shown in Figure 3.4.

5.4.1.2 During the first peak (red) pricing period, from 06h00 to 09h00.

This is a time when energy costs are at their highest (peak). Figure 3.5, shows a low load demand. Looking at Figure 5.2, the pumps are switched OFF, meaning that the optimal control turned OFF the energy supply to the pumps. The reservoir volume in Figure 5.3, maintains a steady increase, which is the result of the rainfall influencing the water volume in the reservoir. Therefore, causing a change in the water volume trajectory in the reservoir referring to Figure 5.3. Evaporation and seepage remain at zero during this time.

5.4.1.3 During the first standard price period (yellow) from 09h00. to 17h00.

The standard costing period is assumed to be between peak and off-peak pricing. The load demand in Figure 3.5, increases as the day activity is about starting. During this moment, the optimal control switch in Figure 5.2, switches ON after being OFF for 35 minutes. It remains on for the remainder of the period, delivering power to the pump to allow it to resume pumping. Because the load demand is just about to pick up, the reservoir state of water volume continues to increase for about 2 hours and 12 minutes, after which it starts to decrease, as shown in Figure 5.3. Meaning that, evaporation and seepage losses

result in a reduction in reservoir water volume, adding to the fact that the load demand is so high at this point. No rain is reported as of yet. However, as shown in Figure 3.4, a small amount of water evaporates, adding to seepage losses.

5.4.1.4 Switching during the second peak (red) pricing period from 17:00 to 19:00

The load demand begins to decrease at this hour of the day, however, at a very slow rate, as shown in Figure 3.5. The optimal control switch in Figure 5.2, shut off the power supply to the pumps. The reservoir volume in Figure 5.3, shows a downward slope, implying the load-demand, the evaporation and seepage losses are the significant contribution to the rate of water decline in the reservoir, as seen in Figure 3.4. Adding to the fact that the optimal control setting looks at the ToU tariff structure, to avoid scheduling the switching ON of the pump, during the peak period.

5.4.1.5 Switching during the second standard (yellow) pricing period, which runs from 19h00 to 22h00.

During this period, the load demand is seen decreasing, as shown in Figure 3.5. The optimal control switch turns ON and remains in the ON state for an hour and 10 minutes before turning off, while the pump is running, as shown in Figure 5.2. At the same time, the water volume in the reservoir is marginally decreasing, as shown in Figure 5.3. As a result, the pumps are turned OFF and remain so for the remainder of the period. However, the rate of evaporation drops to zero, along with a decrease in seepage loss, as seen in Figure 3.4 and rain begins to fall, filling the reservoir.

5.4.1.6 Switching during the 22h00 to 24h00 hour, the second off-peak (green) pricing period

The last part of the day is the off-peak costing period, during which the load demand continues to fall, as shown in Figure 3.5 and the pump is turned off, as shown in Figure 5.2. Figure 5.3, shows a declining trend in the reservoir state of water volume, suggesting that the day is drawing to a close and that the final state of the pump should be addressed, in order to properly analyse the various situations. Figure 3.4, shows an estimated 29ML of rain water filling the reservoir, capable of meeting the load demand in Figure 3.5, as well as the reserve reservoir water content.

5.4.2. VFD-Optimal control switching sequence and reservoir volume state.

Figure 5.4, shows the VFD-Optimal controller switching automated sequence, in order to acquire a lower daily usage charge, while maintaining the consumers' water supply reliability. The pumping rate slows down in some cases, when the load demand is low, as seen in Figure 5.4. The varied colours in Figure 5.4, represent the different pricing zones in a 24 hour period.

The intervals when the pumps are ON/OFF are indicated by the switching sequence in Figure 5.4. Furthermore, the VFD effect, which controls the pump's power, is clearly shown in Figure 5.4, where the power control axis (Y-axis) indicates occasions where the pump power supply is reduced, indicating that VFD control is limiting the power of the pump.

Figure 5.5, shows the VFD-Optimal system switching state of water stored in the reservoir, with the column describing changes in tariff prices over a 24 hour period. The power switching curve in Figure 5.4, controls the system's electrical pump and leads to the VFD-Optimal solution, in terms of reservoir water volume and maximum pumping energy cost, as shown in Figure 5.6.

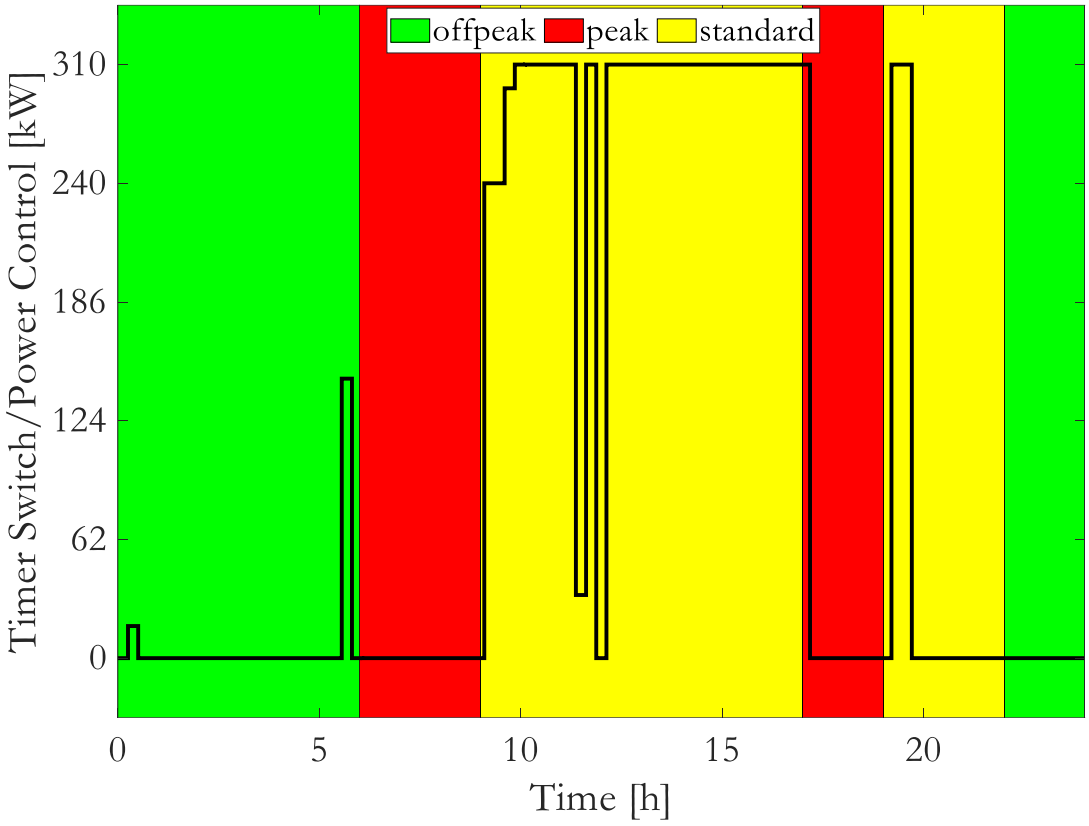

Figure 5.4: Optimal control with VFD switching sequence

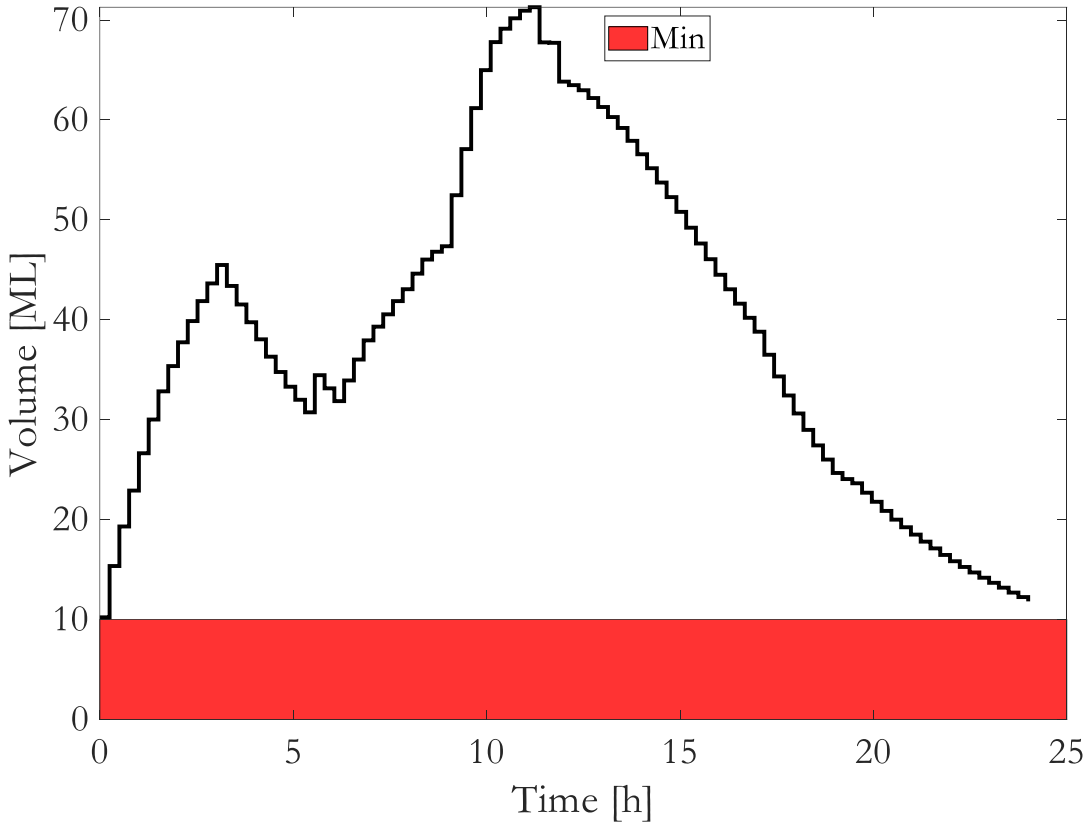

Figure 5.5: Optimal-VFD control state of water stored in the reservoir

This section looks at how the combined VFD-Optimal controller system works.

Explaining the pump switching outcome as it pertains to the reservoir in each tariff period, as shown in Figure 5.4.

5.4.2.1 During the first off-peak (green) pricing period, from 00h00 to 06h00.

The pricing is at its lowest (off-peak) phase, as illustrated by the green delimited period on Figure 5.4. The load demand in Figure 3.5, is on a decline. The switching ON of the pump occurs in two intervals, firstly, the pump turns ON, 25 minutes after the start of the period, with the VFD regulates the power consumption of 16kW and it stays ON for 25

minutes before turning off. The second instance occurs 5 hours later, where the pump is seen turned ON, with a VFD power setting of 145.8kW and stays ON for another 30 minutes. An indication that the rotational power varies, based on the load demand at the time, as shown on Figure 5.4.

Figure 5.5, shows a gradual increase in water volume at the start of the day, with a maximum water level of 45ML. This rate of reservoir water volume growth is related to the rainfall water volume, shown in Figure 3.4, illustrating that rainfall water volume aids in reservoir topping up. As a result, assisting the optimal control system in limiting the switching ON time of the pump, while helping the VFD with the power control of the pump. The pump's power source is turned off near the end of this period. As a result, as shown in Figure 5.5, the reservoir's state of water volume begins to progressively decrease, in response to load demand. During this time, there is no evaporation and merely a minor amount of seepage loss is recorded.

5.4.2.2 During the first peak (red) pricing period, from 06h00 to 09h00.

This is a time when energy costs are at their highest (peak). Figure 3.5, shows a low load demand. Looking at Figure 5.4, the pumps are switched OFF, which means that the VFD-Optimal control switch is turned OFF and the energy supply to the pumps is zero kilowatt (kW). The state of the reservoir volume in Figure 5.5, maintains a steady increase, which is an indication that rainfall influences the water volume in the reservoir, as shown in Figure 3.4. Therefore, causing changes in the water trajectory in the reservoir, referring to Figure 5.5. Evaporation and seepage remain at zero during this time.

5.4.2.3 During the first standard price period (yellow) from 09h00 a.m. to 17h00.

The standard costing period is assumed to be between peak and off-peak pricing. The load demand in Figure 3.5, increases as the day activity is about to start. The optimal control switch in Figure 5.4, turns ON, with a VFD power level regulated to 248kW. It stays ON for 40 minutes before increasing the power to 297.6kW and, later, to 310kW. After pumping for 2 hours and 37 minutes, the VFD slows the power to 33kW and 0kW, respectively, before returning to full capacity for the rest of the period, as shown in Figure 5.5.

The high load demand, indicated in Figure 3.5, together with evaporation and seepage losses, shown in Figure 3.4, allows the reservoir state of water volume to decline as the day proceeds, meaning that the load demand, evaporation and seepage losses result in a reduction in reservoir water volume. Figure 3.4, shows that rain is reported as zero.

5.4.2.4 Switching during the second peak (red) pricing period from 17h00 to 19h00

The load demand begins to decrease during this period of the day, however, at a particularly slow rate, as shown in Figure 3.5. The optimal control switching in Figure 5.4, shut OFF the power supply to the pumps, implying no VFD operation is seen. The reservoir volume in Figure 5.5, shows a downward slope, implying that, the load-demand, the evaporation and seepage losses are the significant contribution to the rate of water decline in the reservoir. Figure 3.4, shows a drop in evaporation and a minimal volume of water loss due to seepage.

5.4.2.5 Switching during the second standard (yellow) pricing period, which runs from 19h00 to 22h00.

During this period, the load demand is seen decreasing, as shown in Figure 3.5. The

optimal control switch turns ON and the VFD set the power to 310kW, it remains in the ON state for 51 minutes, before turning OFF. At the time, the water volume in the reservoir is marginally decreasing, as shown in Figure 5.5. Consequently, the pumps are turned OFF, resulting in zero kilowatts of power and will remain that way for the rest of the time. However, the rate of evaporation drops to zero, along with a decrease in seepage losses, as seen in Figure 3.4 and rain begins to fall, filling the reservoir.

5.4.2.6 Switching during the 22h00 to 24h00 hour, the second off-peak (green) pricing period

The last part of the day is the off-peak costing period, during which the load demand continues to fall, as shown in Figure 3.5 and the pump remains turned OFF, with no power usage, as shown in Figure 5.4. Figure 5.5, shows a declining trend in the reservoir water level, implying that the day and its activities are coming to an end and that the final state of the pump should be addressed, to adequately analyse the various situations. Figure 3.4, shows an estimated 29ML of rainwater filling the reservoir, capable of handling the load demand in Figure 3.5, as well as the reserve reservoir water content.

5.5. DAILY COST AND ENERGY COMPARISON

When supplying the same load demand, the daily operation costs of the various control methods are compared, during which the state of water volume level in the reservoir are considered. When the effects of rainfall, seepage and evaporation are incorporated in the model.

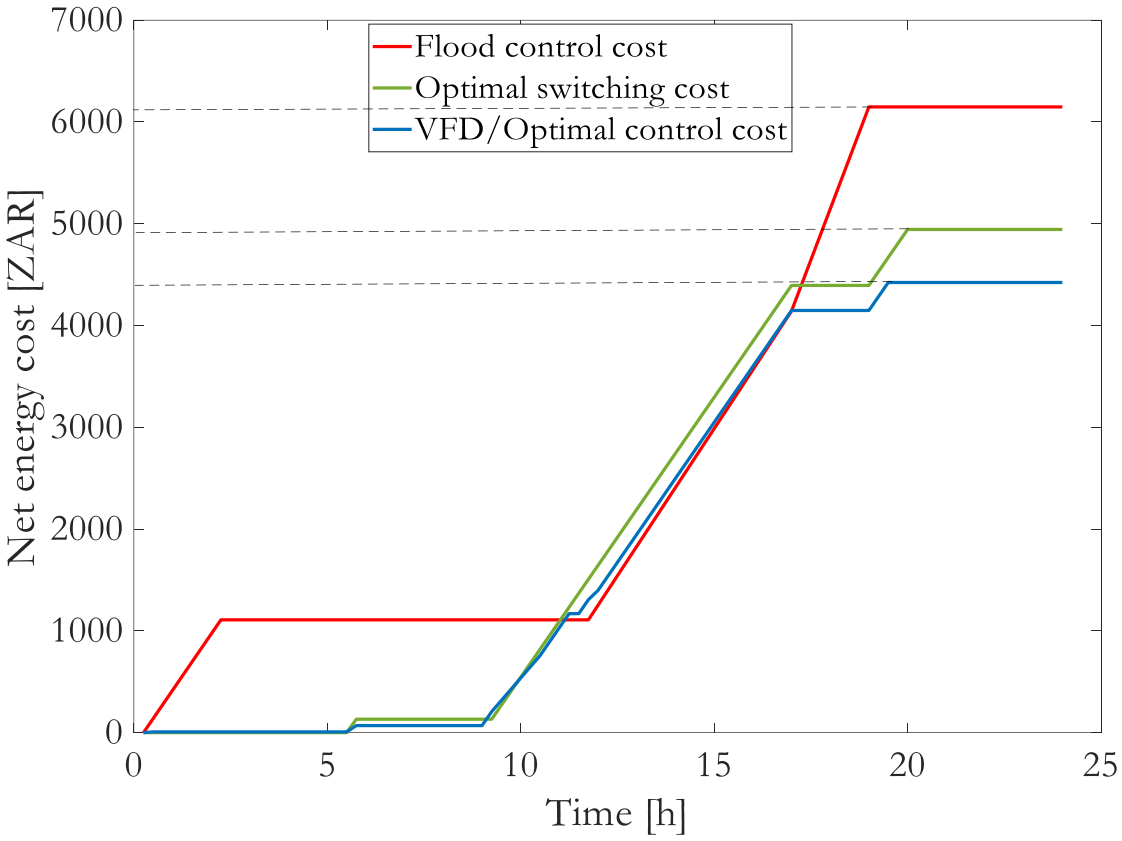

Figure 5.6: Control daily cost

Figure 5.6, shows that the control switching occurs at different intervals, in each of the three switching circumstances, as indicated in Figures 3.10, 5.2 and 5.4, respectively. Starting from the initial value, the flood switching control, optimal control and VFD-Optimal control models, will each record a separate cumulative energy consumption of the pump. Table 5.1 shows the breakdown by time of consumption and total energy cost consumed throughout the course of a 24 hour period. The table equally shows the time at which a change in energy consumption occurs in each control system model.

Table 5.1: Simulation results comparison

Time of operation (hour)	**Cost and energy consumption**					
	Flood switching control		Optimal control		VFD-Optimal control	
	Cost (ZAR)	Energy consumption (kWh)	Cost (ZAR)	Energy consumption (kWh)	Cost (ZAR)	Energy consumption (kWh)
00:00	0	0	0	0	0	0
02:25	1108	620	0	0	0	0
05:55	1108	620	131.80	73.75	69.20	38.72
09:00	1108	620	131.80	73.75	69.20	38.72
09:25	1108	620	131.80	73.75	206.70	156.70
11:55	1108	620	1507	737.5	1307	677.90
17:00	4148	2248	4394	2360	4148	2227
18:00	5145	2558	4394	2360	4148	2227
19:00	6148	2868	4394	2360	4148	2227
19:30	6148	2868	4669	2434	4423	2300
20:00	6148	2868	4944	2655	4423	2374
24:00	6148	2868	4944	2655	4423	2374

The cumulative cost consumption, at every given stage of change in VFD control power, is recorded in Table 5.1, which is separated into the 24 hour time of day. The power

rating for all the pumps, is zero at 00h00, meaning that the pumps are switched OFF and that no power is regulated. When looking at the VFD-Optimal control model at 24h00, it consumes 4423ZAR of energy, compared to 4944ZAR and 6148ZAR, for the optimal control and flood switching control models, respectively; an indicator that the VFD-Optimal control model served more energy when used to control the pumping of water to the reservoir.

Table 5.1, further shows the cumulative energy consumption, for each control system. The energy usage of the flood switching control model, at 18:00 hours, is 2558 kWh, compared to 2360 kWh and 2227 kWh for the optimal and VFD-Optimal control models, respectively. The flood switching control model, on the other hand, costs 5145 ZAR, while the optimal control model costs 4394 ZAR and the VFD-Optimal control model costs 4148 ZAR. When calculating the cost per unit of energy for this hour, the optimal control model saved energy, by controlling its operation according to the ToU tariff, and the VFD-Optimal control model saved more energy, by adjusting the power of the motor-pump.

5.6. SUMMARY

In this Chapter, an optimal control and the VFD are modeled and simulated for a water pumping system. Evaporation losses, rainfall effect and seepage losses are all significant aspects included in the model. The optimal control is used to schedule the pump operating period in a real time load demand changing environment, according to the objective function, that specifically informs shifting water pumping during the period where electricity will be less costly. VFD, on the other hand, controls the power of the pump, by looking at the load demand level at any giving state.

Comparisons are made, in terms of operation and cost, when supplying the same load. The study found that, although the optimal control model performed well in proactively scheduling pumping during a more affordable energy tariff period, in order to achieve a

reduced pumping energy cost. Adding a VFD to this model resulted in a more effective energy cost reduction. Applied to a real time water pumping operating system.

Results have shown that a substantial energy cost is saved using VFD-Optimal control configuration, as compared to using solely optimal control or flood switching control configuration. The study equally embraces a real-time control switching, that takes into consideration changes, such as load demand, rainfall, evaporation, seepage and pipe losses in the reservoir.

CHAPTER 6: TECHNO-ECONOMIC ANALYSIS

6.1. INTRODUCTION

Several economic performance indicators are available, to assess the water pumping system financial cost-effectiveness. These indications, may include the simple payback period (SPP), or the length of time it takes to repay the initial investment. The overall cost of an asset over its lifetime, which includes the asset's initial capital expenditures, ongoing maintenance, ongoing operating expenses and residual value at the asset's end of life, is referred to as life cycle cost (LCC). Benefits-to-cost ratio (BCR), further known as the relationship between relative costs and benefits of a proposed project represented in monetary or qualitative terms and rate of return (RoR), further known as the net gain or loss of an investment, over a specific time period.

The SPP is the most straightforward to comprehend, as its streamlined cost calculation. Nevertheless, it has limitations, in that it does not account for any future inflation, that may affect the overall cost throughout the course of a project. The SPP, further has the flaw of not accounting for cash flows, that occur after the payback period (PBP), as the project lifetime is not taken into account. As a result, the economic analysis is less accurate and investors are left with a rough cost or profit forecast. In light of this, methodologies such as like the BCR, LCC and RoR, provide a more accurate cost analysis, as compared to SPP, as they account for inflation and project duration [128]. In order to increase accuracy, a break-even point (BEP) analysis is performed after a whole life cycle cost evaluation, in terms of the baseline and proposed water pumping control systems. The savings over a particular project lifespan, may further be calculated by comparing the life cycle costs. This case study project lifetime, was set at 20 years.

6.2. INITIAL INSTALLATION COST

The initial investment cost of a flood switching control (baseline) water pumping system, is shown in Table 6.1. The centrifugal electric motor pump combination was selected, due to the manufacturer being approved by the Eskom rebate program. Furthermore, the manufacturers' products, all comply with Eskom and the South African Bureau of Standards (SABS) criteria. The prices, in Table 6.1, obtained from [129-130], are average component prices for the year 2020.

Table 6.1**:** Bill of quantity of the flood control system (Baseline)

Flood control component description	**Quantity**	**Cost (ZAR)**
200kW Centrifugal pump	1	131,373.64
110kW Centrifugal pump	1	60,463.70
Flood switch (level sensor) set	2	16,375.4
Total initial investment cost	4	208,212.74

An increase in investment was made to modernize the flood technique and replace it with the timer setting approach to manage the pumping of water in the water treatment facility. Table 6.2 shows the additional cost associated with purchasing and installing the timer device, if the initial VFD cost was included. The values in Table 6.2 are the typical component prices for 2020 as reported in [131-132].

Table 6.2**:** Bill of quantity of the Timer and VFD control system

Timer control component description	**Quantity**	**Cost (ZAR)**
VFD	2	73,759.68
Timer set	1	9,785.68
Total initial investment cost	4	83545.36

More money was invested in updating the timer control technique and replacing it with the optimal strategy. The extra expense related to getting and implementing the optimal control system is shown in Table 6.3. According to [133], the figures in Table 6.3 represent the typical component pricing for 2020.

Table 6.3**:** Bill of quantity of the optimal control and VFD system

Optimal control component description	**Quantity**	**Cost (ZAR)**
VFD	2	73,759.68
Optimal controller	1	10,000.00
Total initial investment cost	4	83759.68

6.3. MAXIMUM DEMAND CHARGE

Demand fee and energy charge, are the two components that make up the Maximum Demand Tariff. The energy charge, is based on the monthly energy consumption in units (kWh), however, the demand charge is based on the maximum demand in kVA. Therefore, the potential energy costs, incurred for the control case, were calculated, by adding

135.58ZAR/kVA of the maximum demand charge to the unit charge of electricity consumed per month [134].

6.4. DAILY CUMULATIVE ENERGY COST

To determine the daily cumulative energy cost (or energy charge), the primary objective function may be changed, so that Equation (6.1), may be applied, in this case [135]:

$$C_{(daily-EC)} = t_s * \sum_{k=1}^{n} P_{(pump)_k} * C_{ToU_k} * S_w \quad (6.1)$$

Where:

t_s is the sampling time;

$P_{(pump)_k}$ is the variable power of the motor pump (kW);

C_{ToU_k} is the time-of-use cost of electricity at each kth interval (ZAR/kWh);

S_w is the switching setting status of the motor pump.

With this, the daily cumulative daily cost values (ZAR), were obtained for the flood control, without the effect of rainfall, seepage and evaporation (Baseline 1), flood control with the effect of rainfall, seepage and evaporation (Baseline 2), timer setting control, VFD-Timer setting control, optimal control and VFD-Optimal control model, as illustrated in the appendix, Table B and C respectively.

Figure 6.1, illustrates the cumulative cost comparison between the optimally controlled system and the baselines for the water pumping system, respectively.

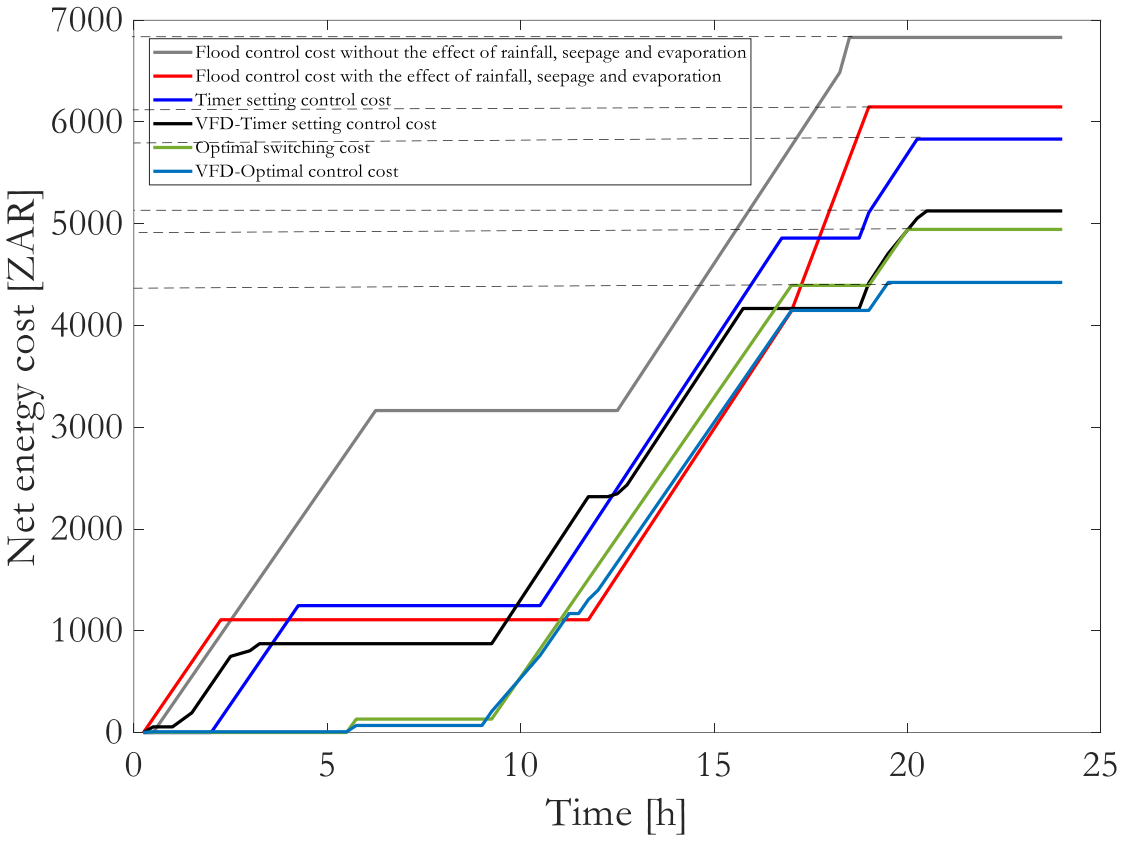

Figure 6.1: Control daily cost projection

Figure 6.1, shows that, using the various control strategies in a water pumping system, results in a gradual reduction in cost. All control mechanisms show zero energy consumption at the beginning of the pumping period, however, as the day goes on, the baseline 1 system, which is the flood switching control, without the effects of evaporation, rainfall and seepage, is observed to consume a significant amount of energy. All systems use the grid electricity, due to the ToU setting and the pump's VFD operation, the curves follow a somewhat sharp downward trend, as the pump is operated throughout the day, using the various control methods. This is particularly apparent for the VFD-Optimal control system. The optimal control case, avoids turning on during peak hours, avoiging high energy costs. In contrast to the peak period for both the baseline 1 & 2 systems, the cumulative cost curve further returns to its typical cumulative trend, for the ensuing standard and off-peak periods. The total cost for the water pumping system using the baseline without constraints (Baseline

1), baseline with constraints (Baseline 2), timer-setting control with fixed motor pump (Timer), VFD-Timer-setting control (Timer-VFD), optimal control with fixed motor pump (Optimal) and VFD-Optimal control (Optimal-VFD), case is currently 6831 ZAR, 6148 ZAR, 5126 ZAR, 4944 ZAR and 4423 ZAR, respectively.

6.4.1. Daily energy consumption.

Table 6.4, displays the energy consumption for the winter and summer seasons. According to the curves, the various control mechanisms, cause the total daily cost to rise every time switching is created within a particular ToU tariff period. The difference in overall cost, is seen at 24:00, the end of the control horizon. Considering Table 3.1, that shows the cost of the winter and summer tariff, according to the industrial tariff structure within a year. The daily total cost for the two seasons of the year, is displayed in Table 6.4.

Table 6.4**:** Daily seasonal energy consumption cost

24:00 cumulative energy cost						
Tariff period	Baseline 1 Cost (ZAR)	Baseline 2 Cost (ZAR)	Timer Cost (ZAR)	Timer-VFD Cost (ZAR)	Optimal Cost (ZAR)	Optimal-VFD Cost (ZAR)
Winter	6831	6148	5832	5126	4944	4423
Summer	4917	4119.20	4201.40	3690.90	3616	3591.70

6.4.2. Annual energy consumption.

Using the information in Table 6.4, the annual cost, as a whole, is computed. The winter season lasts 92 days, overall, while the summer season lasts 273 days, according to Eskom's

pricing structure [64]. The overall seasonal energy cost may be calculated, by multiplying the number of days in the season by the daily total energy cost, for that particular season. An approximation of the annual energy cost, in terms of electricity cost, may be determined, by adding the energy costs of the two seasons. The cost of energy, annually, in 2020, is shown in Table 6.5.

Table 6.5**:** Annual seasonal energy consumption cost

365 days cumulative energy cost						
Tariff period	Baseline 1 Cost (ZAR)	Baseline 2 Cost (ZAR)	Timer Cost (ZAR)	Timer-VFD Cost (ZAR)	Optimal Cost (ZAR)	Optimal-VFD Cost (ZAR)
Winter	628452	565616	536544	471592	454848	406916
Summer	1342341	1124541.60	1146982.20	1007615.70	987168	980534.10
Total annual energy-charge	1970793	1690157.60	1683526.20	1479207.70	1442016	1387450.10
Total annual demand charge	607659.72	607659.72	607659.72	607659.72	607659.72	607659.72
Total charge	2578452.72	2297817.32	2291185.92	2086867.42	2049675.72	1995109.82

6.5. LIFE CYCLE COST ANALSIS

The water pumping system's project lifetime, was set at 20 years, in order to lower the margin of error. The guaranteed collector lifespan of 10 years, served as the basis for choosing the 20-year lifetime, however, further studies indicate that the lifetime may exceed 30 years. As a result, the median number of years between the guaranteed and reported lifespans, was selected.

In order to account for future replacement upgrades to more efficient systems, the salvage costs for both the baseline and further control techniques, were concluded to be 20% of the initial cost of installation.

The future costs of components may be anticipated using the average inflation rate, displayed in Figure 6.2, by assuming that it may be equal to the interest rate [136, 137]. The replacement cost is calculated, using Equation (6.2).

$$C_{rep} = \sum_{k=1}^{N_{rep}} C_{cap} * k(1 + n.r) \quad (6.2)$$

Where:

C_{cap} is the initial capital cost for each component;

N_{rep} is the number of component replacement of the 20-year lifetime;

n is the lifespan for a specific component (years);

r is the average inflation rate, shown as 5.14% in Figure 6.2.

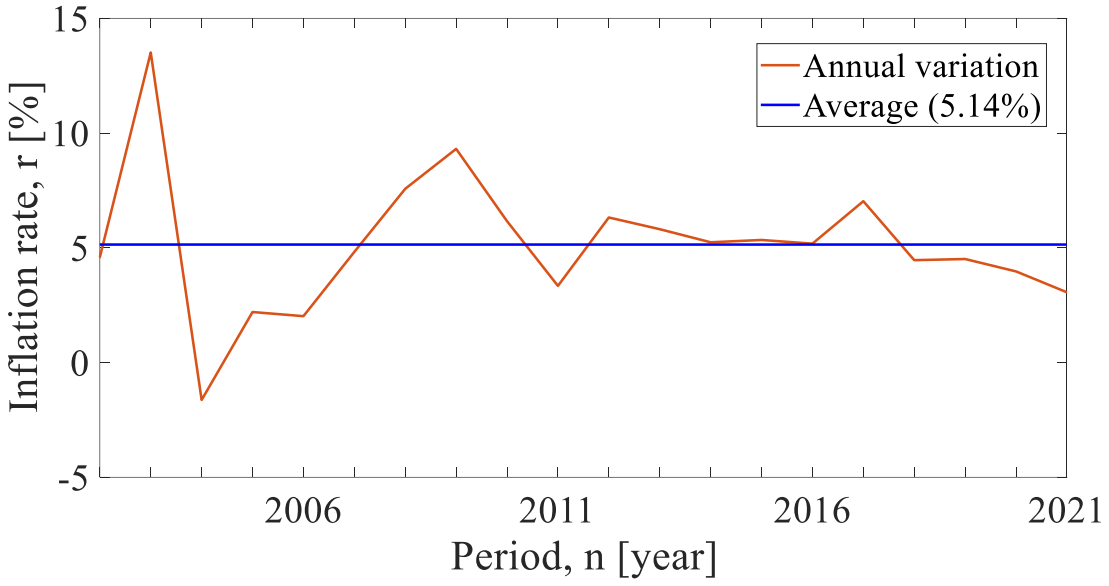

Figure 6.2: Inflation rate of South Africa from 2001 to 2021[138].

6.5.1. Baseline (Flood control water pumping) life cycle cost analysis.

The total replacement cost (C_{rep}), over the 20-year lifespan for the baseline (Flood control), are shown in Table 5.4. The flood switching control water pumping solely has one component, therefore, the total lifecycle replacement costs ($C_{rep-BTC}$), are equal to the replacement costs of the flood control, as denoted in Equation 6.3.

$$C_{rep-BTC} = C_{rep-flood\ control} \tag{6.3}$$

Equation 6.2, is used to calculate the total replacement cost ($C_{rep-flood\ control}$), over the project lifespan and the results are noted in Table 6.6.

Table 6.6: Total replacement cost for the flood switching control water pumping

Parameters	Value
Flood switch (level sensor) set	4
$N_{rep-flood\ control}$	2
$C_{rep-flood\ control}$	55332.82
$C_{rep-BTC}$	55332.82

The cumulative electricity costs, incurred over a 20-year lifespan for the baseline system, is shown in Table 6.5. The cost at the end of year 20, equates to the total cumulative electricity cost (C_{EC}), with an increase of 10% annually taken into account, shown in Equation 6.4.

$$C_{EC} = \sum_{k=1}^{20} C_{initial-EC} * k(1+a) \quad (6.4)$$

Where:

$C_{initial-EC}$ is the cumulative cost of energy at the end of year one (ZAR);

k represents the year at which the cumulative cost should be calculated (years);

a is the annual increase of 10%.

The operation and maintenance costs at the end of each year (k) of the flood switching control water pumping may be taken as 1% of the initial implementation cost, therefore Equation (6.5), is shown as:

$$C_{OM} = \sum_{k=1}^{20} C_{initial-OM} * k(1+r) \quad (6.5)$$

The initial cost of implementation ($C_{initial}$), equal to 208212.74 ZAR, shown in Table 6.1, is the cost of the flood control water pumping system.

A salvage cost ($C_{initial}$), is 20% of the initial implementation cost ($C_{initial}$), of the flood control water pumping system, may be calculated, using Equation 6.6.

$$C_{salvage} = 0.2 * C_{initial} \quad (6.6)$$

The addition of Equations (6.2-6.5) and the subtraction of the salvage cost ($C_{salvage}$), should be equal to the total life cycle cost for the flood control water pumping system, in Equation (6.7):

$$LCC_{flood\ control} = C_{initial} + C_{rep-BTC} + C_{EC} + C_{OM} - C_{salvage} \quad (6.7)$$

Table 6.7: Total life cycle cost for the flood control water pumping system

Cumulative Cost	Value (ZAR)
$C_{initial}$	19650.48
$C_{rep-BTC}$	55332.82
C_{EC}	131607485.84
C_{OM}	5495.49
$C_{salvage}$	3275.08
$LCC_{flood\ control}$	131,684,689.55

The total life cycle cost value $LCC_{flood\ control}$ (ZAR), using Equation (6.7), is shown in Table 6.7. Over a 20-year project lifetime, a total amount of approximately 131684689.55 ZAR, may be spent, in the case of the flood control water pumping system.

6.5.2. Timer setting control water pumping system life cycle cost analysis.

In the case of the timer setting control water pumping system, further components exist, with varying life expectancies. Therefore, Table 6.8 lists the parameters and their values.

Table 6.8: Total replacement cost for the timer switching control system

Parameters	Value
Timer (Electronic) lifetime (years)	20
$N_{rep-timer\ control}$	4
$C_{rep-timer\ control}$	55332.82
$C_{rep-BTC}$	55332.82

The total replacement costs (C_{rep}), calculated using Equation 6.2, for the 20 year project lifespan for all the timer setting control water pumping system's components, shown in Table 6.9 are added, in order to obtain the total lifecycle replacement costs (C_{rep-TC}), denoted in Equation (6.8).

$$C_{rep-TC} = C_{rep-timer\ control} \tag{6.8}$$

The same method for cumulating the electricity cost, with an annual 10% increment, was implemented for the timer control system, using Equation (6.4), for the timer setting control water pumping, in Equation (6.5) and (6.6), respectively. Equation (6.9), shows the calculation of the life cycle cost, for the timer setting control water pumping.

$$LCC_{flood\ control} = C_{initial} + C_{rep-Timer} + C_{EC} + C_{OM} - C_{salvage} \quad (6.9)$$

Table 6.9: Total life cycle cost for the timer control water pumping system

Cumulative Cost	Value (ZAR)
$C_{initial}$	11742.82
C_{rep-TC}	55332.82
C_{EC}	131227672.41
C_{OM}	3284.02
$C_{salvage}$	1957.13
$LCC_{flood\ control}$	131296074.93

Table 6.10: Total life cycle cost for the timer and VFD control water pumping system

Cumulative Cost	Value (ZAR)
$C_{initial}$	100254.43
C_{rep-TC}	55332.82
C_{EC}	119525330.42
C_{OM}	28037.36
$C_{salvage}$	16709.07
$LCC_{flood\ control}$	119692245.97

Equation (6.7), is used to calculate the total life cycle cost (LCC), for the timer-controlled water pumping system using the information in Table 6.9. The timer setting control water pumping system, should cost approximately 131296074.93 ZAR, in total, throughout the course of the 20 year project, using a fixed motor pump.

In a similar approach, using the information in Table 6.10 and Equation (6.9), the VFD and timer setting control water pumping system, should cost approximately 119692245.97 ZAR, in total, over the course of its 20 year lifespan.

6.5.3. Optimal control water pumping system life cycle cost analysis.

The optimal control water pumping system, has additional components with varying life expectancies. Therefore, Table 6.11 lists the parameters and their values [135].

Table 6.11: Total replacement cost for the optimal control water pumping

Parameters	Value
Optimal control (Computer system) lifetime	20
$N_{rep-optimal\ control}$	2
$C_{rep-optimal\ control}$	55332.82
$C_{rep-BTC}$	55332.82

The optimal control water pumping system's total replacement costs (C_{rep}), calculated using Equation 6.2, during the 20 year project lifespan, are added, to obtain the entire life cycle replacement costs (C_{rep-TC}), denoted in Equation (6.10) [139].

$$C_{rep-TC} = C_{rep-optimal\ control} \quad (6.10)$$

Equation (6.4), was used to calculate cumulative electricity costs, with an annual 10% increase, for the optimal control system. Equations (6.5) and (6.6), were used, to determine cumulative operation, maintenance expenses and salvage costs, respectively. The life cycle cost calculation, for the optimal control water pumping system, is shown in Equation (6.11) [139].

$$LCC_{flood\ control} = C_{initial} + C_{rep-TC} + C_{EC} + C_{OM} - C_{salvage} \quad (6.11)$$

Table 6.12: Total life cycle cost for the optimal control water pumping system

Cumulative Cost	Value (ZAR)
$C_{initial}$	12000.00
C_{rep-TC}	55332.82
C_{EC}	117395175.82
C_{OM}	3355.95
$C_{salvage}$	2000
$LCC_{flood\ control}$	117463864.59

Table 6.13: Total life cycle cost for the optimal and VFD control water pumping system

Cumulative Cost	Value (ZAR)
$C_{initial}$	100511.61
C_{rep-TC}	55332.82
C_{EC}	114269913.93
C_{OM}	28109.29
$C_{salvage}$	16751.93
$LCC_{flood\ control}$	114437115.72

Using Equation (6.11) and the information in Table (6.13), the optimal control water pumping system, total lifespan cost (LCC) value, is calculated. The optimal control water pumping system, should cost approximately 117463864.59 ZAR, in total, over the course of its 20 year lifespan. When using a fixed motor pump.

The total life cycle cost (LCC) value of the VFD and optimal control water pumping system, using Equation (6.11), with the data shown in Table 6.13, is calculated. Over a 20 year project lifetime, a total amount of approximately 114437115.72 ZAR, may be spent, in the case of the VFD and optimal control water pumping system, with the implementation of an optimal control energy management strategy.

6.6. BREAKEVEN POINT

When the total costs of two systems are equal, that is when the breakeven point (BEP), is reached. The proposed water pumping system, with the controlled energy management strategy, is contrasted to the baseline water pumping system, in terms of the overall cumulative yearly energy costs, for the course of the 20 year project [139]. The initial investment cost and the total annual cost are included in the cumulative cost curves. Costs

for the baseline and controlled pumping systems, over this time span, are shown on a similar axis, the point in time (years) in which these two curves intersect, is indicated as the systems breakeven point.

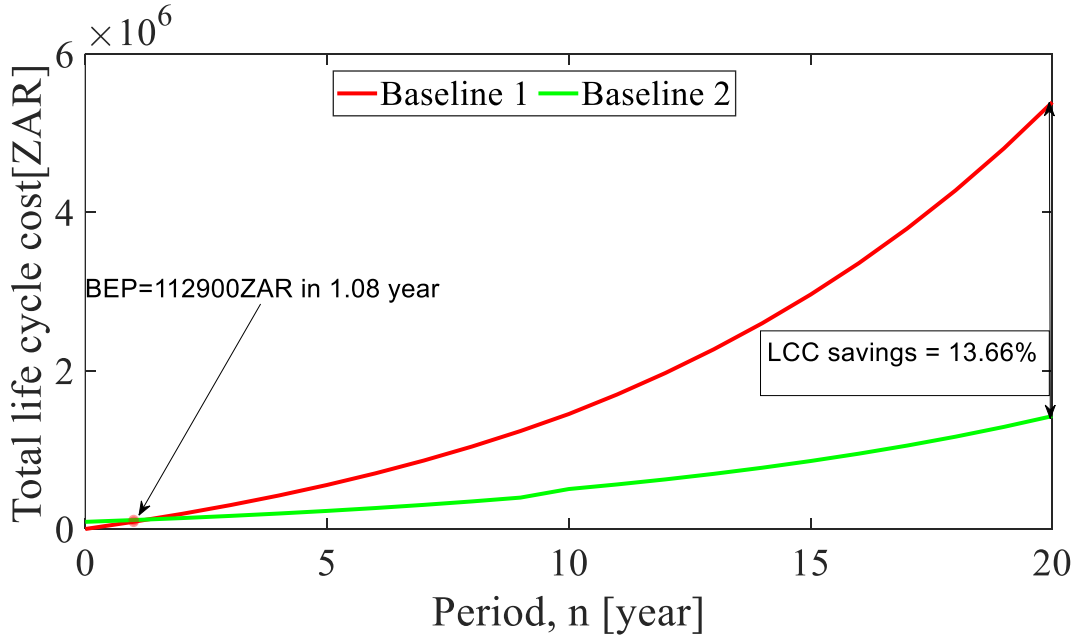

Figure 6.3: Baseline breakeven point

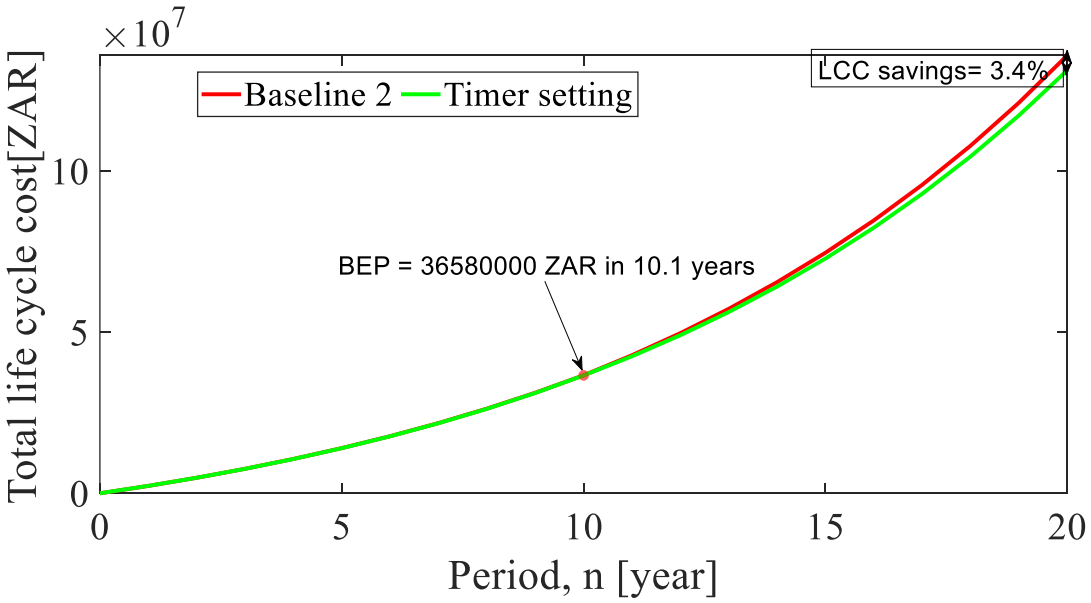

Figure 6.4: Baseline 2 and timer breakeven point

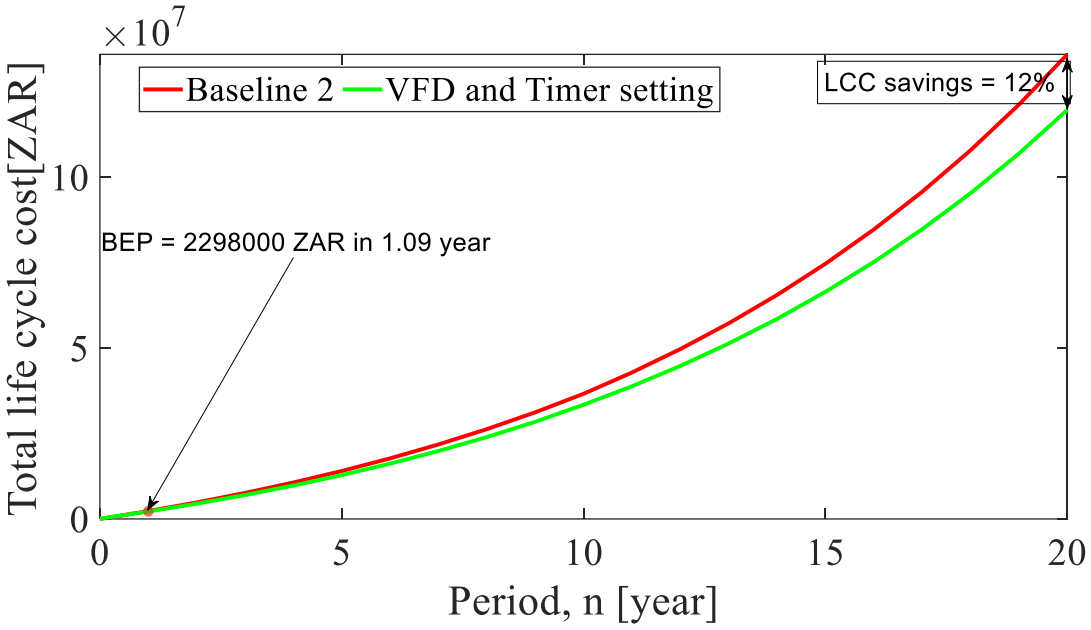

Figure 6.5: Baseline 2 and VFD-Timer breakeven point

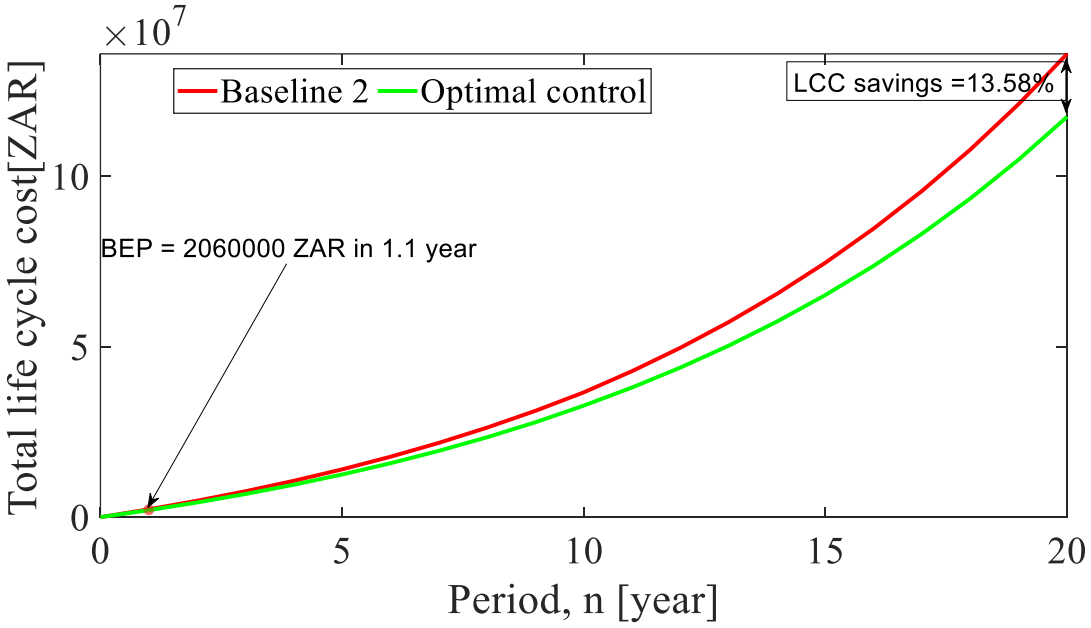

Figure 6.6: Baseline 2 and optimal control breakeven point

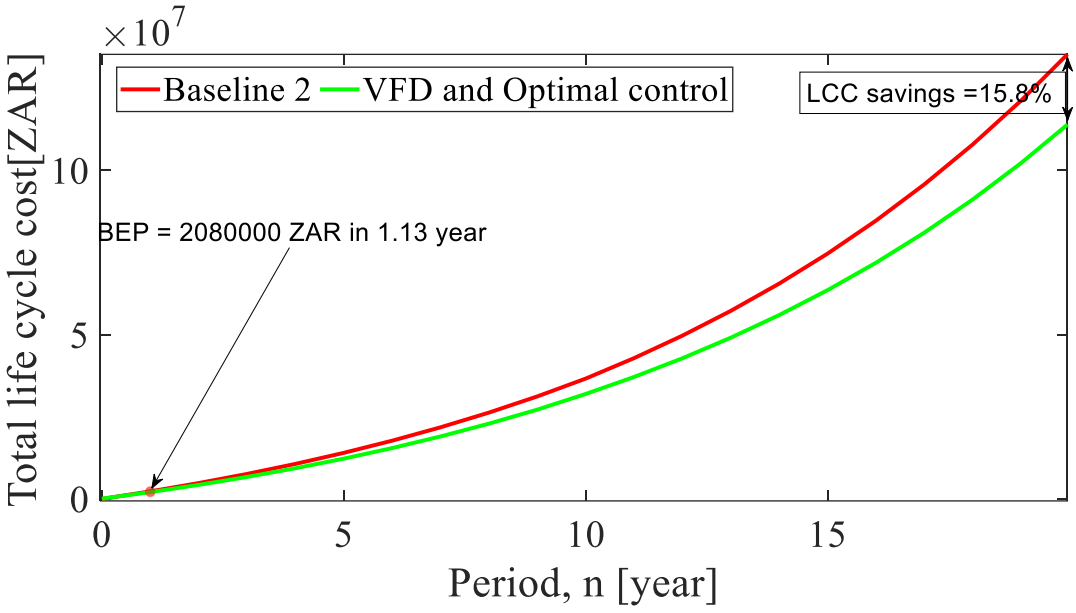

Figure 6.7: Baseline 2 and VFD-Optimal control breakeven point

The initial total cost of implementing the flood switching control, timer setting control, VFD-timer setting control, optimal control and VFD-optimal control, in the water pumping system, is shown in Table 6.1, 6.2 and 6.3, with further costs of 16375.40 ZAR, 9785.68 ZAR, 83545.36 ZAR, 10000.00 ZAR and 83759.68 ZAR, respectively. These values are, therefore, additional costs of implementing the control system to the traditional baseline system. The initial investment cost, which is the total present cost of energy, stated in Table 6.4, is increased by the entire yearly cost of energy, once the first year has passed. This amount is an accurate reflection of the first year amount of accumulated costs. In order to determine the annual energy expenses for the second year, following implementation, a 10% increase in the price of electricity, is used. This sum, is once more, added to the first year total cumulative cost. The same method is followed for years 3 to 10, as shown in Figures 6.3 to 6.7. In this curve, the statistics on the replacement costs and useful lives of each component, are taken into account, for increased accuracy of cumulative cost representation. It is evident, from the relevant Figures, that the breakeven point arrives early in the project's lifespan, showing a low investment capital in installing the control system in

place. A crucial economic performance measure, is the variations in total expenditure, at the conclusion of the project's lifespan, which is covered in Section 6.12.

6.7. LIFE CYCLE COST COMPARISON

Table 6.10, compares the life cycle costs of the baseline water pumping system, with those of the timer, VFD-timer, optimal and VFD-optimal control systems. The time required for cumulative cost equalization, is represented by the breakeven point analysis. The difference in LCC is computed to reflect the cost savings at the project's 20 year lifespan.

The gain in monitory value, over the course of 20 years, is seen in Table 6.14, when these control methods are applied to the water pumping system. As seen in Table 6.14, the baseline flood switching control system may generate savings of 16600700.90 ZAR, when the effects of precipitation, evaporation and seepage, are taken into account.

When the flood control switch is changed to a timed setting control system, an approximate sum of 4628965.20 ZAR, is saved. In a configuration that used the VFD and timer setting control, to manage the pumping system of a municipal water facility, observed an increase of 16232794.20 ZAR savings, observed over a 20 year period.

In a similar calculation, as shown in Table 6.14, when an optimal control system is employed to manage the pumping in a water facility, 18461175.50 ZAR is saved over 20 years. However, an additional 21487924.40 ZAR is saved, if a VFD is added to the optimal control system. Therefore, the long-term cost savings from a small technological and equipment enhancement, in a water pumping system over the course of the system's 20 year life cycle, is seen in Table 6.14.

Table 6.14: Life cycle cost comparison

LCC	Value (ZAR)
$LCC_{baseline\ 1}$	152,525,741.07
$LCC_{baseline\ 2}$	135,925,040.18
$LCC_{baseline\ savings}$	**16,600,700.90**
$LCC_{baseline\ 2}$	135,925,040.18
$LCC_{timer\ control}$	131,296,074.93
$LCC_{baseline\ 2\ and\ timer\ savings}$	**4,628,965.20**
$LCC_{baseline\ 2}$	135,925,040.18
$LCC_{VFD-timer\ control}$	119,692,245.97
$LCC_{baseline\ 2\ and\ VFD-timer\ savings}$	**16,232,794.20**
$LCC_{baseline\ 2}$	135,925,040.18
$LCC_{optimal\ control}$	117463864.60
$LCC_{baseline\ 2\ and\ optimal\ control\ savings}$	**18,461,175.50**
$LCC_{baseline\ 2}$	135,925,040.18
$LCC_{VFD-optimal\ control}$	114,437,115.72
$LCC_{baseline\ 2\ and\ VFD-optimal\ control\ savings}$	**2,1487,924.4**

6.8. SUMMARY

In this Chapter, the cost effectiveness of a water pumping system, was evaluated. The differences in cumulative energy consumption, unit and maximum demand costs, were noted, so that the annual energy usage and cost savings comparisons, were able to be made.

A breakeven point analysis, was carried out, to calculate when the proposed system would have an equivalent cumulative cost as compared to the baseline system. The analysis

showed that, in all the control systems implemented, after a minimum of a year, the cumulative costs were lower for the proposed system, as opposed to the baseline. It was observed that, after the breakeven point, the difference in cumulative costs significantly increased, with the baseline cost following an exponential trend.

To determine the savings over a 20 year project lifespan, a complete life cycle cost analysis was conducted, after the breakeven point analysis. When compared to baseline 1, the proposed baseline 2 flood control system, exhibited a cost reduction of 20841051.5 ZAR (or 13.66%), throughout the course of the project in the LCC analysis. The proposed timer control system, showed a cost savings of 4628965.2 ZAR, relating to 3.4% savings, throughout the course of the project, when compared to baseline 2, in the LCC analysis. The proposed VFD-timer control system, reflects a cost savings of 16232794.2 ZAR, which is equal to 12% savings, throughout the course of the project, when compared to baseline 2, in the LCC analysis. The proposed optimal control system, showed a cost savings of 18461175.6 ZAR, throughout the course of the project, when compared to baseline 2, in the LCC analysis, calculated as 13.58% cost savings, for a 20 year period. The proposed VFD-optimal control system, showed a cost savings of 21487924.45 ZAR, throughout the course of the project, when compared to baseline 2, in the LCC analysis. This was put into perspective, by calculating a cost savings of 15.8%.

The LCC analysis supports the hypothesis, in Chapter 1, Section 1.6, that the current pumping system (baseline), has a higher energy consumption rate, due to the lack of an efficient control water pumping system. However, the proposed system, may possess significantly lower costs than the baseline system, over the long term.

The LCC calculations, for the proposed systems, used a relatively low interest rate, which, if it were to be greater than the average estimated 5.14%, shown in Figure 6.2, may increase the costs of replacing components. Furthermore, given that previous cost increases were substantially higher in contrast, a 10% increase in electricity costs, may further be considered as a conservative assumption. In light of this, it may be concluded that the

calculated cost savings of 15.8%, in the VFD-optimal control system, represents the minimum savings that the suggested method is capable of achieving.

CHAPTER 7: CONCLUSION AND FUTURE STUDIES

7.1. SUMMARY

This Chapter serves as a conclusion on the research carried out on the optimal water pump scheduling in an open reservoir water-treatment system, incorporating the evaporation and seepage effect.

The major problem identified in Chapter 1, that was the substantial energy consumption by the pumps in a water pumping system, which is further due to evaporation, seepage and insufficient control during rainy periods. As a result, consumers are paying a high price for potable water.

Chapter 2 examines the numerous studies that deal with water pumping and the various proposed ways for reducing energy usage to a large extent. In a sustainable water development and service system, the energy management plan is reviewed using the POET based concept. The review highlights the fact that energy management, based on the POET concept, has an efficient coordinated energy saving capability under the performance, operation, equipment and technological operation of its processes.

The architecture of water purification processes was examined, and limits were identified, with the aim of achieving a result that minimizes both pumping and water expenses, while ensuring that the community always has access to drinkable water. The Chapter further covers the various control systems used in the field of water pumping, to determine the most optimal and accurate pump energy consumption control strategy. The flood switching control, timer-setting control, optimal control, and the inclusion of a VFD control system, were all examined.

Chapter 3 aims at developing and simulating a model that consists of a flood switching control system to regulate a water pump. The flood switching control system forms the

baseline of this research, known to be the early control system for water pumping into the reservoir. A proposed energy-saving configuration for a water-pumping system is modelled and developed, that uses the mechanical flood approach, to limit the pump's running time. The pump is turned ON/OFF, by the help of the flood switch and the energy cost calculated to indicate the cost of energy usage over a 24 hour period.

The construction of a mathematical model and simulations of the various control methods of the water pumping system are discussed in Chapters 3 through 5. These control methods employ diverse principles, including:

- Timer-setting control with a fixed motor pump.
- Optimal control using a fixed motor pump.
- Timer-setting control applied to a VFD control motor pump.
- Optimal control applied to a VFD control motor pump.

The aim of these controls in a water pumping system, is to reduce energy consumption when pumping water from one level to another.

To demonstrate the level of energy savings performance, in accordance with load demand-supply stabilization, the following comparison was made; a timer-setting control with a fixed motor pump was used against the baseline flood switching control. An optimal control with a fixed motor pump was used against the baseline flood switching control. A timer-setting control applied to a VFD motor pump was used against the baseline flood switching control and an optimal control applied to a VFD motor pump was used against the baseline flood switching control.

Simulations were conducted in comparing the energy usage of the various controllers, when applied to a water pump system. The model and simulated cases that were developed have further been used to:

- Analyze the relationship between the variation of the water load demand.

- Examine the relationship between variations in water evaporation, seepage and the influence of rainfall in the state of reservoir water levels.
- Examine the electrical pumps' switching relationships with the various control systems.
- Demonstrate the necessity of matching the water pump level to the demand of the user.
- Conduct the techno-economic assessments of the various control systems.

Objective-function and constraints were identified, modelled, developed and simulated, using MATLAB software, in solving a water pumping system. The system is powered by the utility grid energy, with the aim of obtaining a lower energy cost of pumping water from one state to another, in a water facility.

Figure 6.1, shows the growing sequence of energy costs over a 24 hour period, when the various models were tested against the identical load demand, as shown in Figure 3.5, taking into account variations due to rainfall, seepage and evaporation.

The various daily cost savings of the control systems are shown in Figure 3.11, 4.8 and 5.6. Various restrictions, such as pipe losses, the effect of water evaporation at the reservoir, seepage losses and the rainfall effect, remain the same in all the control systems, as does the fact that the load demand in this simulation remains the same as in Figure 3.5. In each simulated model, the net energy cost saving results found that:

- Comparing the cost of flood switching control energy without the effects of rainfall, seepage, or evaporation, against the cost of flood switching control energy with these effects included. Figure 3.11, shows that the rainfall effect contributes positively to the reservoir's water volume by increasing the reservoir's water volume, therefore, decreasing the rate at which the pumps are turned on. While the seepage and evaporation effects have a negative impact on the reservoir's water volume, they do so by lowering the reservoir's water level. The flood switching control system, on the other hand, helps in maintaining water volume stability at the reservoir's top and

bottom levels, preventing overflow or the water level falling below the reservoir's minimum limit. The introduction of these effects, to a water pumping system, may allow the pump to be stopped during the rainy period, thereby, reducing the pump energy consumption, according to the economic perspective described in Chapter 6. Over a 20-year period, energy costs are reduced by approximately 13,66%.

- Comparing the cost of timer-setting control energy versus the cost of a VFD-Timer setting control system. Energy is saved when a timer is used to control the ON/OFF of a water pump that pumps water into the reservoir, as shown in Figure 4.8. Adding a variable frequency drive (VFD) control to the system, on the other hand, further saves additional energy of about 8.83% ZAR, of the total timer control cost. Nonetheless, the timer programming is dependent on the operator's knowledge of the projected load demand, which in this case is based on historical load demand, making the system unsuitable for a fluctuating load demand, according to this study.
- Taking the optimal control energy cost and comparing it to the VFD-Optimal control cost. Figure 5.6, shows that utilizing the optimal control model to control the turning ON/OFF of a water pump in a water pumping system, saves energy. This is due to the model real-time operating principle, which examines the many permutations in real time, before making a pumping decision. However, by adding a variable frequency drive (VFD) to this system, an additional real-time energy savings amounts to 2.57% ZAR, of the optimal control costs, making it suitable for a changing load demand application.

It is further concluded that, when an optimal control system is used with a VFD power control water pump, the outcome indicates a significant reduction in energy usage, when pumping water in a water pumping system. As a result, lowering the energy usage of a water pumping system, could result in more affordable water for users.

7.2. PERFORMANCE ANALYSIS OF THE CONTROL STRATEGIES

The performance of the three major control strategies, is compared (i.e. flood switching control, timer-setting control and optimal control). The three major control methods, were to manage the pumping rate of water into the reservoir, as shown in the control daily cost projection, in Figure 6.1; taking into account, that all of the constraints are included and have an impact on their performance. The flood switching control approach, on the other hand, does not consider the energy supply ToU tariff, causing it to consume significantly more energy than the other control methods. In addition, the operator may choose the operating duration of the timer-setting control system, taking into account the ToU tariff and setting the operational time, to avoid the peak tariff periods. There is a drawback, in that the operator setting data is drawn from historical operations, which may not be accurate given changes that may occur in due time and calls on a change in water demand; the second drawback may occur, as the constraints change (i.e. evaporation, precipitation, seepage and leakage), may harm the system.

The optimal control method, as discourse in Chapter 2 and 5, works in real time, meaning that it makes a decision, by looking at the load demand and the constraints in real time changes, therefore, it is a unique method for controlling large water pumping systems.

7.3. MAJOR CONTRIBUTION

This study has contributed to the development of a model that responds to daily load demand in real time, by automatically adjusting the pumping rate of water to the reservoir in response to the load demand.

The developed model will further compensate for water losses, due to evaporation and seepage, which occur because of the reservoir being built with the top left open and the concrete constructed surroundings.

The operating model handles the effect of rainfall filling up the reservoir; the model manages the pump operation to maintain the water level at the required load demand level. Consequently, the optimal control model employs the ToU tariff structure for scheduling pumping operations, resulting in lower pump energy consumption.

7.4. SUGGESTIONS FOR FURTHER WORKS

To validate the produced model and simulation results, the proposed water-pump control system model could be applied in real time, on a physical prototype in future study.

The above technology is recommended for use in bulk water pumping plants and will offer a pleasing result, when combined with renewable energy supply systems.

Further research into the influence of distribution-pipe losses on water pumping, could be conducted; an area that was not covered in this study.

REFERENCES

[1] Franks, Water. Cambridge, UK: Royal Society of Chemistry, 2000.

[2] Bruins, H. J., 2000. Proactive Contingency Planning vis-a-vis Declining Water Security in the 21ste Century. Journal of Contingencies and Crisis Management, 8(2), pp. 63-72.

[3] A. Dai, K. Trenberth and T. Qian, "A Global Dataset of Palmer Drought Severity Index for 1870–2002: Relationship with Soil Moisture and Effects of Surface Warming", Journal of Hydrometeorology, vol. 5, no. 6, pp. 1117-1130, 2004.

[4] Clark, R. M., 2011. Modeling Water Quality in Distribution Systems Second Edition. s.l.: American Water Works Association.

[5] National Research Council, 2012. Water reuse: potential for expanding the nation's water supply through reuse of municipal wastewater. National Academies Press.

[6] Mukheibir, P., 2008. Water resources management strategies for adaptation to climate-induced impacts in South Africa. *Water Resources Management*, *22*(9), pp.1259-1276.

[7] Rasul, G., 2021. Twin challenges of COVID-19 pandemic and climate change for agriculture and food security in South Asia. *Environmental Challenges*, *2*, p.100027.

[8] Institute of Development Studies. 2022. *IDS Annual Review 2020 - Institute of Development Studies*. [online] Available at: <https://www.ids.ac.uk/publications/ids-annual-review-2020/> [Accessed 31 May 2022].

[9] Molobela, I.P. and Sinha, P., 2011. Management of water resources in South Africa: A review. African Journal of Environmental Science and Technology, 5(12), pp.993-1002.

[10] Kingsford, R.T., 2000. Ecological impacts of dams, water diversions and river management on floodplain wetlands in Australia. *Austral Ecology*, *25*(2), pp.109-127.

[11] Bukhary, S., Batista, J. and Ahmad, S., 2020. An analysis of energy consumption and the use of renewables for a small drinking water treatment plant. *Water*, *12*(1), p.28.

[12] Bloemwater.co.za. 2020. *Annual Reports – Bloemwater*. [online] Available at: <https://www.bloemwater.co.za/annual-reports/> [Accessed 2020].

[13] Pmg.org.za. 2021. DWS; Mhlatuze Water Board, Sedibeng Water Board and Overberg Water Board 2019/20 Annual Reports; with Deputy Minister | PMG. [online] Available at: <https://pmg.org.za/committee-meeting/33292/> [Accessed 13 July 2021].

[14] Förster, J.J., Downsborough, L. and Chomba, M.J., 2017. When policy hits practice: Structure, agency, and power in South African water governance. *Society & Natural Resources*, *30*(4), pp.521-536.

[15] Gov.za. 2022. *Water and sanitation | South African Government*. [online] Available at: <https://www.gov.za/about-sa/water-affairs> [Accessed 2022].

[16] "Reconciliation Strategy for the Large Bulk Water Supply System: Greater Bloemfontein Area", Dwa.gov.za, 2012. [Online]. Available: http://www.dwa.gov.za/Projects/Bloem/contacts.aspx. [Accessed: Jun- 2012].

[17] Ngancha, P.B., Kusakana, K. and Markus, E.D., 2018, October. Optimal Pump Scheduling in an Open Reservoir Water-Treatment Incorporating Evaporation and Seepage Effect. In *2018 Open Innovations Conference (OI)* (pp. 102-106). IEEE.

[18] Biehl, W.H. and Inman, J.A., 2010. Energy optimization for water systems. *Journal-American Water Works Association*, *102*(6), pp.50-55.

[19] Pulido-Calvo, I. and Gutiérrez-Estrada, J.C., 2011. Selection and operation of pumping stations of water distribution systems. *Environ. Res. J*, *5*(3), pp.1-20.

[20] Reca, J., García-Manzano, A. and Martínez, J., 2014. Optimal pumping scheduling for complex irrigation water distribution systems. Journal of Water Resources Planning and Management, 140(5), pp.630-637.

[21] Planells Alandi, P., Carrión Pérez, P., Ortega Álvarez, J.F., Moreno Hidalgo, M.Á. and Tarjuelo Martín-Benito, J.M., 2005. Pumping selection and regulation for water-distribution networks. Journal of Irrigation and Drainage Engineering, 131(3), pp.273-281.

[22] Moradi-Jalal, M., Marino, M.A. and Afshar, A., 2003. Optimal design and operation of irrigation pumping stations. *Journal of Irrigation and Drainage Engineering*, *129*(3), pp.149-154.

[23] Friedrich, K., Grossman, R.L., Huntington, J., Blanken, P.D., Lenters, J., Holman, K.D., Gochis, D., Livneh, B., Prairie, J., Skeie, E. and Healey, N.C., 2018. Reservoir evaporation in the Western United States: current science, challenges and future needs. *Bulletin of the American Meteorological Society*, *99*(1), pp.167-187.

[24] Craig, I., Aravinthan, V., Baillie, C., Beswick, A., Barnes, G., Bradbury, R., Connell, L., Cooper, P., Fellows, C., Fitzmaurice, L. and Foley, J., 2007. Evaporation, seepage and water quality management in storage dams: a review of research methods. *Environmental Health*, *7*(3), pp.84-97.

[25] Hohne, P.A., Kusakana, K. and Numbi, B.P., 2018. Scheduling and economic analysis of hybrid solar water heating system based on timer and optimal control. *Journal of Energy Storage*, *20*, pp.16-29.

[26] Physics.weber.edu. 2021. Law Of Gravity. [online] Available at: <http://physics.weber.edu/amiri/physics1010online/WSUonline12w/OnLineCourseMovies/CircularMotion&Gravity/reviewofgravity/ReviewofGravity.html> [Accessed 8 January 2021].

[27] Gupta, V.K., Ali, I., Saleh, T.A., Nayak, A. and Agarwal, S., 2012. Chemical treatment technologies for waste-water recycling—an overview. Rsc Advances, 2(16), pp.6380-6388.

[28] Wimalawansa, S.J., 2013. Purification of contaminated water with reverse osmosis: effective solution of providing clean water for human needs in developing countries. *International journal of emerging technology and advanced engineering*, *3*(12), pp.75-89.

[29] Ormsbee, L.E. and Lansey, K.E., 1994. Optimal control of water supply pumping systems. Journal of Water Resources Planning and Management, 120(2), pp.237-252.

[30] Gopal, C., Mohanraj, M., Chandramohan, P. and Chandrasekar, P., 2013. Renewable energy source water pumping systems—A literature review. Renewable and Sustainable Energy Reviews, 25, pp.351-370.

[31] Ramos, H.M., Costa, L.H.M. and Gonçalves, F.V., 2012. Energy efficiency in water supply systems: GA for pump schedule Optimization and ANN for hybrid energy prediction. Water Supply System Analysis-Selected Topics.

[32] Tawanda, T., Optimal Pump Scheduling Considering Resetting Reservoir to Minimum Level and Rescheduling due to Pump Maintenance.

[33] Reca, J., García-Manzano, A. and Martínez, J., 2015. Optimal pumping scheduling model considering reservoir evaporation. Agricultural Water Management, 148, pp.250-257.

[34] Yannopoulos, S.I., Lyberatos, G., Theodossiou, N., Li, W., Valipour, M., Tamburrino, A. and Angelakis, A.N., 2015. Evolution of water lifting devices (pumps) over the centuries worldwide. *Water*, *7*(9), pp.5031-5060.

[35] Xia, X. and Zhang, J., 2010. Energy efficiency and control systems–from a POET perspective. IFAC Proceedings Volumes, 43(1), pp.255-260.

[36] Gleick, P.H., 1994. Water and energy. *Annual Review of Energy and the environment*, *19*(1), pp.267-299.

[37] Del Borghi, A., Strazza, C., Gallo, M., Messineo, S. and Naso, M., 2013. Water supply and sustainability: life cycle assessment of water collection, treatment and distribution service. The International Journal of Life Cycle Assessment, 18(5), pp.1158-1168.

[38] Hohne, P.A., Kusakana, K. and Numbi, B.P., 2020. Improving energy efficiency of thermal processes in healthcare institutions: A review on the latest sustainable energy management strategies. *Energies*, *13*(3), p.569.

[39] Wanjiru, E.M. and Xia, X., 2015. Energy-water optimization model incorporating rooftop water harvesting for lawn irrigation. Applied energy, 160, pp.521-531.

[40] Malinowski, P.A., Stillwell, A.S., Wu, J.S. and Schwarz, P.M., 2015. Energy-water nexus: Potential energy savings and implications for sustainable integrated water management in urban areas from rainwater harvesting and gray-water reuse. Journal of Water Resources Planning and Management, 141(12), p.A4015003.

[41] Xu, Z., Guan, X., Jia, Q.S., Wu, J., Wang, D. and Chen, S., 2012. Performance analysis and comparison on energy storage devices for smart building energy management. IEEE Transactions on Smart Grid, 3(4), pp.2136-2147.

[42] Matsubayashi, S. and Nagamitsu, S., Panasonic Corp, 2006. Energy management system, energy management method, and unit for providing information on energy-saving recommended equipment. U.S. Patent 6,983,210.

[43] Sallem, S., Chaabene, M. and Kamoun, M.B.A., 2009. Energy management algorithm for an optimum control of a photovoltaic water pumping system. Applied Energy, 86(12), pp.2671-2680.

[44] Shalaby, M.M., Nassar, I.N. and Abdallah, A.M., 2021. Evaporation suppression from open water surface using various floating covers with consideration of water ecology. *Journal of Hydrology*, *598*, p.126482.

[45] Saggaï, S. and Bachi, O.E.K., 2018. Evaporation reduction from water reservoirs in arid lands using monolayers: Algerian experience. *Water resources*, *45*(2), pp.280-288.

[46] Condie, S.A. and Webster, I.T., 1997. The influence of wind stress, temperature, and humidity gradients on evaporation from reservoirs. *Water Resources Research*, *33*(12), pp.2813-2822.

[47] Benzaghta, M.A. and Mohamad, T.A., 2009, May. Evaporation from reservoir and reduction methods: An overview and assessment study. In *International Engineering Convention. Domascus, Syria and Medinah, Kingdom of Saudi Arabia* (Vol. 11, p. 18). Domascus Syria.

[48] Martínez-Granados, D., Maestre-Valero, J.F., Calatrava, J. and Martínez-Alvarez, V., 2011. The economic impact of water evaporation losses from water reservoirs in the Segura basin, SE Spain. *Water Resources Management*, *25*(13), pp.3153-3175.

[49] Mousavi, N., Kothapalli, G., Habibi, D., Khiadani, M. and Das, C.K., 2019. An improved mathematical model for a pumped hydro storage system considering electrical, mechanical and hydraulic losses. *Applied energy*, *247*, pp.228-236.

[50] Sears, D.W. and Moore, S.R., 2005. On laboratory simulation and the evaporation rate of water on Mars. Geophysical research letters, 32(16).

[51] Rigaudier, T., Lécuyer, C., Gardien, V., Suc, J.P. and Martineau, F., 2011. The record of temperature, wind velocity and air humidity in the δD and δ18O of water inclusions in synthetic and Messinian halites. Geochimica et Cosmochimica Acta, 75(16), pp.4637-4652.

[52] Lurie, M. and Michailoff, N., 1936. Evaporation from free water surface. *Industrial & Engineering Chemistry*, *28*(3), pp.345-349.

[53] Ngancha, P.B., Kusakana, K. and Markus, E.D., 2020, July. Energy Management Methodology for Sustainable Water Development and Servicing, Considering the POET Based Concept. In *Journal of Physics: Conference Series* (Vol. 1577, No. 1, p. 012043). IOP Publishing.

[54] Puust, R., Kapelan, Z., Savic, D.A. and Koppel, T., 2010. A review of methods for leakage management in pipe networks. *Urban Water Journal*, *7*(1), pp.25-45.

[55] Hunaidi, O., Wang, A., Bracken, M., Gambino, T. and Fricke, C., 2004, May. Acoustic methods for locating leaks in municipal water pipe networks. In *International conference on water demand management* (pp. 1-14). Jordan: Dead Sea.

[56] Global Water, C. (2018). TREADING WATER Corporate Responses to Rising Water Challenges. CDP Worldwide Level 4. [online] 60 Great Tower Street London EC3R 5AD. Available at: https://www.cdp.net/en/responses [Accessed 2018].

[57] El-Zahab, S. and Zayed, T., 2019. Leak detection in water distribution networks: an introductory overview. *Smart Water*, *4*(1), pp.1-23.

[58] Bond, A., Mergelas, B. and Jones, C., 2004. Pinpointing leaks in water transmission mains. In *Pipeline Engineering and Construction: What's on the Horizon?* (pp. 1-10).

[59] Kisch, M., 1959. The theory of seepage from clay-blanketed reservoirs. *Geotechnique*, *9*(1), pp.9-21.

[60] Omofunmi, O.E., Kolo, J.G., Oladipo, A.S., Diabana, P.D. and Ojo, A.S., 2017. A review on effects and control of seepage through earth-filled dam. *Current Journal of Applied Science and Technology*, *22*(5), pp.1-11.

[61] Oblinger, J.A., Moysey, S.M., Ravindrinath, R. and Guha, C., 2010. A pragmatic method for estimating seepage losses for small reservoirs, with application in rural India. *Journal of Hydrology*, *385*(1-4), pp.230-237.

[62] Yu, S., Ren, X., Zhang, J., Wang, H., Wang, J. and Zhu, W., 2020. Seepage, deformation and stability analysis of sandy and clay slopes, with different permeability anisotropy characteristics affected by reservoir water level fluctuations. *Water*, *12*(1), p.201.

[63] Listenlights. n.d. *Tariff And Its Types - Listenlights.* [online] Available at: <https://university.listenlights.com/2017/09/02/tariff-and-its-types/> [Accessed 15 January 2022].

[64] Distribution. 2021. *Tariffs and charges - Distribution.* [online] Available at: <https://www.eskom.co.za/distribution/tariffs-and-charges/> [Accessed 1 April 2021].

[65] Nelik, L. and Brennan, J., 2013. Gulf Pump Guides: Progressing Cavity Pumps, Downhole Pumps and Mudmotors. Elsevier.

[66] Moreira, D.F. and Ramos, H.M., 2013. Energy cost optimization in a water supply system case study. Journal of Energy, 2013.

[67] Yannopoulos, S.I., Lyberatos, G., Theodossiou, N., Li, W., Valipour, M., Tamburrino, A. and Angelakis, A.N., 2015. Evolution of water lifting devices (pumps) over the centuries worldwide. Water, 7(9), pp.5031-5060.

[68] Luo, X., Niu, Z., Shi, Z. and Hu, J., 2011. Analysis and design of an axial piston water-pump with piston valve. Journal of Mechanical Science and Technology, 25(2), p.371.

[69] Tackett, H.H., Cripe, J.A. and Dyson, G., 2008. Positive displacement reciprocating pump fundamentals-power and direct acting types. In Proceedings of the 24th International Pump Users Symposium. Texas A&M University. Turbomachinery Laboratories.

[70] Breit, F., Pumpenfabrik Urach, 1974. Diaphragm pumps for delivering liquid or gaseous media. U.S. Patent 3,807,906.

[71] Springer, C.M., Theis, B.O., Wawra, G. and Juffa, R., Bayer AG and Binks Manufacturing Co, 1983. Flushable rotary gear pump. U.S. Patent 4,400,147.

[72] Volk, M., 2013. Pump characteristics and applications. CRC Press.

[73] Liu, H.C., Tong, S.H. and Yang, D.C., 2000. Trapping-free rotors for high-sealing lobe pumps. Journal of Mechanical Design, 122(4), pp.536-542.

[74] Inaguma, Y. and Yoshida, N., 2015. Small High-Efficiency Vane Pump Based on Vane Pump Theory. SAE International Journal of Passenger Cars-Mechanical Systems, 8(2015-01-1496), pp.614-623.

[75] Cerdà, V., Estela, J.M., Forteza, R., Cladera, A., Becerra, E., Altimira, P. and Sitjar, P., 1999. Flow techniques in water analysis. Talanta, 50(4), pp.695-705.

[76] Larsson, E., 1977. Helical gear pump and method of manufacturing the same. U.S. Patent 4,030,862.

[77] Akin, O. and Rockwell, D., 1994. Flow structure in a radial flow pumping system using high-image-density particle image velocimetry. Journal of fluids engineering, 116(3), pp.538-544.

[78] Furukawa, A., Shigemitsu, T., Takano, T., Okuma, K. and Watanabe, S., 2005. Air/water two-phase flow performance of contra-rotating axial flow pump and rotational speed control of rear rotor. Nihon Kikai Gakkai Ronbunshu, B Hen/Transactions of the Japan Society of Mechanical Engineers, Part B, 71(708), pp.2047-2052.

[79] Haavik, H.K. and Sweet, D.F., Nash Engineering Co, 1999. Mixed flow liquid ring pumps. U.S. Patent 5,961,295.

[80] Gerlach, T. and Wurmus, H., 1995. Working principle and performance of the dynamic micropump. Sensors and Actuators A: Physical, 50(1-2), pp.135-140.

[81] Tackett, H.H., Cripe, J.A. and Dyson, G., 2008. Positive displacement reciprocating pump fundamentals-power and direct acting types. In *Proceedings of the 24th International Pump Users Symposium*. Texas A&M University. Turbomachinery Laboratories.

[82] Hohne, P.A., Kusakana, K. and Numbi, B.P., Economic Power Dispatch for Energy Cost Reduction of a Hybrid Energy System Considering Maximum Demand Charges and Time-based Pricing in a Healthcare Institution. In *2020 6th IEEE International Energy Conference (ENERGYCon)* (pp. 395-400). IEEE.

[83] Ahonen, T., Orozco, S.M., Ahola, J. and Tolvanen, J., 2016, September. Effect of electric motor efficiency and sizing on the energy efficiency in pumping systems. In *2016 18th European Conference on Power Electronics and Applications (EPE'16 ECCE Europe)* (pp. 1-9). IEEE.

[84] Burt, C.M., Piao, X., Gaudi, F., Busch, B. and Taufik, N.F.N., 2008. Electric motor efficiency under variable frequencies and loads. *Journal of irrigation and drainage engineering*, *134*(2), p.129.

[85] Trianni, A., Cagno, E. and Accordini, D., 2019. Energy efficiency measures in electric motors systems: A novel classification highlighting specific implications in their adoption. *Applied Energy*, *252*, p.113481.

[86] NEMA. 2022. *Motors and Generators*. [online] Available at: <https://www.nema.org/standards/view/motors-and-generators> [Accessed 15 July 2022].

[87] Magneticinnovations.com. 2022. *What are IEC standards? – Magnetic Innovations*. [online] Available at: <https://www.magneticinnovations.com/faq/what-are-iec-standards/> [Accessed 15 July 2022].

[88] Schleicher-Tappeser, R., 2012. How renewables will change electricity markets in the next five years. Energy policy, 48, pp.64-75.

[89] Urmee, T. and Md, A., 2016. Social, cultural and political dimensions of off-grid renewable energy programs in developing countries. *Renewable Energy*, *93*, pp.159-167.

[90] Gopal, C., Mohanraj, M., Chandramohan, P. and Chandrasekar, P., 2013. Renewable energy source water pumping systems—A literature review. *Renewable and Sustainable Energy Reviews*, *25*, pp.351-370.

[91] Xia, X. and Zhang, J., 2010. Energy efficiency and control systems–from a POET perspective. *IFAC Proceedings Volumes*, *43*(1), pp.255-260.

[92] Zhang, H., Xia, X. and Zhang, J., 2012. Optimal sizing and operation of pumping systems to achieve energy efficiency and load shifting. *Electric Power Systems Research*, *86*, pp.41-50.

[93] Moreira, D.F. and Ramos, H.M., 2013. Energy cost optimization in a water supply system case study. *Journal of Energy*, *2013*.

[94] Tang, Y., Zheng, G. and Zhang, S., 2014. Optimal control approaches of pumping stations to achieve energy efficiency and load shifting. *International Journal of Electrical Power & Energy Systems*, *55*, pp.572-580.

[95] Phiri, S.F., Kusakana, K. and Numbi, B.P., 2020, July. A survey of technical efficiency in crane systems using POET structure. In *Journal of Physics: Conference Series* (Vol. 1577, No. 1, p. 012037). IOP Publishing.

[96] Boiten, W., 2020. Hydrometry: IHE Delft lecture note series. CRC press.

[97] Sumi, T., Kantoush, S.A. and Shirai, A., 2011. *Worldwide Flood Mitigation Dams: Operating and Designing Issues*. na.

[98] Xu, Z., Guan, X., Jia, Q.S., Wu, J., Wang, D. and Chen, S., 2012. Performance analysis and comparison on energy storage devices for smart building energy management. IEEE Transactions on Smart Grid, 3(4), pp.2136-2147.

[99] DeBenedictis, A., Haley, B., Woo, C.K. and Cutter, E., 2013. Operational energy-efficiency improvement of municipal water pumping in California. Energy, 53, pp.237-243.

[100] Ahmad, H. and Atikol, U., 2018. Retracted: A simple algorithm for reducing the operation frequency of residential water pumps during peak hours of power consumption. *Energy Science & Engineering*, *6*(4), pp.253-271.

[101] Lumen Vault. 2022. Digital Timer Switch - Digital Mains Timer Relay Socket With LCD Display 7 Days Electronic Programable Relay Time Switch 16on&8off Timer | Lumen Vault Kenya. [online] Available at: <https://lumenvault.co.ke/product/digital-timer-switch-digital-mains-timer-relay-socket-with-lcd-display-7-days-electronic-programable-relay-time-switch-16on%EF%BC%868off-timer/> [Accessed 20 January 2022].

[102] Zazueta, F.S., Smajstrla, A.G. and Clark, G.A., 1994. *Irrigation system controllers*. University of Florida Cooperative Extension Service, Institute of Food and Agriculture Sciences, EDIS.

[103] Abhilash, P., Kumar, R.N. and Kumar, R.P., 2021. Solar powered water pump with single axis tracking system for irrigation purpose. *Materials Today: Proceedings*, *39*, pp.553-557.

[104] Getu, B.N. and Attia, H.A., 2015, September. Automatic control of agricultural pumps based on soil moisture sensing. In *AFRICON 2015* (pp. 1-5). IEEE.

[105] Kirk, D.E., 2004. *Optimal control theory: an introduction*. Courier Corporation.

[106] Bagirov, A.M., Barton, A.F., Mala-Jetmarova, H., Al Nuaimat, A., Ahmed, S.T., Sultanova, N. and Yearwood, J., 2013. An algorithm for minimization of pumping costs in water distribution systems using a novel approach to pump scheduling. *Mathematical and Computer Modelling*, *57*(3-4), pp.873-886.

[107] López-Ibáñez, M., Prasad, T.D. and Paechter, B., 2008. Ant colony optimization for optimal control of pumps in water distribution networks. *Journal of water resources planning and management*, *134*(4), pp.337-346.

[108] Shankar, V.K.A., Umashankar, S., Paramasivam, S. and Hanigovszki, N., 2016. A comprehensive review on energy efficiency enhancement initiatives in centrifugal pumping system. *Applied Energy*, *181*, pp.495-513.

[109] Duan, Z. and Bastiaanssen, W.G.M., 2017. Evaluation of three energy balance-based evaporation models for estimating monthly evaporation for five lakes using derived heat storage changes from a hysteresis model. Environmental Research Letters, 12(2), p.024005.

[110] Tanny, J., Cohen, S., Assouline, S., Lange, F., Grava, A., Berger, D., Teltch, B. and Parlange, M.B., 2008. Evaporation from a small water reservoir: Direct measurements and estimates. *Journal of Hydrology*, *351*(1-2), pp.218-229.

[111] Quinn, F.H., 1979. An improved aerodynamic evaporation technique for large lakes with application to the International Field Year for the Great Lakes. *Water Resources Research*, *15*(4), pp.935-940.

[112] Ndunguru, M.G. and Hoko, Z., 2016. Assessment of water loss in Harare, Zimbabwe. *Journal of Water, Sanitation and Hygiene for Development*, *6*(4), pp.519-533.

[113] Farley, M. and Trow, S., 2003. Losses in water distribution networks. IWA publishing.

[114] Anagnostopoulos, J.S. and Papantonis, D.E., 2012. Study of pumped storage schemes to support high RES penetration in the electric power system of Greece. *Energy*, *45*(1), pp.416-423.

[115] Cedergren, H.R., 1997. *Seepage, drainage, and flow nets* (Vol. 16). John Wiley & Sons.

[116] Sichilalu, S.M., 2016. *Optimal control of renewable energy/grid hybrid systems with heat pump load* (Doctoral dissertation, University of Pretoria).

[117] Hohne, P.A., Kusakana, K. and Numbi, B.P., 2018. Operation cost minimisation of hybrid solar/electrical water heating systems: model development. *Advanced Science Letters*, *24*(11), pp.8076-8080.

[118] Liszka, T. and Orkisz, J., 1980. The finite difference method at arbitrary irregular grids and its application in applied mechanics. Computers & Structures, 11(1-2), pp.83-95.

[119] Shojaei, A., Galvanetto, U., Rabczuk, T., Jenabi, A. and Zaccariotto, M., 2019. A generalized finite difference method based on the Peridynamic differential operator for the solution of

problems in bounded and unbounded domains. *Computer Methods in Applied Mechanics and Engineering*, *343*, pp.100-126.

[120] Hohne, P.A., Kusakana, K. and Numbi, B.P., 2018, April. Operation cost and energy usage minimization of a hybrid solar/electrical water heating system. In *2018 international conference on the domestic use of energy (DUE)* (pp. 1-7). IEEE.

[121] Population, E., Africa, P., Botshabelo, P., Africa, F., counted?, ⚡., Africa?, ⚡., Africa, L., Brakpan, P., Bay, P., Witbank, P., Vervoerdburg, P. and Uitenhage, P., 2021. *Population of Botshabelo 2021 | Botshabelo population - statistics*. [online] Population HUB. Available at: <https://population-hub.com/en/za/population-of-botshabelo-5764.html> [Accessed 4 October 2021].

[122] The Southern African Universities Radiometric Network (SAURAN):Available online at: https://sauran.ac.za/ [Accessed 24 Mar. 2020].

[123] Plus, C.P.M., 2007. Operation Manual. *Signal*, *20*(20.00), pp.5-000.

[124] Eskom.co.za. 2021. Tariffs And Charges. [online] Available at: <https://www.eskom.co.za/CustomerCare/TariffsAndCharges/Pages/Tariffs_And_Charges.aspx> [Accessed 8 January 2021].

[125] Hohne, P.A., Kusakana, K. and Numbi, B.P., 2020. Model validation and economic dispatch of a dual axis pv tracking system connected to energy storage with grid connection: A case of a healthcare institution in South Africa. *Journal of Energy Storage*, *32*, p.101986.

[126] Albaghdadi, A.M., Baharom, M.B. and bin Sulaiman, S.A., 2021, February. Parameter design optimization of the crank-rocker engine using the FMINCON function in MATLAB. In *IOP Conference Series: Materials Science and Engineering* (Vol. 1088, No. 1, p. 012072). IOP Publishing.

[127] Hohne, P.A., Kusakana, K. and Numbi, B.P., 2018, August. Techno-economic comparison of timer and optimal switching control applied to hybrid solar electric

water heaters. In *2018 International Conference on the Industrial and Commercial Use of Energy (ICUE)* (pp. 1-6). IEEE.

[128] Numbi, B. P., and S. J. Malinga. "Optimal energy cost and economic analysis of a residential grid-interactive solar PV system-case of eThekwini municipality in South Africa." Applied Energy 186 (2017): 28-45.

[129] Alibaba.com. 2022. *Radar Level Gauge And Water Level Controller Automatic Fluid Level Sensor For Digital Iiot Water Hydrology Management System - Buy Radar Level Gauge,Water Level Controller Automatic,Fluid Level Sensor Product on Alibaba.com*. [online] Available at: <https://www.alibaba.com/product-detail/Radar-Level-Gauge-and-Water-Level_1600087768833.html?spm=a2700.details.0.0.60231e284kjs2c> [Accessed 24 July 2022].

[130] STEP Building Supplies. 2022. *Speroni Centrifugal Pump Nm200-500*. [online] Available at: <https://www.stepbuildingsupplies.co.za/products/speroni-centrifugal-pump-nm200-500?currency=ZAR&variant=34197742747779&utm_medium=cpc&utm_source=google&utm_campaign=Google%20Shopping&gclid=CjwKCAjwrNmWBhA4EiwAHbjEQD9MTP5xhVGNaqdyzmwm1IuYtDIY1OY9oa7ibIXrSZWCkG1pPAQ5ARoCIRAQAvD_BwE> [Accessed 19 July 2022].

[131] Alibaba.com. 2022. *Toky Digital Display Good Price Mechanical Outlet Timer - Buy Mechanical Outlet Timer,Digital Display Mechanical Outlet Timer,Good Price Mechanical Outlet Timer Product on Alibaba.com*. [online] Available at: <https://www.alibaba.com/product-detail/Toky-digital-display-good-price-mechanical_60779438217.html?spm=a2700.pccps_detail.normal_offer.d_image.15c35450GTQ0pO> [Accessed 19 July 2022].

[132] Made-in-china.com. 2022. *Vfd, vfd in Variable-Frequency Drive, China vfd Manufacturers*. [online] Available at: <https://www.made-in-china.com/productdirectory.do?word=vfd&file=&searchType=0&subaction=hunt&st

yle=b&mode=and&comProvince=nolimit&order=0&isOpenCorrection=1&org=top&code=1642000000&log_from=1> [Accessed 19 July 2022].

[133] Electric, S., SYSTEMS, P., Electric, T. and Electric, T., 2022. *TM221CE24T Schneider Electric*. [online] Wiautomation. Available at: <https://za.wiautomation.com/schneider-electric/plc-systems/TM221CE24T?utm_source=shopping_free&utm_medium=organic&utm_content=ZA92081&gclid=Cj0KCQjw2_OWBhDqARIsAAUNTTE0p6_GNq3Neqax7gSnQQHB7Szd_xIPxlUzX_WCjCENVJrs1rrlwdIaAlyrEALw_wcB> [Accessed 24 July 2022].

[134] Cousins, T., 2009. Using time of use (TOU) tariffs in industrial, commercial and residential applications effectively. *TLC Engineering Solutions*.

[135] Hohne, P.A., Kusakana, K. and Numbi, B.P., 2022. Energy cost minimization of a multifarious water heating system with energy recovery: A case of a healthcare institution. *Journal of Energy Storage*, *51*, p.104451.

[136] King, R.G. and Kerr, W., 1996. Limits on interest rate rules in the IS model. *FRB Richmond Economic Quarterly*, *82*(2), pp.47-75.

[137] Hohne, P.A., 2017. *Optimal energy management of a hybrid solar water heating system with grid connection under time-based pricing* (Doctoral dissertation, Bloemfontein: Central University of Technology, Free State).

[138] Media, T., 2022. *Historic inflation South Africa – historic CPI inflation South Africa*. [online] Inflation.eu. Available at: <https://www.inflation.eu/en/inflation-rates/south-africa/historic-inflation/cpi-inflation-south-africa.aspx> [Accessed 18 July 2022].

APPENDICES

Table A: 2020 Load demand, Evaporation and Rainfall data

Date and Time	Evaporation Data (ML)	Load demand Data (ML)	Rainfall Data (ML)	Seepage Data (ML)
6/22/2020 0:00	0	50.02	14.20	2.50
6/23/2020 0:00	0	50.02	14.20	2.50
6/22/2020 0:30	0	45.27	15.35	2.26
6/23/2020 0:30	0	45.27	15.35	2.26
6/22/2020 1:00	0	45.12	16.80	2.25
6/23/2020 1:00	0	45.12	16.80	2.25
6/22/2020 1:30	0	45.17	16.08	2.25
6/23/2020 1:30	0	45.17	16.08	2.25
6/22/2020 2:00	0	40.47	16.03	2.02
6/23/2020 2:00	0	40.47	16.03	2.02
6/22/2020 2:30	0	40.18	16.42	2.00
6/23/2020 2:30	0	40.18	16.42	2.00
6/22/2020 3:00	0	35.42	17.03	1.77
6/23/2020 3:00	0	35.42	0.50	1.77
6/22/2020 3:30	0	30.12	0.50	1.50
6/23/2020 3:30	0	30.12	0.50	1.50
6/22/2020 4:00	0	30.43	0.50	1.52
6/23/2020 4:00	0	30.43	0	1.52
6/22/2020 4:30	0	25.12	0	1.25
6/23/2020 4:30	0	25.12	0	1.25
6/22/2020 5:00	0	20.31	0	1.01
6/23/2020 5:00	0	20.31	0	1.01
6/22/2020 5:30	0	20.02	0	1.00
6/23/2020 5:30	0	20.02	0	1.00
6/22/2020 6:00	0	20.48	0	1.02
6/23/2020 6:00	0	20.48	22.32	1.02
6/22/2020 6:30	0	20.28	23.68	1.01
6/23/2020 6:30	0	20.28	23.68	1.01
6/22/2020 7:00	0	25.10	21.67	1.25
6/23/2020 7:00	0	25.10	21.67	1.25
6/22/2020 7:30	0	20.43	22.62	1.02
6/23/2020 7:30	0	20.43	22.62	1.02
6/22/2020 8:00	0	20.24	26.84	1.01

6/23/2020 8:00	0	20.24	26.84	1.01
6/22/2020 8:30	0	25.43	23.52	1.27
6/23/2020 8:30	0	30.43	23.52	1.52
6/22/2020 9:00	0	40.23	21.27	2.01
6/23/2020 9:00	0	40.23	21.27	2.01
6/22/2020 9:30	0	60.03	16.76	3.00
6/23/2020 9:30	0	60.03	16.76	3.00
6/22/2020 10:00	1.85	65.49	12.95	3.27
6/23/2020 10:00	1.85	65.49	0	3.27
6/22/2020 10:30	2.93	65.39	0	3.26
6/23/2020 10:30	2.93	65.39	0	3.26
6/22/2020 11:00	3.49	70.42	0	3.52
6/23/2020 11:00	3.49	70.42	0	3.52
6/22/2020 11:30	3.78	75.38	0	3.76
6/23/2020 11:30	3.78	75.38	0	3.76
6/22/2020 12:00	4.09	80.35	0	4.01
6/23/2020 12:00	4.09	80.35	0	4.01
6/22/2020 12:30	4.46	85	0	4.25
6/23/2020 12:30	4.46	85	0	4.25
6/22/2020 13:00	4.42	85.17	0	4.25
6/23/2020 13:00	4.42	85.17	0	4.25
6/22/2020 13:30	4.39	90.01	0	4.50
6/23/2020 13:30	4.39	90.01	0	4.50
6/22/2020 14:00	4.26	90.40	0	4.52
6/23/2020 14:00	4.26	90.40	0	4.52
6/22/2020 14:30	4.16	90.45	1.55	4.52
6/23/2020 14:30	4.16	90.45	1.55	4.52
6/22/2020 15:00	3.47	95.16	1.55	4.75
6/23/2020 15:00	2.86	95.16	2.80	4.75
6/22/2020 15:30	2.86	95.09	2.80	4.75
6/23/2020 15:30	1.80	95.095	2.80	4.75
6/22/2020 16:00	1.80	90.40	10.75	4.52
6/23/2020 16:00	0.50	90.40	10.75	4.52
6/22/2020 16:30	0	90.03	10.18	4.50
6/23/2020 16:30	0	90.03	10.18	4.50
6/22/2020 17:00	0	85.05	10.79	4.25
6/23/2020 17:00	0	85.05	0	4.25
6/22/2020 17:30	0	75.23	0	3.76
6/23/2020 17:30	0	75.23	0	3.76
6/22/2020 18:00	0	70.45	0	3.52
6/23/2020 18:00	0	70.45	0	3.52

6/22/2020 18:30	0	65.43	0	3.27
6/23/2020 18:30	0	65.43	0	3.27
6/22/2020 19:00	0	65	0	3.25
6/23/2020 19:00	0	65	0	3.25
6/22/2020 19:30	0	55.445	0	2.77
6/23/2020 19:30	0	55.445	0	2.77
6/22/2020 20:00	0	60.08	0	3.00
6/23/2020 20:00	0	60.08	0	3.00
6/22/2020 20:30	0	50.465	0	2.52
6/23/2020 20:30	0	50.465	14.315	2.52
6/22/2020 21:00	0	50.175	14.425	2.50
6/23/2020 21:00	0	50.175	14.425	2.50
6/22/2020 21:30	0	50.065	14.075	2.50
6/23/2020 21:30	0	50.065	14.075	2.50
6/22/2020 22:00	0	45.43	14.875	2.27
6/23/2020 22:00	0	45.43	14.875	2.27
6/22/2020 22:30	0	45.49	16.145	2.27
6/23/2020 22:30	0	45.49	16.145	2.27
6/22/2020 23:00	0	45.29	16.975	2.26
6/23/2020 23:00	0	45.29	16.975	2.26
6/22/2020 23:30	0	40.255	17.58	2.01
6/23/2020 23:30	0	40.255	17.58	2.01

Table B: Energy calculation

Time of operation (hour)	**energy consumption**					
	Flood switching control		Timer-setting control		VFD-Timer-setting control	
	Energy consumption (kWh)	Energy in (kVA)	Energy consumption (kWh)	Energy in (kVA)	Energy consumption (kWh)	Energy in (kVA)
00:00	0	0	0	0	0	0
02:25	620	746.98	155	186.75	341	410.84
03:25	620	746.98	465	560.24	488.30	588.31
04:25	620	746.98	697.50	840.36	488.30	588.31
09:25	620	746.98	697.50	840.36	488.30	588.31
10:50	620	746.98	697.50	840.36	875.80	1055.18
11:55	620	746.98	1008	1214.46	1186	1428.92
15:55	1783	2148.19	2248	2708.43	2178	2624.09
16:55	2093	2521.68	2558	3081.93	2255	2716.87
17:00	2248	2708.43	2635	3174.70	2255	2716.87
18:55	2713	3268.67	2635	3174.70	2255	2716.87
19:00	2868	3455.42	2713	3268.67	2333	2810.84
20:25	2868	3455.42	3100	3734.94	2674	3221.68

20:50	2868	3455.42	3100	3734.94	2713	3268.67
24:00	2868	3455.42	3100	3734.94	2713	3268.67

Table C: Energy calculation

Time of operation (hour)	energy consumption					
	Flood switching control		Optimal control		VFD-Optimal control	
	Energy consumption (kWh)	Energy in (kVA)	Energy consumption (kWh)	Energy in (kVA)	Energy consumption (kWh)	Energy in (kVA)
00:00	0	0	0	0	0	0
02:25	620	746.98	0	0	0	0
05:55	620	746.98	73.75	88.85	38.72	46.65
09:00	620	746.98	73.75	88.85	38.72	46.65
09:25	620	746.98	73.75	88.85	156.70	188.79
11:55	620	746.98	737.5	88.85	677.90	816.75
17:00	2248	2708.43	2360	2843.37	2227	2683.13
18:00	2558	3081.93	2360	2843.37	2227	2683.13
19:00	2868	3455.42	2360	2843.37	2227	2683.13
19:30	2868	3455.42	2434	2932.53	2300	2771.08
20:00	2868	3455.42	2655	3198.79	2374	2860.24
24:00	2868	3455.42	2655	3198.79	2374	2860.24

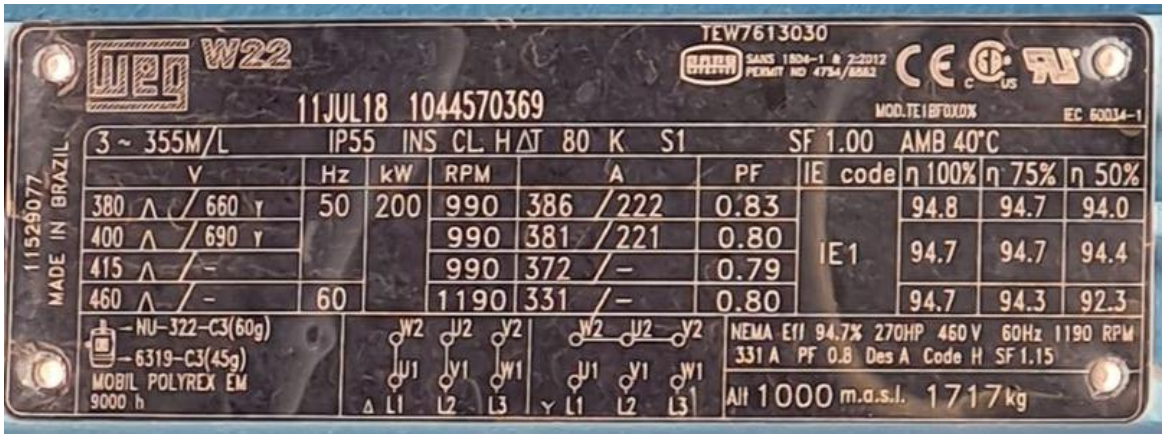

Figure A: 200kW Electrical water pump specifications

Figure B: Allen-Bradley VFD driver